Stress Analysis of Spiral Bevel Gear Drives

Mohammad Qasim Abdullah
University of Baghdad/ College of Engineering
Mechanical Engineering Department

Humam Abdulrahiem Abdulwahid
University of Baghdad/ College of Engineering
Mechanical Engineering Department

ABSTRACT

This paper presents numerical and experimental stress analyses to evaluate the contact and bending stresses on the teeth of spiral bevel gear drive. Finite Element Method has been adopted as a numerical technique which accomplished basically by using ANSYS software package. The experimental stress analysis has been achieved by using a gear tooth model made of Castolite material which has photoelastic properties. The main goal of this research is detecting the maximum tooth stresses to avoid the severe areas that caused tooth failure and to increase the working life for this type of gear drives.

Keywords: spiral, bevel, gear, generation, simulation, teeth meshing, stress analysis

الخلاصة

هذا البحث يقدم تحليلا للاجهادات التي تظهر على المسنن المخروطي الحلزوني عدديا باستخدام تقنيه العناصر المحددة وعمليا باستخدام طريقة التحليل الضوئي للمرونة لايجاد قيم اجهادات التلامس والحناية على سطح السن.

الهدف الرئيسي من هذا البحث هو تحديد قيم إجهادات التلامس والحناية القصوى التي يتعرض لها هذا النوع من المسننات لتجنب حدوث الفشل وضمان عمل المسنن لفترة زمنية أطول.

.

INTRODUCTION

Bevel gear are most suitable widely used in transmission power and motion from the shafts oriented in intersecting axes , therefore the gear have conical pitch surfaces. Spiral bevel gear has a spiral angle and the teeth of such gear drive are curved and oblique and as a result have a considerable amount of overlap. Because of continuous contact the spiral bevel has large load-carrying capacity and run in high speed and more smoothly and quietly than straight bevel gears of the same size. The curved teeth of spiral bevel gear drive ensures more than one tooth in contact at all time and results in gradual engagement and continuous pitch-line contact.

EXPERIMENTAL ANALYSIS

Photoelastic analysis is a widely used technique to perform stress analysis experimentally with a reasonable percent of errors. The present photoelastic study conducted successfully and values of stresses has been determined. Essentially such a problem defined as a three-dimensional problem and it required using a stress-freezing method. Therefore, this study has been reduced to series of two-dimensional problem by calculating the stresses at a number of thin cross sections along the

tooth length **,M. Q. Abdullah, 1997**. The distribution of contact and bending stresses had been determined.

THE PHOTOELASTICITY METHOD OF STRESS ANALYSIS

Basically we used a transparent material which has a properties leads to simplifying such problems experimentally. One of these properties is transparency to the light which employed in the polariscope. These materials are so called photoelastic materials or birefringent materials **,Robert F. and George D., 1999**.

The basic equation which calculates experimental stresses is:

$$(\sigma_1 - \sigma_2) = n\, f / h \qquad (1)$$

Where n represent the number of fringes, f is material fringe constant and $(\sigma_1 - \sigma_2)$ is the difference between principal stresses.

PHOTOELASTIC MATERIAL

The used material for models was"Castolite" with (4 mm) thickness such material can be applied for two dimensional studies.

Table 1. shows the material properties that conducted from calibration test of sample which has been taken from same material of sheet used to fabricate the tooth model.

PHOTOELASTIC MODEL

The segment model with one tooth profile has been chosen carefully to matching the output of theoretical design with curved-edged tool of cutting. The gear teeth model was made 7 times actual size. The dimensions of gear geometry of the chosen profile are given in **Table 2.**

EXPERIMENTAL APPARATUS AND CALIBRATION METHOD

In such analysis the stress distribution in a complex model is sought as a function of the load **, Litvin and Alfonso, 2003.**

The accurate calculations of stress distribution need a careful calibration of the material fringe value. These values affected with many parameters such as applied load, temperature and the age of material **, Lelkes and Marialigeti, 2002.**

As an example of the concept of using a calibration specimen that exhibits several fringe orders simultaneously, beam tensile stress is useful and this method used in the present work. An axial load applied on specimen that causes appearance of fringe pattern in the center of the specimen as shown in Fig. (3).

The calculation of the tensile stress for a rectangular specimen of thickness t and width b is:

$$\sigma_1 = \sigma_x = F / dt \qquad (2)$$

Referring to eq. (1):

$$F / dt = nf / h \qquad (3)$$

Here $t = h$, so

$$f / t = \sigma_1 / n \qquad (4)$$

After applying sufficient load F, several orders of fringes appeared. Table (3) shows the results of calibration. Fig.(4) shows the results of photoelastic fringes, gradually increasing the contact and bending stresses for both light and dark field.

EXPERIMENTAL PROCEDURE

The gear teeth model was positioned in the loading fixture such that the point of contact on the gear tooth profile matched the point of contact on the pinion tooth profile. The model of the gear tooth was firmly clamped to prevent rotation and connected to the load sensor which was connected to the load cell to read the load applied, and another gear (pinion) tooth was connected to the arm which connects to the crank handle to apply load by turning the load crank on the loading fixture. Both a light and dark field was employed to increase the accuracy of the account of the fringes in the calibration specimen. Once the load was established, alight field and dark field photograph were taken of the fringe pattern in the gear model. Before conducting any test on the model, the calibration of load cell must be checked. The model is then aligned in the field of the polariscope, and the load is gradually applied to the models. The above procedure is carried out for all the photoelastic models.

TRANSITION FROM MODEL TO PROTOTYPE

For many practical two-dimensional elastic problems with forces applied to external boundaries, stresses depend upon geometry and external forces only. A model must then be geometrically similar to the prototype and the applied loads must be similarly distributed, but they may differ in magnitude by a factor of proportionality. Any stress, σ_{th} in the prototype is determined from the corresponding stress, $\sigma_{\exp}$ at the corresponding point in the model **, Litvin F. L. and Lee H., 1989.**

$$p_{\max} = \sigma_{\max} = \frac{3}{2} C_p W^{1/3} \left(\frac{B+A}{\phi}\right)^{2/3} (A/B)^{0.186} \tag{5}$$

Where

$$\phi = \frac{1-v_1^2}{E_1} + \frac{1-v_2^2}{E_2}$$

Then

$$\frac{\sigma_{\max})_{th}}{\sigma_{\max})_{\exp}} = \frac{\frac{3}{2} C_p W_{th}^{\ 1/3} \left(\frac{\{B+A\}_{th}}{\phi_{th}}\right)^{2/3} (A/B)_{th}^{\ 0.186}}{\frac{3}{2} C_p W_{\exp}^{\ 1/3} \left(\frac{\{B+A\}_{\exp}}{\phi_{\exp}}\right)^{2/3} (A/B)_{\exp}^{\ 0.186}} \tag{6}$$

Since the gear teeth models were made 7 times of actual size, thus

$$A, B)_{th} = \frac{1}{7} A, B)_{\exp} \tag{7}$$

Where (A) and (B) are the length of major and miner axis of the contact ellipse.

The material is steel with the properties of Young's Modulus $E = 2.068 \times 10^5\ MPa$ and Poisson's ratio $\nu = 0.29$, and the material properties of photoelastic is shown in Table (1) thus

$$\phi)_{th} = 8.857833 \times 10^{-12}\ m^2 / N \quad \& \quad \phi)_{\exp} = 4.085732 \times 10^{-10}\ m^2 / N$$

Then
$$\frac{\sigma_{\max})_{th}}{\sigma_{\max})_{\exp}} = 47.064519 \left(\frac{W_{th}}{W_{\exp}} \right)^{1/3} \tag{8}$$

NUMERICAL ANALYSIS

In accordance with the described procedure for calculation of stresses on tooth flanks, it can be concluded that the solving of the defined task by the analytical methods is very complex and possible only with many assumptions. So, for this problem, as well as for almost all problems in theory of elasticity, the numerical methods must be used. Instead of a system of differential (simple, partial and integral) equations, which are defined for solving some problem in theory of elasticity, numerical methods form corresponding system of simple algebraic equations. By using computers, that system can be solved quickly and successfully. So, for studying the problem of contact stresses on tooth flanks, the Finite Element Method (FEM) is chosen. The Finite Element Method formulates the differential equations of balance of an elastic body. By taking into consideration the boundary conditions, the number of unknown quantities in these equations becomes smaller **Gosselin and Cloutier, 1991**.

The tooth model has been adopted from previous generation computer program **, M. Q. Abdullah and I. A. Hussain, 1999.** with means of CAD software package and solid works program, the basic input design data imported by Gleason works standards **, M. Q. Abdullah, 2007**. Fig.(2) shows three teeth of generated gear and pinion.

DEVELOPMENT OF FINITE ELEMENT MODELS

The development approach for finite element models is accomplished as follows:

1- Tooth surface equations of pinion and gear and portions of corresponding rim are considered for determination of the volumes of the designed bodies. Loss of accuracy introduced by CAD computer programs for the generation is avoided**, Robert F. Handschuh, 1997.**

2- The proposed approach does not require an assumption on the load distribution in the contact area. To get the contact area and stresses the contact algorithm of the general purpose (Ansys) is used.

3- F.E. models of three pairs of teeth are applied and therefore the boundary conditions are far enough from the loaded areas of the teeth.

4- Setting of boundary conditions is accomplished automatically and is shown in **Fig. 1.**

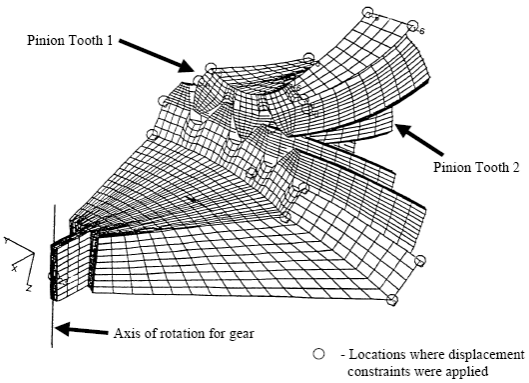

Figure 1. Boundary conditions for pinion and gear.

The following ideas are considered:
Nodes on the two sides and bottom part of the portion of the gear rim are considered as fixed.
Nodes on the two sides and bottom part of the portion of the pinion rim are considered as a rigid body.
Input torque can be expressed as the sum of applied nodal forces at radius of shaft (r_{sh}), thus

$$\mathbf{T}_1 = \sum_{i=1}^{n} F_i \, r_{sh} \tag{9}$$

Where T1 is the input torque load, n is the total number of constrained nodes and F_i is the tangential nodal force (usually $F_i = F$, where F is a constant value). The displacement of two sides and bottom part on the pinion tooth has a unique value because a coupled equation was used to enable these surfaces to be rigid in motion.

5-The contact algorithm of the FEA computer program requires definition of contacting surfaces **,David G. and Ron L., 2003.**To define a contact pair completely, contact and target elements have to be referred to the same characteristic parameters. The element Solid 92 with 10 nodes is used as a contact surface to surface in the present analysis.

6-The select contact algorithm was the Penalty Method. The penalty method uses a contact “spring” to establish a relationship between the two contact surfaces.

NUMERICAL EXAMPLE

The finite element analysis has been performed. A three teeth model has been applied for each case of design. The element "solid 10 node 92" has been adopted to build the finite element mesh. The total number of elements is 72820 with 84614 nodes. The material steel is applied for both pinion and gear. A torque of 400 N.m has been applied to the pinion for all cases of design.
Figs.(5, 6) show the results of execution of Ansys program to evaluate contact and bending stresses numerically by choosing Von-Mises failure criterion with changing design parameters. Also **Tables (4, 5)** shows the comparison between experimental and numerical results.

Table 1.Photoelastic material properties.

Elastic Limits N/m^2	Tensile Strength N/m^2	Young's Modulus N/m^2	Poisson's Ratio
2.068427e+007	4.136854e+007	4.295434e+009	0.35

Table 2. Dimensions of gear tooth model.

Normal Module (mm)	Normal Pressure Angle (Deg)	Spiral Angle (Deg)	Face Width (mm)	Number of Pinion Teeth	Number of Gear Teeth
5	25	35	4	19	62

Table 3. Results of Calibration test.

Fringe Order, ***n***	Load, ***F*** (N)	Stress, **σ** (MPa)
0	0	0
1	624.28	10.404
2	836.72	13.945
3	1024.52	17.075
4	1266.98	21.1163
5	1472.61	24.5435
6	1682.23	28.0371
7	1870.79	31.179
8	2063.82	34.397
9	2283.17	38.0528
10	2503.17	41.7226

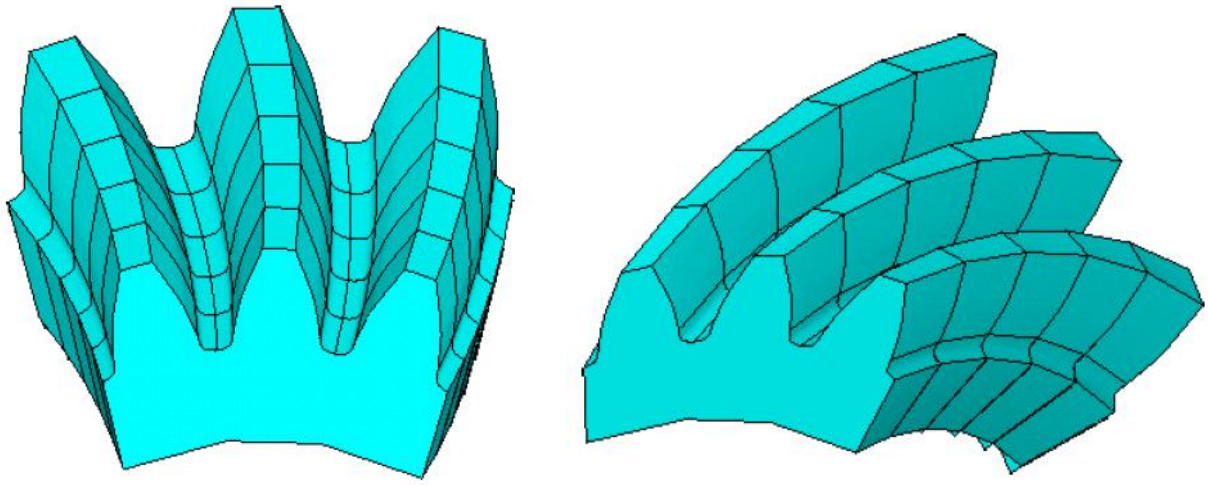

Figure 2. Three generated teeth of gear and pinion.

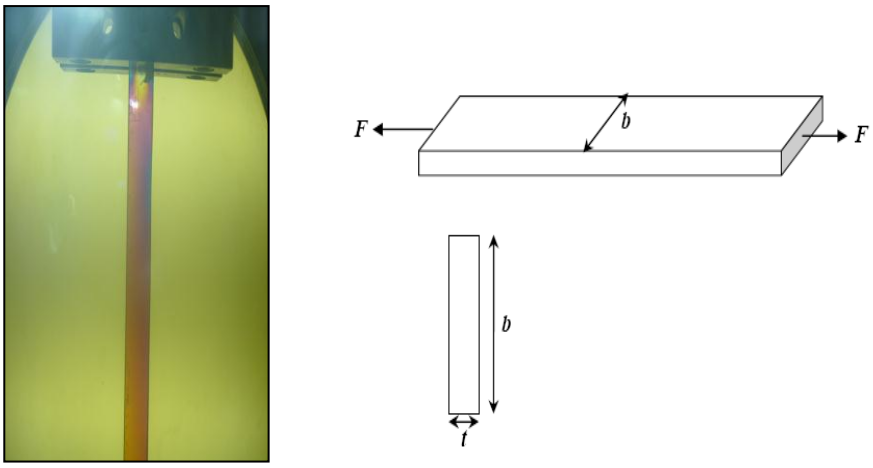

Figure 3. Schematic diagram for the tensile specimen geometry.

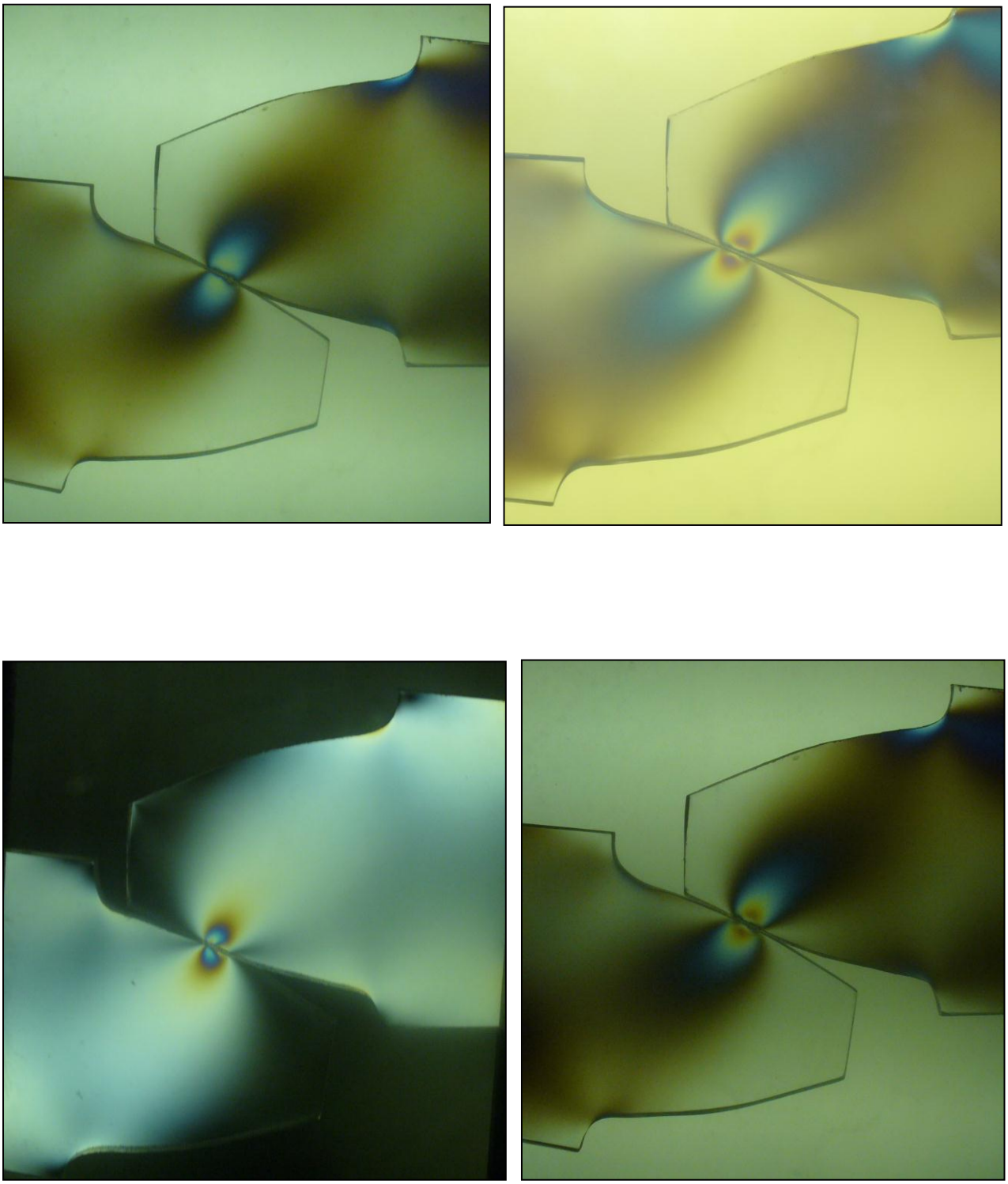

Figure 4. Results of photoelastic fringes shows gradually increasing the contact and bending stresses for both light and dark field.

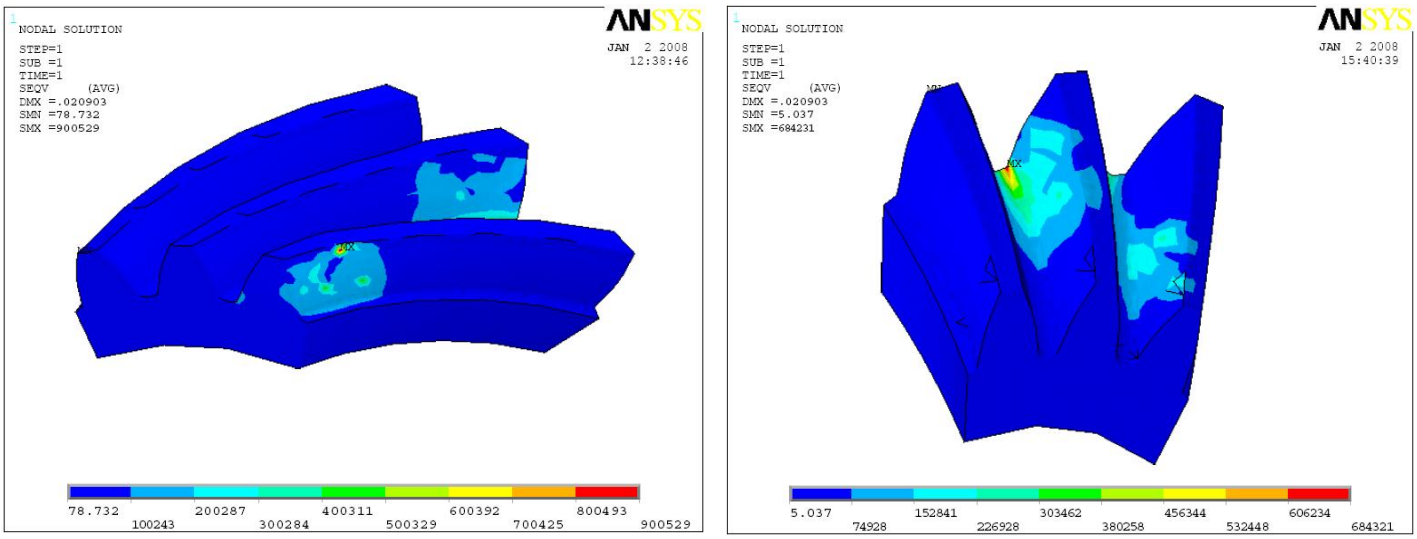

(a)

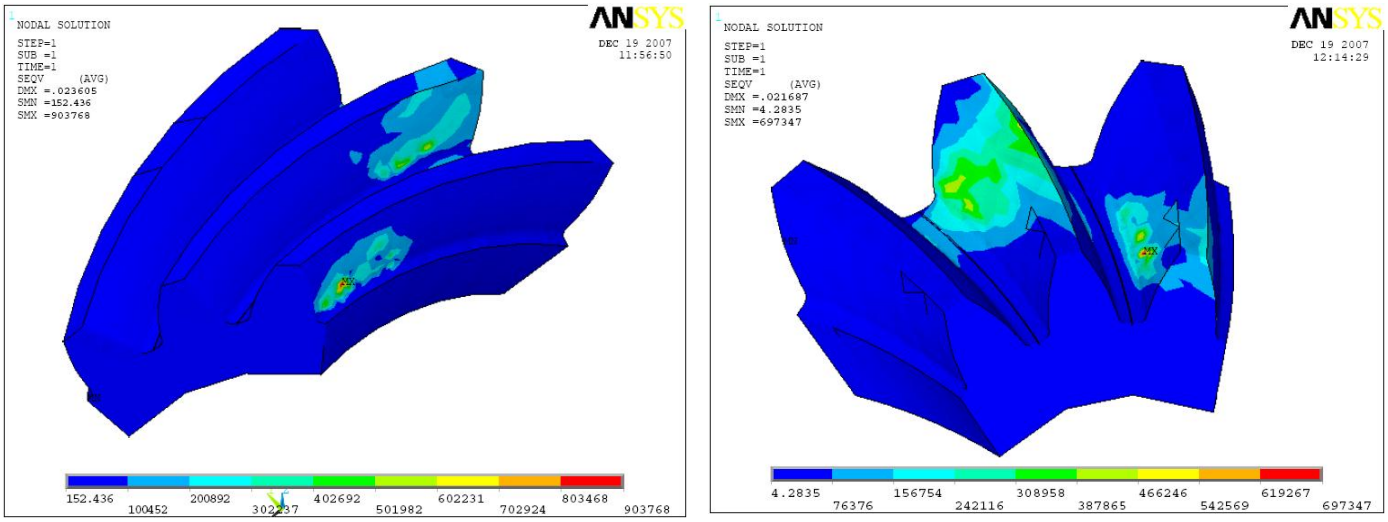

(b)

Figure 5. Von Mises contact and bending stresses with changing of spiral angle.
(a) ß=25.0°, (b) ß=35.0°

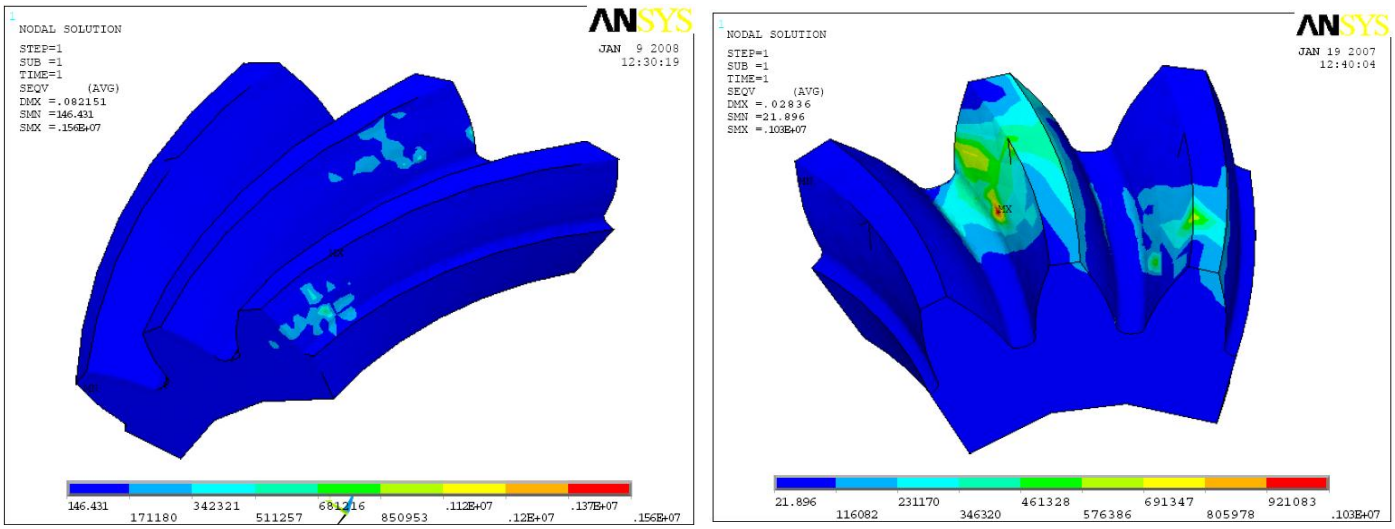

(a)

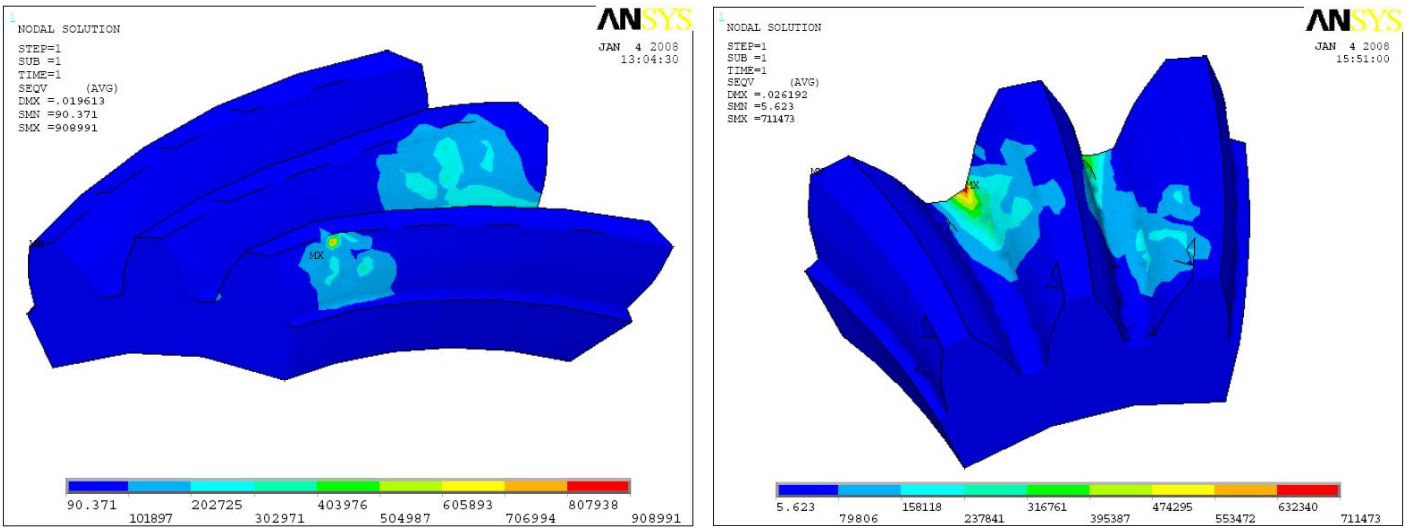

(b)

Figure 6. Von Mises contact and bending stresses with changing of Normal Module.
(a) Mn=3mm, (b) Mn=9 mm

Table 4. Comparison between experimental and numerical contact stresses.

	Experimental Contact Stress (Mpa)	Numerical Contact Stress (Mpa)	Percentage Error (%)
Pinion	1328.02	1372.5	3.34
Gear	1162.35	1247.3	7.308

Table 5. Comparison between experimental and numerical bending stresses.

	Experimental Bending Stress (Mpa)	Numerical Bending Stress (Mpa)	Percentage Error (%)
Pinion	288.7	248.9	15.9
Gear	242.3	221.3	9.48

CONCLUSIONS

1. Experimental and numerical analyses have been successfully conducted.
2. Automatic generation of finite element models have been developed to perform multi-tooth stress analysis for several contact points along the path of contact and obtain the contact and bending tooth stresses.
3. The investigation shows that the increasing of mean spiral angle causes increase contact stresses while the bending stresses decrease, also the increasing in the normal module leads to decrease the both contact and bending stresses, all of that indicate the improvement in the shape of transmission error function from linear to parabolic function from the point of view of minimizing transmission error which caused by misalignment.

NOMENCLATURES

A	length of major axis of contact ellipse
B	length of major axis of contact ellipse
b	width of specimen
C_p	constant
E	modulus of elasticity
F	tangential Force
f	material fringe constant
Mn	normal module
n	fringe order
T	input torque
t	thickness of specimen
r_{sh}	radius of shaft
W	applied load
ß	mean spiral angle
σ_1	first principal stress
σ_2	second principal stress
ν	poisson's Ratio

REFERENCES

- David G. Lewicki, Ron L. Woods, Evaluation of low-noise, improved bearing contact spiral bevel gears, NASA TR-2970, 2003.
- Faydor L. Litvin, Alfonso Fuentes, Computerized design, Generation, Simulation of meshing and contact, and stress analysis of formate cut spiral bevel gear drives, NASA CR-525, 2003.
- Gosselin C, Cloutier L., Brousseau J., Tooth contact analysis of high conformity spiral bevel gear, NASA CR-341, 1991.
- Litvin F. L., Lee H., Generation and tooth contact analysis of spiral bevel gears with predesigned parabolic functions of transmission errors, NASA TR-C-014, 1989.
- Lelkes M., Marialigeti J., Cutting definition for kinematic optimization of spiral bevel gears, Hungary 2002.
- Mohammad Qasim Abdullah, Influence of Varying The Normal Load Position on Maximum Tensile Stresses on Unsymmetrical Gear Tooth, University of Baghdad Engineering Journal, ISSN 1726-4073, Vol.3, No.2, 1997.

- Mohammad Qasim Abdullah, Imad Ahmed Hussain, Computer Aided Graphics of Involute Gear Tooth Profile, University of Baghdad Engineering Journal, ISSN 1726-4073, Vol.5, No.1, 1999.
- Mohammad Qasim Abdullah, Machine-tool settings to provide optimal TCA of spiral bevel gear drives, University of Baghdad Engineering Journal, ISSN 1726-4073, Vol.13, No.4, 2007.
- Robert F. Handschuh , Recent advances in the analysis of spiral bevel gears, NASA ARL-TR-1316, 1997.
- Robert F. Handschuh, George D. Bibel, Comparison of experimental and analytical tooth bending stress of aerospace spiral bevel gears, NASA ARL-TR-1891, 1999.

Evaluating the Performance of High Modulus Asphalt Concrete Mixture for Base Course in Iraq

Amjad H. K. Albayati
Assistant Professor
Engineering College-University of Baghdad
Sirtransportation@yahoo.com

Roaa H. Lateif
M.Sc Candidate
Engineering College-University of Baghdad
roaahamed47@yahoo.com

ABSTRACT

In the 1980s, the French Administration Roads LCPC developed high modulus mixtures (EME) by using hard binder. This type of mixture presented good resistance to moisture damage and improved mechanical properties for asphalt mixtures including high modulus, good fatigue behaviour and excellent resistance to rutting. In Iraq, this type of mixture has not been used yet. The main objective of this research is to evaluate the performance of high modulus mixtures and comparing them with the conventional mixture, to achieve this objective, asphalt concrete mixes were prepared and then tested to evaluate their engineering properties which include moisture damage, resilient modulus, permanent deformation and fatigue characteristics. These properties have been evaluated using indirect tensile strength, uniaxial repeated loading and repeated flexural beam tests. EME mixes were found to have improved fatigue and permanent deformation characteristics, also showed more resistance to moisture damage than conventional mix by 9.3 percent and the resilient modulus at temperature 60 ^{o}C increased by 63 percent. The general theme viewed from the results of this study has added to local knowledge the ability to produce more durable asphalt concrete mixtures with better serviceability using EME mixes.

Key words: high modulus asphalt mixture, fatigue, rutting.

تقييم اداء الخلطة الاسفلتية العالية الجساءة لطبقة الاساس في العراق

ا.م.د. امجد حمد البياتي
استاذ مساعد
كلية الهندسة-جامعة بغداد

رؤى حامد لطيف
ماجستير هندسة مدنية
كلية الهندسة-جامعة بغداد

الخلاصة

في سنة ١٩٨٠، طورت المؤسسة الفرنسية للطرق (LCPC) الخلطات العالية الجساءة، (EME) بواسطة استخدام اسفلت بتدرج صلب. هذا النوع من الخلطات يعطي مقاومة جيدة لضرر الرطوبة و يحسن الخواص الميكانيكية للخلطات الاسفلتية التي تشمل جساءة عالية،تصرف جيد للكلل ومقاومة ممتازة للتخدد. هذا النوع من الخلطات لم يستخدم بعد في العراق. الهدف الرئيسي من هذا البحث هو تقييم اداء الخلطات العالية الجساءة ومقارنتها بالخلطات الاعتيادية، للوصول لهذا الهدف، تم تحضير خلطات الخرسانة الاسفلتية وفحصها لتقييم الخصائص الهندسية. هذه الخصائص تم تقييمها بأستخدام فحوصات نسبة الشد غير المباشر، الحمل المتكرر احادي المحور وفحص الانحناء المتكرر. أنشأت خلطات ال EME لتحسين خصائص الكلل و التشوهات الدائمية، وكذلك اظهرت مقاومة للضرر الحاصل بسبب الرطوبة اكثر من الخلطات الاعتيادية بنسبة 9,3 % و ومعامل المرونة عند درجة حرارة 60 ^{o}س ازداد بنسبة 63 %. اضيف الى المعرفة المحلية الموضوع العام الذي يعرض من نتائج هذه الدراسة هو القابلية لانتاج خلطات خرسانية اسفلتية بتحمل اعلى مع خدمة افضل بأستخدام خلطات EME.

الكلمات الرئيسية: الخلطة الاسفلتية العالية الجساءة، الكلل، التخدد.

1. INTRODUCTION

Several distresses hamper the performance of flexible pavements in Iraq and result in premature failure. In flexible pavements, the primary forms of distress are fatigue cracking and rutting. These distresses manifest themselves most of the time due to construction material quality, poor maintenance, and improper structural design. The necessity to increase the service life of pavement subjected to high traffic volume imposes the use of asphalt mixture with high performance. This led to the development of EME (Enrobés à Module Elevé) or High- Modulus Asphalt (HiMA) in the 1980s by French road administration (LCPC), bitumen producers and road contractors. In view of this, the need for the use of EME mixture to improve mechanical properties including high resilient modulus, good moisture damage resistance, good fatigue behaviour and excellent resistance to rutting.

With this purpose in mind, the primary objective of this study is to evaluate the performance of high modulus mixtures and compare them with the conventional mixture for base course based on the following tests, Marshall properties (mix design parameters), indirect tensile test (moisture damage resistance), uniaxial repeated load test (resilient modulus and permanent deformation) and repeated flexural beam test (fatigue characteristics).

2. BACKGROUND

The specification for EME (High Modulus Mixture) is shown in specification NF P 98-140, **AFNOR, 1999**. There are two classes of EME mixture, EME Class 1 (EME1) and Class 2 (EME2). Both mixtures are designed to have high modulus, but EME2 has a higher asphalt content requirement and specified for most heavily trafficked roads. As noted by **Dariuze, et al., 2010**, bitumen with harder grades are used, mainly 10/20, 15/25, and even 5/15; polymer modified bitumen (PMB) is also used. In **Sanders, and Nunn, 2005**, the UK Highways Agency recommends a 10/20 and 15/25 grade bitumen as binder for use in EME base/binder coarse asphalt mixtures while **Denneman, et al., 2011** and **Vaitkus, et al., 2013** used hard binder (20-30).

EME is designed to satisfy criteria determined using laboratory tests developed by French Administration Roads LCPC for **Delorme, et al., 2007** to measure the performance properties of laboratory compacted test specimens in respect of compatibility, water sensitivity, deformation resistance, stiffness and fatigue cracking resistance. The binder content is controlled by a richness modulus (K), which is a function of the mass of the soluble binder expressed as a percentage of total dry mass of aggregate, the specific surface area of aggregate and the density of the aggregate, **AFNOR, 1999**. **Lee, and Park, 2007** found out that the rutting resistance of HMAC is twice higher than that of hot mix asphalt, and the fatigue resistance is 5–10 times higher by using polymer modified 20/30 bitumen. **Rohde, et al., 2008** analyzed the HMAC to find that the accumulated permanent deformation 6.7% after 10,000 loading cycles. On the other hand, the comparison mixture with conventional binder (50/70) presented permanent deformation higher than 23% just after 1,300 cycles. According to **Hussain Bahia, et al., 2013**, the HMABs can be effective in reducing layer thickness. One grade increase in the continuous high temperature performance grade reduces the thickness of asphalt layer by 0.065 inch without an increase in total permanent deformation. The asphalt layer thickness is reduced by 0.89 to 4.4 inches by replacing the neat binder with HMABs produced in this study. The results of **Grobler, et al., 2011** indicated that the higher stiffness and increase in fatigue life (2 to 3 times more than normal asphalt) a decrease in asphalt thickness up to 30% is possible. In **Hussain Bahia, et al., 2013**, there are still some barriers

which prevent hard binder from being used as a worldwide road construction material. First of all, the viscoelastic properties of hard binder are not well understood. Secondly, because hard binder is stiff with a higher viscosity, workability and thermal cracking resistance become critical factors that need further evaluation. Finally, the effectiveness of hard binder as wearing course and binder course materials is still debated and needs further evaluation (**Hussain Bahia, et al., 2013**).

3. MATERIAL CHARACTERIZATION

Asphalt cement, aggregate, and filler used in this work have been characterized using routine type of tests and the results were compared with State Corporation for Roads and Bridges specifications (SCRB, 2003). All experimental works have been performed in highway Materials and Construction Materials Laboratories in Civil Engineering Department, College of Engineering, University of Baghdad.

3.1 Asphalt Cement

In this study, two asphalt grades are considered: grade (20-30) and grade (40-50). Grade (20-30) type AIWIN was brought from Jordan and grade (40-50) was brought from Dora refinery, south-west of Baghdad. The physical properties of the asphalt cement are shown in Table (1).

3.2 Aggregate

EME is typically produced using fully crushed fractured aggregate for base course but rounded aggregate used in Iraqi practice. The aggregate used in this work was obtained from Amanat Baghdad asphalt concrete mix plant located in Taji, north of Baghdad, its source is Al-Nibaie quarry. This type of aggregate is widely used in Baghdad city for asphaltic mixes. EME shall be designated as EME 0/10, EME 0/14 or EME 0/20 (minimal/maximal particle size in mm, where 0 represents the 0.075 mm) according to aggregate size as specified in **Sanders, and Nunn, 2005**. In this study, the appropriate grading for the base course based on **SCRB, 2003** is EME 0/20. The coarse and fine aggregates used in this work were sieved and recombined in the proper proportions to meet the base course gradation as required by SCRB specification **SCRB, 2003**. The aggregate gradation properties are presented in Table (2) and gradation curve is shown in **Fig.1**. Routine tests were performed on the aggregate to evaluate their physical properties. The results together with the specification limits as set by the **SCRB, 2003** are summarized in Table (3). Tests results show that the chosen aggregate met the **SCRB, 2003** specifications.

3.3 Filler

The filler is non-plastic materials that passes sieve No.200 (0.075mm). Mineral filler used in this work is limestone dust obtained from Amanat Baghdad asphalt concrete mix plant; its source is the lime factory in Karbala governorate, south east of Baghdad. The physical properties of the used filler are presented in **Table 4.**

4. EXPERIMENTAL WORK

The experimental work was started by Marshall Test to find optimum asphalt content for conventional and high modulus asphalt mixtures (EME). Indirect tensile test to evaluate the moisture damage resistance and the mechanical properties which include resilient modulus,

permanent deformation and fatigue characteristics. The mechanical properties have been evaluated using uniaxial repeated loading and repeated flexural beam tests.

4.1 Marshall Test

To obtain the optimum asphalt content (O.A.C) for base course, Marshall specimens were prepared according to the Marshall method as outlined in Asphalt Institute manual (series No.2 ,1981) using 75 blows (SCRB, 2003) of the automatic Marshall compactor on each side of specimen. The specimens were evaluated for Marshall Stability, flow value, percent air voids (AV) and percent voids in mineral aggregate (VMA).The optimum asphalt content for HMAC and conventional mixtures were 4.6% and 3.8% respectively. Table (5) presents the mixtures properties at optimum asphalt contents.

4.2 Indirect Tensile Test

The moisture susceptibility of the bituminous concrete mixtures was evaluated according to (ASTM- D-4867-96). The result of this test is the indirect tensile strength (ITS) and tensile strength ratio (TSR). In this test, a set of specimens was prepared for each mix according to Marshall Procedure and compacted to 7±1 % air voids using different numbers of blows per face, varying from 17 to 19 (targeted air voids content were prepared to voids is not meant to mimic the actual field conditioning process but to accelerate the moisture damage in a manner that can be measured under laboratory conditions). The set consists of six specimens and was divided into two subsets, one set (control) was tested at 25°C and the other set (soaked) was subjected to one cycle of freezing and thawing then tested at 25°C. The test is shown below in **Fig. 2**. It involved loading the specimens with compressive load at a rate of 50.8 mm/min acting parallel to and along the vertical diametric plane through 0.5 in. wide steel strips which are curved at the interface with the specimens. These specimens failed by splitting along the vertical diameter. The indirect tensile strength calculated according to Eq. (1) of the soaked specimens (ITS_c) is divided by that of the control specimens (ITS_d), which gives the tensile strength ratio (TSR) as the following Eq. (2).

$$ITS = \frac{2\,P}{\pi\,t\,D} \qquad (1)$$

$$TSR = \frac{TSR\ c}{TSR\ d} \qquad (2)$$

Where

ITS= indirect tensile strength
P = ultimate applied load
t = thickness of specimen
D = diameter of specimen
Other parameters are defined previously

4.3 Uniaxial Repeated Loading Test

The uniaxial repeated loading tests were conducted for cylindrical specimens, 101.6 mm (4 inch) in diameter and 203.2 mm (8 inch) in height, using the pneumatic repeated load system (shown in **Fig. 3**). In these tests, repetitive compressive loading with a stress level of 20 psi was applied in the form of rectangular wave with a constant loading frequency of 1 Hz (0.1 sec. load duration and 0.9 sec.

rest period) and the axial permanent deformation was measured under the different loading repetitions. All the uniaxial repeated loading tests were conducted at 20, 40 and 60 °C. The specimen preparation method for this test can be found elsewhere **Albayati, 2006**. The permanent strain (ε_p) is calculated by applying the following equation:

$$\varepsilon_p = \frac{Pd \times 10^6}{h} \quad (3)$$

Where:
ε_p = axial permanent microstrain
pd = axial permanent deformation
h = specimen height

Also, throughout this test the resilient deflection is measured at the load repetition of 50 to 100, and the resilient strain (εr) and resilient modulus (Mr) are calculated as follows:

$$\varepsilon_r = \frac{r_d \times 10^6}{h} \quad (4)$$

$$M_r = \frac{\sigma}{\varepsilon r} \quad (5)$$

Where:
ε_r = axial resilient microstrain
rd = axial resilient deflection
h = specimen height
M_r = Resilient modulus
σ = repeated axial stress
εr = axial resilient strain

The permanent deformation test results for this study are represented by the linear log-log relationship between the number of load repetitions and the permanent microstrain with the form shown in Eq. (6) below which is originally suggested by **Monismith, et al., 1975** and **Barksdale, 1972.**

$$\varepsilon_p = a\, N^b \quad (6)$$

Where:
ε_p = permanent strain
N = number of stress applications
a = intercept coefficient
b = slope coefficient

Once regression coefficients had calculated (a and b), the permanent deformation coefficients Alpha (α) and Mu (μ) were computed using the relationship given in Eq. (7) and (8) (Huang, 1993):

$$\alpha = 1-b \quad (7)$$

$$\mu = \frac{a\,b}{\varepsilon r} \quad (8)$$

Where (μ) is the permanent deformation parameter representing the constant of proportionally between permanent strain and resilient strain (i.e. plastic strain at N =1) and α is a permanent deformation parameter indicating the rate of decrease in incremental permanent deformation as the number of load applications increases.

4.4 Flexural Beam Fatigue Test

Within this study, third-point flexural fatigue bending test was adopted to evaluate the fatigue performance of asphalt concrete mixtures using the pneumatic repeated load system, this test was performed in stress controlled mode with flexural stress level varying from 15 to 45 psi applied at frequency of 2 Hz with 0.1 sec loading and 0.4 sec unloading times and in rectangular waveform shape. All tests were conducted at 10°C on beam specimens 76 mm (3 in) x 76 mm (3 in) x 381 mm (15 in) prepared according to the method described in **Alkhashab, 2009**. In the fatigue test, the initial tensile strain of each test has been determined at the 50th repetition by using Eq. (9) shown below and the initial strain was plotted versus the number of repetition to failure on log scales, collapse of the beam was defined as failure, the plot can be approximated by a straight line and has the form shown below in Eq. (10).

$$\varepsilon_t = \frac{\sigma}{E_S} = \frac{12d\Delta}{3L^2-4a^2} \quad (9)$$

$$Nf = K_1\, \varepsilon t^{-K2} \quad (10)$$

Where:
ε_t = Initial tensile strain
σ = Extreme flexural stress
Es = Stiffness modulus based on centre deflection.
h = Height of the beam
Δ = Dynamic deflection at the centre of the beam.
L = Length of span between supports.
a = Distance from support to the load point (L/3)
N_f = Number of repetitions to failure
k_1 = fatigue constant, value of N_f when = 1
k_2 = inverse slope of the straight line in the logarithmic relationship

5. TEST RESULTS AND DISCUSSION

5.1 Asphalt Concrete Mixture Properties

The optimum asphalt content (O.A.C) and Marshall stability for HMAC were more than conventional mixture by 21% and 31% respectively. Therefore, the highest Marshall stability, flow and voids in mineral aggregate are achieved with the stiff binder type (20-30).

5.2 Durability Performance

The durability of HMAC is assessed in France using an unconfined compressive test (EN 12697-12) on moisture conditioned specimens (Duriez test). In this study, the modified Lottman test in accordance with ASTM D4867 is generally used for this purpose.

The Tensile Strength Ratio (T.S.R.) test results are shown in Table (6) for conventional and HMAC mixture at optimum asphalt content (O.A.C). Generally a minimum TSR of 0.70 is recommended. The TSR results corresponding to HMAC and "conventional" specimens were 0.79 and 0.72, respectively, showing that both mixtures present good resistance to moisture damage. The results showed that the high modulus asphalt mixture had a resistance to moisture damage more than the conventional asphalt mixture approximately by 9.3 %.

5.3 Resilient Modulus

Table (7) and **Fig. 4** show the values of Mr for the conventional and HMAC mixtures. When using HMAC instead of conventional mixture at (O.A.C), the value of (Mr) increased by 29, 102 and 63% for temperature 20, 40 and 60 ^{0}C respectively. In case of decreasing the asphalt content for HMAC mixture from 4.6 to 4%, the value of (Mr) increased by 13, 17 and 11% for temperature 20, 40 and 60 ^{0}C respectively.

5.4 Permanent Deformation

Based on the data shown in Table (8), **Fig. 5** and **Fig. 6**, it appears that the hard binder contents have influence on the plastic parameter of the material as characterized by the (α) and (μ) values.When using HMAC instead of conventional mixture, the value of (μ) decreased and the variable (α) has an opposite effect.

5.5 Flexural Fatigue

For the hard binder used in this study, increase asphalt content significantly affect the number of cycles to failure NF and provide an increased level of protection against cracking due to repetitive loading because higher asphalt content increases the thickness of the binder film between aggregates, which results in lower stress in the binder film. Fatigue cracking coefficient (K_1) and exponent (K_2) are presented in Table (9) for the conventional mix and mixes for HMAC. Values of k_1 and k_2 can be used as indicators of the effects of stiff binder on the fatigue characteristics of a paving mixture. The flatter the slope of the fatigue curve, the larger the value of k_2 which indicates a

potential for longer fatigue life. On the other hand, a lower k_1 value represents a shorter fatigue life. As can be seen from **Fig. 7** as the stiff binder used with high asphalt content the k_2 value increases and the k_1 value decreases. These results highlight the improvement in fatigue resistance for mixes with high content of stiff binder. The fatigue life increases for HMAC more than conventional mixture as illustrated in **Fig. 8**.

6. MINIMUM BINDER CONTENT using RICHNESS FACTOR (K)

The French specification includes two classes of HMAC (EME) mixes for base course: Class 1 for light traffic, and Class 2 for heavy traffic. To find out the class of the HMAC mixture used in this study, the equation of the minimum binder content is applied as follows:

$$TL = K * \alpha * \sqrt[5]{\sum} \quad (11)$$

The correction coefficient (α) was computed by finding the effective specific gravity of aggregate (Gse) and (∑) value depending on the aggregate grading. The minimum binder content (TL) is the percentage by the mass of aggregate. Therefore, to find the percentage of binder content by the mass of the total mix (P_b), the following equation is used, **AFNOR, 2002, Denneman et al., 2011** and **Sanders, and Nunn, 2005**:

$$TL = \frac{100 * Pb}{100 - Pb} \quad (12)$$

The result obtained from the above equations is illustrated in Table (10). The optimum asphalt content for HMAC mixture is (4.6 percent). Therefore, the content of O.A.C-0.6 (4 percent) is less than the minimum binder content of Class 2 (5.3 percent) so the mixture of HMAC in this study can be classified as Class 1.

7. EVALUATION of PRESENT SERVICEABILITY INDEX (PSI)

In order to reduce the risk of unsatisfactory pavement performance to an unacceptable level, engineers must be able to reliably predict pavement behavior with time. In this study, VESYS 5W software is used to predict the present serviceability index with time. An analysis period of 20 years is used in the analysis. For the practical example, the geometry of the pavement structure is shown in **Fig. 9**. The Mean Air Pavement Temperature (MAPT) is required as an input value. The assumed MAPT was 40^0C, which temperature expected to occur in the middle of the asphalt concrete pavement layer during the hot summer seasons in Iraq.

VESYS 5W needs to be provided with parameters to run the analyses in form of inputs data. VESYS 5W software has been successfully used to analyze the asphalt pavement performance under field traffic and under accelerated pavement testing loads. VESYS 5W needs to be provided with parameters to run the analyses in form of inputs data. These input parameters include material properties of the layers, thickness, traffic data and environmental conditions (Appendix **A**).

The VESYS analysis procedure uses advanced mechanistic concepts to predict the behavior and performance of flexible pavements. Strain and deflection responses are computed, and then used in conjunction with failure criteria to predict pavement distress in terms of cracking, rutting and roughness. Distress is used to define pavement performance in terms of life history of the present serviceability index (PSI). All of the components of the design procedure have been formulated to take into account the inherent variability in traffic estimates, materials properties, and environmental conditions and in the many forms of construction practices used (VESYS 5W user Manual 2003).

These input parameters include (K_1, K2, α, μ and Mr) which can be obtained from fatigue and rutting test. The Percent Serviceability Index (PSI) relationship with time is shown in **Fig. 10**. For a pavement section with 20 years design life, the drop in serviceability index value for the pavement section with EME mixes was less than 1 whereas for conventional mixes the corresponding value is 2.5.

8. CONCLUSIONS

Within the limitations of materials and testing program used in this work, the following principal conclusions are made based on the findings of the investigations:

1. Using HMAC instead of conventional mixture at (O.A.C) lead to increased the resilient modulus (Mr) by 29, 102 and 63% for temperature 20, 40 and 60 ^{0}C respectively. Further decrease in asphalt content beyond the optimum resulted in increased of Mr value.

2. The EME has an excellent resistance to rutting as compared with the conventional mixture at their optimum asphalt content, which was 4.6 for the former and 3.8% for the later. The (α) value for EME mix was more than that of conventional mix by 4.1, 39.7 and 56.7 % for temperature 20, 40 and 60 ^{0}C respectively.

3. Fatigue test results reflected better performance for the EME mix against fatigue cracking as compared to the conventional mix, the fatigue parameter (K1) for the conventional mixture was (6.906 E-10) whereas for EME the corresponding value was (6.777 E-10) for O.A.C (4.6 %). The K2 (inverse slope of fatigue line) for the EME was 3.731 at 4.6 % asphalt content whereas for the conventional mix the value was 3.704. The EME mix with 4% asphalt content introduced less resistance to fatigue cracking as compared with conventional mixture.

4. The results of indirect tensile test showed that the HMAC mix had more resistance to moisture damage than conventional mix approximately by 9.3 % so the HMAC passed the requirement for EME specification for durability performance.

5. The optimum asphalt content (O.A.C) and Marshall stability for EME was more than that of conventional mixture by 21% and 31% respectively. Therefore, the highest Marshall stability, flow and voids in mineral aggregate are achieved with the use of stiff bitumen.

6. Based on minimum Richness factor (K) equation, the HMAC mixture for this study is EME Class1 with minimum binder content of 4 percent.

7. The drop in serviceability index value for the pavement section with EME mixes was less than 1 whereas for conventional mixes the corresponding value is 2.5. With this result in view, the use of EME mixes has added to local knowledge the ability to produce more durable asphalt concrete mixtures with better serviceability.

9. REFERENCES

- AFNOR, 1999, *Enrobés Hydrocarbonés - Couches d'assises: Enrobés à Module Elevé (EME)*. AFNOR, Norme Française, NF P 98-140 (in French), Paris, France.

- Albayati, A. H., 2006, *Permanent Deformation Prediction of Asphalt Concrete Under Repeated Loading*, Ph.D. Thesis, University of Baghdad, College of Engineering.

- AI, 1981, *Thickness Design-Asphalt Pavements for Highways and Streets*, Asphalt Institute, Manual Series No.1, College Park, Maryland, USA.

- Alkhashab, Y.Y., 2009, *Development of Fatigue Prediction Model for Local Asphalt Paving Materials*, Ph.D. Thesis, Baghdad University.

- Barksdale, R., 1972, *Laboratory Evaluation of Rutting in Base Course Materials*, Proceedings, Third International Conference on the Structural Design of Asphalt Pavements, London

- Delorme, J., De La Roche, C., and Wendling, L., 2007, *LCPC Bituminous Mixtures Design Guide*, Director. Paris: Laboratoire Central des Ponts et Chaussees.

- Erik Denneman, Matsopole, N., Joseph, A., and James, W., M., 2011, *Transfer of High Modulus Asphalt Technology to South Africa*, CSIR Built Environment, PO Box 395, Pretoria, 0001, South Africa.

- Grobler, J., E., Pretorius, F., J., Agema, P. and Bowker, I., 2011, *The Performance of Environmentally Beneficial Asphalt Products: Practical Case Studies at or Tambo International Airport Over the Last 5 Years*, 10th Conference on Asphalt Pavements for Southern Africa (CAPSA), South Africa.
- Han Geng, Cristian, S., Clopotel, Hussain Bahia and Lihan Li, 2013, *Effects of high Modulus Asphalt Binders on performance of Typical Asphalt Pavement Structure*, Construction and Building Materials, Volume 44, PP. 207-213, Washington, D.C.

- Huang, Y. H., 1993, *Pavement Analysis and Design*, Second Edition.

- Lee, H., J., and Park, H., M., 2007, *Performance evaluation of high modulus asphalt mixtures for long life asphalt pavements*, ITRD E131554 TRL, Volume: 21, PP. 1079-1087, Issue Number: 5.

- Monismith, C., Ogawa, N. and Freeme, C., 1975, *Permanent Deformation Characteristics of Subgrade Soils Due to Repeated Loadings*, TRR 537.

- Rohde, E. L., Ceratti, J., A., Nūnez, P.,V., and Vitorello, T., 2008, *Using APT and Laboratory Testing to Evaluate the Performance of High Modulus Asphalt Concrete for*

Base Courses in Brazil, in Procceding of the 3rd Internation Conference on Impacts and Benefits from APT Programs, P.11 , 2008, Madrid, Spain.

- Sanders, P. J., and Nunn, M., 2005, *The Application of Enrobe a Module Eleve in Flexible Pavements*, Transport Research Laboratory, Report 636, ISBN 1-84608-653, Crowthorne, UK.

- Sybilski, D., Bankowski, W., and Krajewski, M., 2010, *High Modulus Asphalt Concrete with Limestone Aggregate*, Internationa Journal of Pavement Research and Technology (ISSN: 1996-6814), Vol. 3, No. 2, pp 96-101.

- SCRB, 2003, *General Specification for Roads and Bridges*, Section R/9, Hot-Mix Asphalt Concrete Pavement, Revised Edition, State Corporation of Roads and Bridges, Ministry of Housing and Construction, Republic of Iraq.

- Vaitkus, F., H, Audrius, K., O., Vorobjovas, T., E., and Viktoras, A., D., 2013, *Use of Local Aggregates in High Modulus Asphalt Concrete Layers*, Journal of the Croatian Association of Civil Engineers (HSGI), Zagreb, Vol. 65, PP. 353-360.

10. NOMENCLATURE

a	intercept coefficient, dimensionless
a	distance from support to the load point (L/3), mm
Av	air voids, %
b	slope coefficient, dimensionless
D	diameter of specimen, in
Es	stiffness modulus based on centre deflection, N/mm^2
Gse	effective specific gravity of aggregate, gm/cm^3
h	height of the beam, mm
ITS	indirect tensile strength, psi
K	richness modulus, dimensionless
k_1	fatigue constant, value of N_f when = 1, dimensionless
k_2	inverse slope of the straight line in the logarithmic relationship, dimensionless
L	length of span between supports, mm
M_r	resilient modulus, psi
N	number of stress applications
N_f	number of repetitions to failure
P	ultimate applied load, Ib
P_b	percentage of binder content by the mass of the total mix, %
pd	axial permanent deformation
rd	axial resilient deflection
T	thickness of specimen, in
TL	percentage of binder content by the mass of aggregate, %
TSR	tensile strength ratio, %

VMA voids in mineral aggregate, %
Δ dynamic deflection at the centre of the beam
α correction coefficient, dimensionless
ε_p axial permanent strain, microstrain
ε_r axial resilient strain, microstrain
ε_t initial tensile strain, microstrain
σ repeated axial stress, psi

Table 1. Properties of asphalt cement.

Properties before TFOT					
Test	ASTM Designation	Penetration grade 40-50		Penetration grade 20-30	
		Results	SCRB Specification (2003)	Results	EN-12591 Specification
Penetration at 25 ^{0}C, 100gm, 5 sec (0.1mm)	D5	44	40-50	24	20-30
Ductility at 25 ^{0}C, cm	D113	116	>100	18	-----
Flash Point, ^{0}C	D92	260	232 Min.	300	240 Min.
Softening Point, ^{0}C	D36	48	-----	61.5	55-63
Penetration Index	-----	-1.98	-----	-0.27	+0.7 Max. -1.5 Min.
Properties after TFOT					
Penetration at 25 ^{0}C	D5	29	29	18	-----
Retained Pen. %	------	66	55 (Min.)	75	55(Min.)
Change of Mass, %	------	-0.057	0.5 (Max.)	-0.074	0.5(Max.)
Ductility at 25 ^{0}C, cm	D113	43	25	13	-----
Softening Point, ^{0}C	D36	50.6	-----	68.4	-----
Increase in Softening Point, ^{0}C	------	2.6	-----	6.9	8 (Max.)

Table 2. Percent pass by weight of selected aggregate gradation (25 mm nominal maximum size, base course).

EME 0/20			SCRB (R/9, 2003)			
Sieve size (mm)	% passing by weight		English Sieve.	Standard Sieves (mm)	% passing by weight	
	Selected Limit	Specification range			Selected Limit	Specification range
31.5	100	100	1½"	37.5	100	100
20	92	90-99	1"	25	95	90-100
14	78	75-95	3/4"	19	89	76-90
10	66	60-90	1/2"	12.5	72	56-80
6.3	59	42-75	3/8"	9.5	65	48-74
4	-	-	No.4	4.75	47	29-59
2	28	20-35	No.8	2.36	30	19-49
0.25	13	8-18	No.50	0.3	14	5-17
0.063	7	5-9	No.200	0.075	7	2-8

Table 3. Physical properties of aggregates.

No.	Laboratory Test	ASTM Designation	Test Results	SCRB Specification (2003)
Coarse Aggregate				
1	Apparent Specific Gravity	C-127	2.678	-
2	Bulk Specific Gravity	C-127	2.61	-
3	Water Absorption,%	C-127	0.21	-
4	Fractured pieces,%	D-5821	96	90 Min
5	Flat & Elongated particles,%	D-4791	5	10 Max
6	Percent Wear (Los Angeles Abrasion),%	C-131	17.5	30 Max
7	Soundness Loss by Magnesium Sulfate solution, %	C-88	3.83	18 Max
8	Clay Lumps & Friable Particles,%	C-142	0.6	3 Max
Fine Aggregate				
1	Apparent Specific Gravity	C-128	2.683	-
2	Bulk Specific Gravity	C-128	2.621	-
3	Water Absorption,%	C-128	0.4	-
4	Fine Aggregate Angularity,%	AASHTO TP33	54.78	-

5	Sand Equivalent,%	D-2419	68.45	45 Min.
6	Clay Lumps & Friable Particles,%	C-142	2.85	3 Max

Table 4. Physical properties of fillers.

Property	Test Result
Specific gravity	2.72
%Passing Sieve No.200 (0.075 mm)	96

Table 5. Marshall properties.

Marshall property	Mixture Type		Specification requirements (SCRB, 2003)
	Conventional	HMAC	
Binder content, %	3.8	4.6	3-5.5
Stability ,kN	13.40	17.50	5 Min.
Flow, mm	2.50	3.30	2-4
Air Voids, %	3.50	3.20	3-6
VMA, %	13.05	14.20	12 Min.

Table 6. Indirect tensile strength results.

Grade Type	I.T.S. Unconditioned specimens (psi)	I.T.S. Conditioned specimens (psi)	TSR (%)
20-30	154.09	121.84	79.07
40-50	146.51	104.46	71.70

Table 7. Resilient modulus test results.

Temperature ^{0}C	Mixture Type		
	Conventional (3.8%)	HMAC (4%)	HMAC (4.6%)
20	194048	283712	250853
40	114518	269924	231264
60	69050	125155	112640

Table 8. Plastic parameter results (Rutting test).

Mixture Type		Conventional 3.8%			HMAC 4%			HMAC 4.6%		
Temp. ^{o}C		20	40	60	20	40	60	20	40	60
Variables	α	0.752	0.539	0.386	0.810	0.784	0.669	0.783	0.753	0.605
	μ	0.330	0.590	0.799	0.310	0.398	0.551	0.301	0.377	0.537

Table 9. Fatigue tests result.

Fatigue Coefficient	Mixture Type		
	Conventional (3.8%)	HMAC (4%)	HMAC (4.6%)
K_1	6.906E-10	1.467E-7	6.777E-10
K_2	3.704	2.874	3.731

Table .10 Minimum binder content based on EME class.

EME Class	K min.	α	∑	TL min. percent	P_b min. percent
Class 1	2.5	1.0192	11.001	4.12	4
Class 2	3.4	1.0192	11.001	5.6	5.3

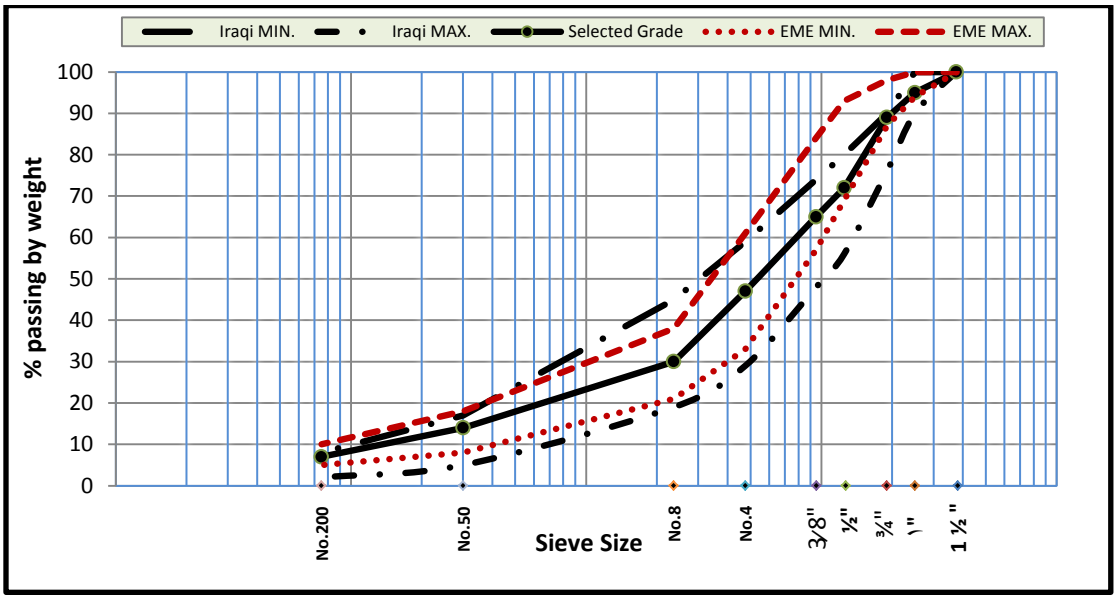

Figure 1. Aggregate gradation.

Figure 2. Photograph for ITS test.

Figure 3. Photograph for the PRLS.

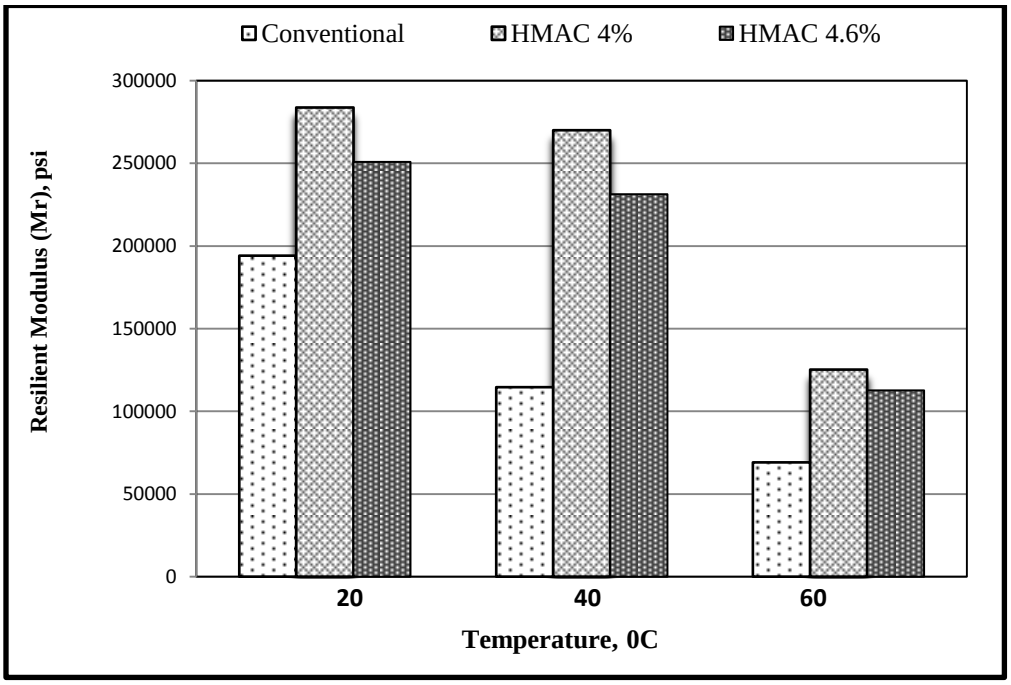

Figure 4. Effect of stiff binder on resilient modulus (Mr).

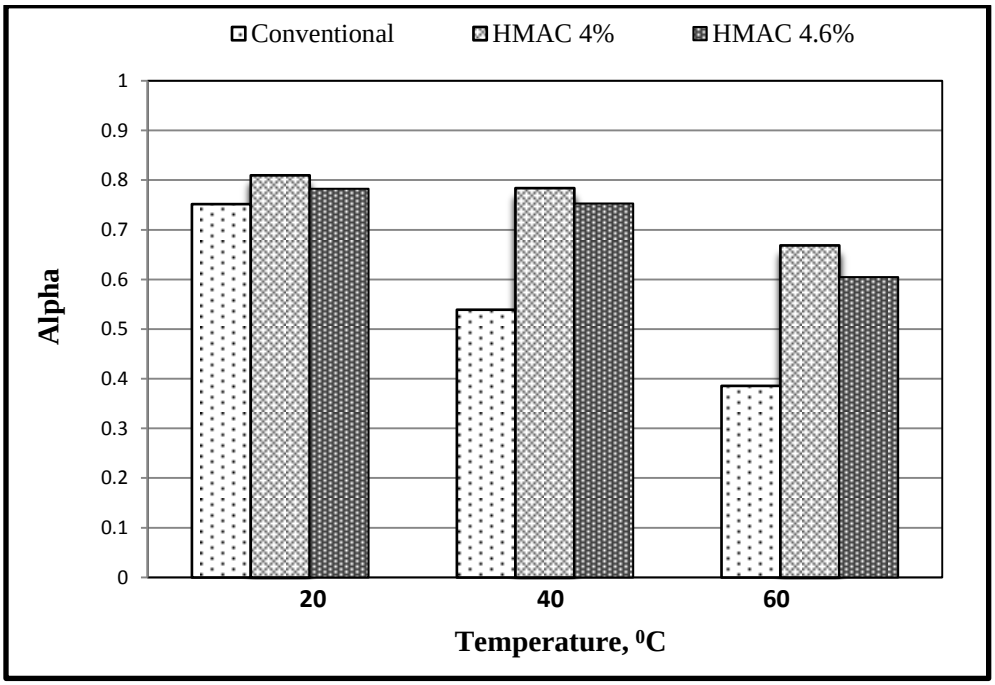

Figure 5. Effect of stiff binder on plastic parameter alpha (α).

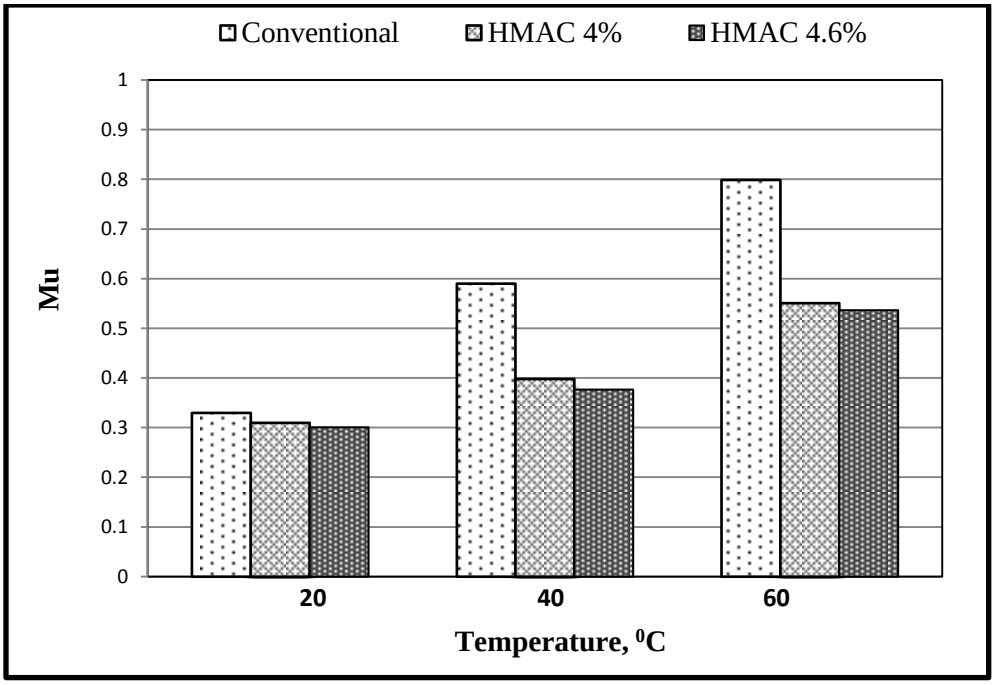

Figure 6. Effect of stiff binder on plastic parameter Mu (μ).

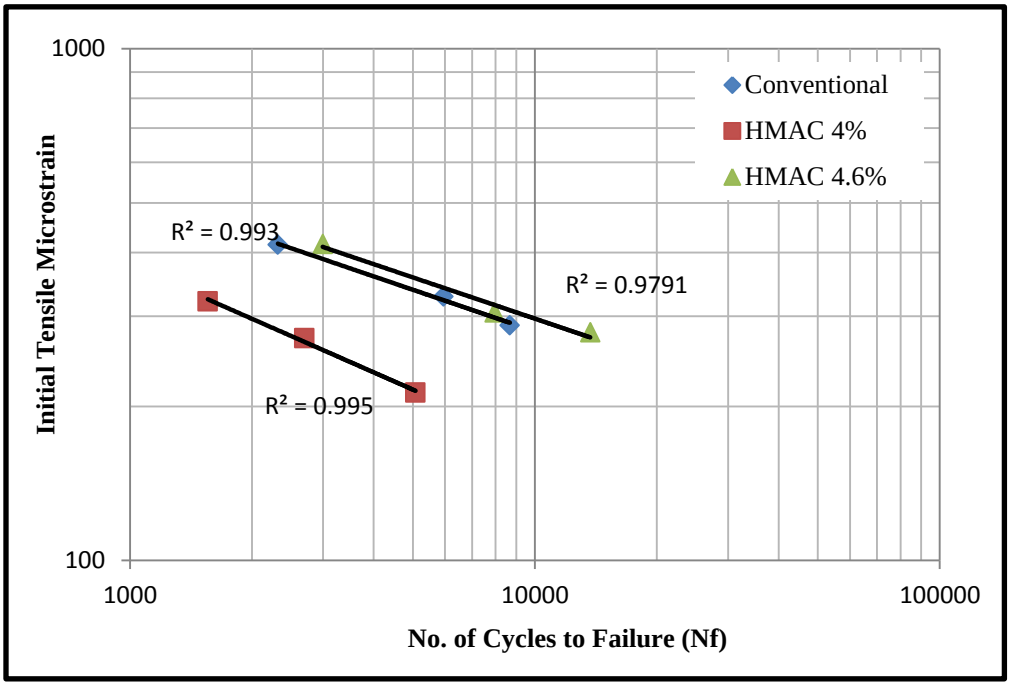

Figure 7. Effect of stiff binder content on fatigue performance.

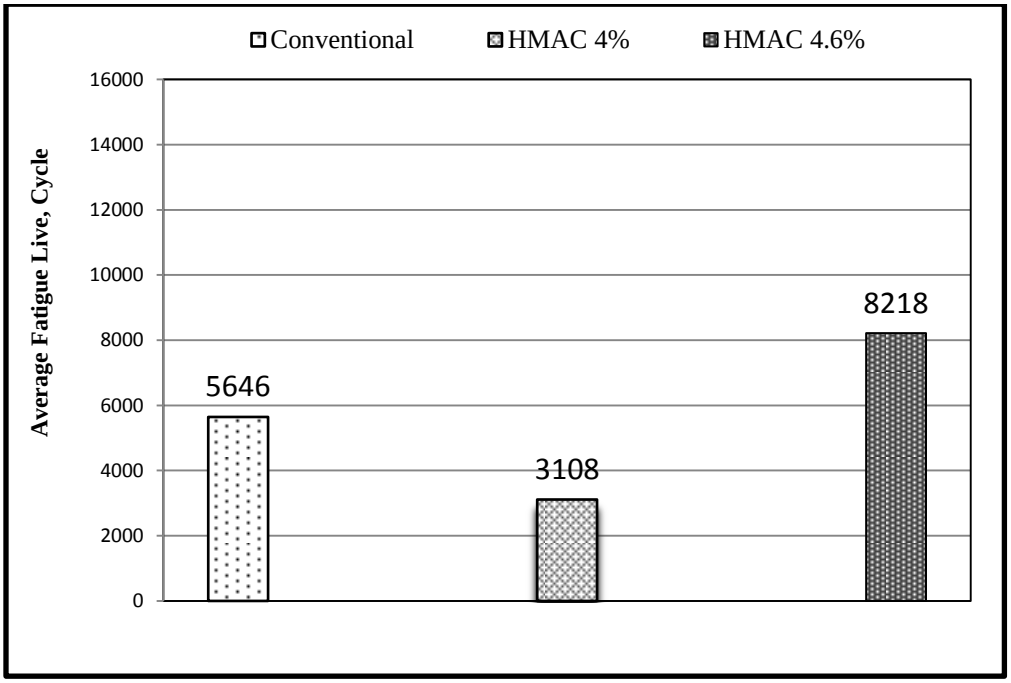

Figure 8. Effect of stiff binder content on fatigue life.

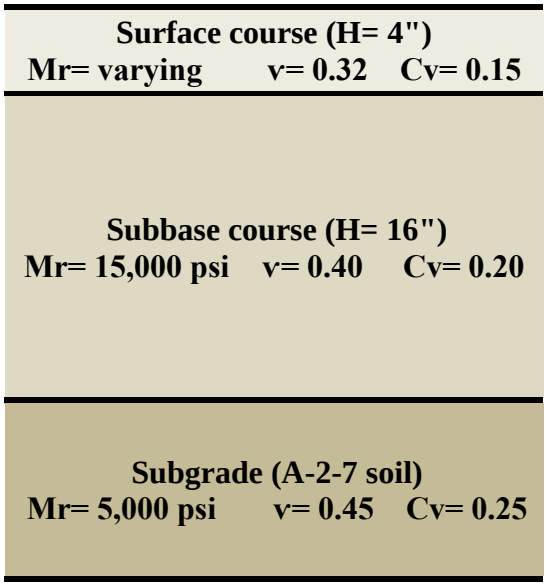

Figure 9. Geometry of the pavement structure.

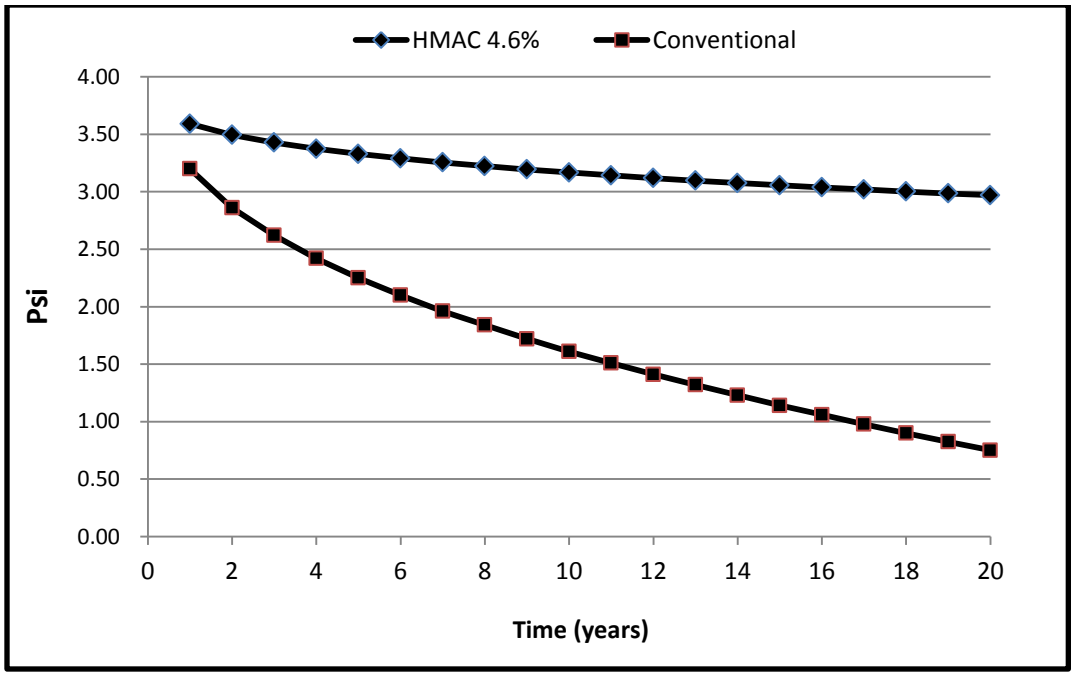

Figure 10. Percent serviceability index (PSI).

Stabilization of Clay Soil Using Tyre Ash

Mahmood Dheyab Ahmed
Assistant Professor
Engineering College-Baghdad University
Email: mahmoud_baghdad@yahoo.com

Ahmed Mohamed. Adkel
Engineering College-Baghdad University
Email:Ahmed87_ce@yahoo.com

ABSTRACT

The planning, designing, construction of excavations and foundations in soft to very soft clay soils are always difficult. They are problematic soil that caused trouble for the structures built on them because of the low shear strength, high water content, and high compressibility. This work investigates the geotechnical behavior of soft clay by using tyre ash material burnt in air. The investigation contains the following tests: physical tests, chemical tests, consolidation test, Compaction tests, shear test, California Bearing Ratio test CBR, and model tests. These tests were done on soil samples prepared from soft clay soil; tyre ash was used in four percentages (2, 4, 6, and 8%). The results of the tests were; The soil samples which gave the value of plasticity test were 2% (25), 4% (25.18), 6% (25.3), and 8% (26.7).The soil samples which gave the value of specific gravity were 2% (2.65), 4% (2.61), 6% (2.5), and 8% (2.36).The value of maximum dry density in a compaction test observed with 2% percentage gave the value 15.8 kN/m3, the 4% gave the value 15.4 kN/m^3, 6% gave 15.3 kN/m^3 and 8%with 15.2 kN/m^3.Samples that gave the values of undrained shear strength test were 2% (55 kN/m^2), 4% (76 kN/m^2), 6% (109 kN/m^2), and 8% (122 kN/m^2). The best of them is 8%.
The sample that gave the best value for swelling test was 8%.The best value for compression index Cc was in 8%.The results of CBR test, were improved in all soil samples. The soil samples which gave the value for CBR were 2% (3.507%), 4% (4.308%), 6% (5.586%), and 8% (9.569%). The best value was obtained from 8%.

Keywords: soft soil, stabilization, shallow foundation**,** tyre Ash

تثبيت الترب الطينية الضعيفة باستخدام رماد الإطارات

احمد محمد ادخيل
باحث
كلية الهندسة- جامعة بغداد

محمود ذياب احمد
أستاذ مساعد
كلية الهندسة- جامعة بغداد

الخلاصة

التخطيط والتصميم وأنشاء الحفريات ووالأسس في الترب الطينية الضعيفة والضعيفة جدا تكون دائما صعبة للمهندسين وتمثل تحديا صعبا لهم التي تكون ذات مشاكل مسببة أضرارا في أعمال الإنشاء عليها بسبب ضعف مقاومة القص ومحتوى الماء العالي ووالانضغاطية العالية لها. هذا العمل تحرى في سلوك خواص الرص للترب الطينية الضعيفة باستخدام رماد الإطارات المحروقة في الهواء. أعمال التحريات تحتوي على الفحوصات التالية: الفحوصات الفيزيائية ,الفحوصات الكيميائية , فحص الانضمام وفحوصات الحدل و فحص القص و فحص ونسبه التحمل لكاليفورنيا وفحوصات الموديل. تلك الفحوصات أجريت على نماذج من التربة الطينية الضعيفة ,واستعمل رماد الإطارات بأربع نسب من رماد الإطارات (2 , 4 , 6 , و

8%) . وكانت نتائج الفحوصات لنماذج التربة التي تعطي قيم فحص اللدونة للنسب2%(25) , 4%(25.18) , 6%(25.3) , و8%(26.7). ونماذج التربة التي تعطي قيم الوزن النوعي للنسب 2%(2.65) , 4%(2.61) , 6%(2.5) , و8%(2.36) .وقيم فحص الحدل عند إضافة 2% تعطي قيمه ,kN/m^3(15.8) 4% تعطي قيمه kN/m^3(15.4), 6% أعطت kN/m^3(15.3)و8% أعطتkN/m^3(15.2) .والنماذج التي أعطت قيم مقاومة القص الغير مبزولة كانت 2%kN/m^2 (55) , 4%kN/m^2 (76) , 6%kN/m^2 (109) , و8%kN/m^2 (122), حيث كانت أفضل قيمه بينهما هي 8% .والنموذج الذي أعطى أفضل قيمة لفحص الانتفاخ هو 8%.وكذلك أفضل قيمة لدليل الانضغاط هي 8%.ونتائج فحص CBR لكل نماذج التربة المحسنة, هذه النماذج أعطت 2%(3.507%) , 4%(4.308%) , 6%(5.586%) , و8%(9.569%) . وأفضل قيمة أعطتها نسبة 8% .

كلمات مفتاح: تربة ضعيفة، التثبيت ، الأسس الضحلة، رماد الإطارات.

1. INTRODUCTION

The engineering properties of the soil are important not only in foundation materials for the projects, but also in the materials for construction in embankments, dams, and other works. The improvement of soil properties is necessary to solve many engineering problems. An improvement is needed in the locations where the soils cannot support loads, for example the necessity for such improvement arises in the airfield runways and sub grade soil of roads, **Atkins, 1980**. One of the fundamental techniques by which the properties of natural materials can be improved is stabilization. In the middle and southern parts of Iraq, soft soils are encountered in many places low shear strengths and high settlements. Random data collected from several sites demonstrated values of undrained shear strength less than 30kPa in Basra governorate and less than 40kPa in Missan and Nasiriya governorates **Rahil, 2007**. In order to improve the behavior of such soils, attempts are made to utilize low cost local materials including waste products materials. Those studies consider stabilizing agents such as (cement-fly ash and lime-fly ash) as in the ground modification of soft compressible clays. Ali- AL Garbi clay belongs to such type of soil; it has greater softness and high compressibility. The suitable use of tyre ash can reduce the cost of stabilization of soft soil, as tyre ash is a waste material. **Afolagboye, and Talabi, 2013**.The choice of method depends on many factors that depend mainly on soil characteristics, type of equipment available, the economy, the type of structure and the time available.

Chemical stabilization includes mixing chemical additives (binding agents) with natural soils by removing moisture and improving strength properties of the soil. Commonly, the role of the stabilizing (binding) agent in the treatment process is either to reinforce the bounds between the particles or fill the pore spaces. Chemical stabilization can be classified into two types depending on the depth of the problematic soil and the type of geotechnical application. The traditional surface stabilization begins by excavating and breaking up the clods of the soil followed by the addition of the stabilization agent. Soil and additives are mixed together with known amounts of water and compacted.

The soil classification and the degree of improvement in the required quality of the soil, its relationship to choose the type determine the percentage added **Misra, and Biswas, 2005**.

As environmental protection is a major concern in the modern world, effective use of tyre ash for large-scale stabilization works can be regarded as economically fruitful and environmentally beneficial. Soil stabilization is used to achieve one or more of the following five items; In-

creasing the strength of the soil, improving the stability of the soil to withstand the small deformations produced by loading under any weather condition, controlling soil permeability to prevent surface water from entering the soil, and reducing compressibility.

2. BACKGROUND FOR SOFT CLAYS IN IRAQ

Soft clays are recent alluvial deposits probably formed within the last 10,000 years characterized by their flat and featureless ground surface. **Brand,** and **Bernner, 1981** are identified by their low undrained shear strength (Cu < 40 kPa (B.S,C.p.8004:1986)) and high compressibility (Cc between 0.19 to 0.44). They found that high natural moisture content, typically ranging from 40-60% with plasticity index ranging from 45-65% **Broms, 1987**. Soils with such characteristics create serious problems to geotechnical engineering associated with stability and settlements problems. The Tigris and Euphrates meet at Qurnah to form the Shatt AL-Arab which flows southward entering the Arabian Gulf at the city of Fao. The scanning of a number of site investigation reports led to some regions of soft clays in Iraq. Most of those locations are concentrated in the middle and southern parts of Iraq. Random data collected from several site investigation reports demonstrated values of undrained shear strength less than 30 kPa in Basrah governorate and less than 40 kPa in Missan and Nasirya governorates; also compression indices as high as 0.3 were also reported. The textures of those soils consist of fine silty clay loams, silty clay and clay fraction with up to 50-70% **Buringh, 1960**.These constituents with high water table throughout most of the southerly of the basins revealed a fair to poor soft deposit. **Al-Qayssi, 2001** studied 41 site investigation reports carried out by the Central Laboratory of Directorate of Military Work in the southern part of Iraq, from the early 1970 up to 200. Most of locations exhibit average undrained shear strength of less than 50 kPa and S.P.T. values less than 5 blows. In At 3000 B.C, the shoreline of the Arabian Gulf was located farther north near Basrah, where the rivers emerged part of the old river trance in the present inlet between Khor AL-Zubair and Umqaser. This wide triangle area is composed mainly of clayey soil and may be classified in the following two types according to **Rahil, 2007:**-

1. Normally consolidated young clay.
2. Normally consolidated aged clay.

The former is the clay distributed along the present river (Abu-Flus, Fao area) and the latter is the clay found distributed along the old river trace (Umqasr, Khor AL-Zubair).

2.1 Scrap Tyre

Waste tyres generated every day in Diobu part of Port Harcourt, Nigeria, can be used as light weight material either in the form of whole tyres, shredded or chips, or in mix with soil. Many studies regarding the use of scrap tyres in geotechnical applications have been done **Ghani, et al., 2002.**The re-use applications for tyres depends on how the tyres are processed. Processing basically includes shredding, removing of metal reinforcement and further shredding until the desired material is achieved **Carreon, 2006**.

Bernal, et al., 1996 reported the technical, economic and environmental benefits of using tyre shreds and rubber-sand, which include reduced weight of fill, adequate stability, low settlements, good drainage and use of large quantities of local waste tyres, which would have a positive impact on the environment. **Akbulut, et al., 2007** studied the modification of clayey soils

using scrap tyre rubber and synthetic fibers and concluded that they improved the strength properties and dynamic behavior of clayey soils.

Afolagboye, and **Talabi, 2013** assessed the consolidation properties of compacted lateritic soils stabilized with up to 8% tyre ash. This was carried out using time dependent one dimensional consolidation test to enhance the usage of the material in geotechnical engineering.

Afolagboye, and **Talabi,2014** assessed the effect of tyre ash on the geotechnical characteristics of compacted lateritic soils derived from migmatite gneiss in order to discover a conventional and cheaper stabilizer for pavement construction. The effects of engineering properties of clayey soil when blended with tyre ash are the main focus of this research. The enhanced engineering properties of various soils, resulting from the utilization of industrial byproducts or agricultural wastes bring about environmental and economic benefits **Walid,** and **Harichane**, **2010**. Addition of such additives reduced the plasticity index, increased optimum moisture content, decreased maximum dry density and improved both the compressive strength and California Bearing Ratio of soils **Rahman, 1986, Ferguson, 1993; Zia,** and **Fox, 2000, Parsons** and **Basha, et al., 2005; Senol et al., 2006 and Amu et al.,2011**.

3. EXPERIMENTAL WORK

3.1 Material Used

3.1.1 Soft soil

Soil used in this study was obtained from Ali-AL Girbi city south east of Baghdad city. The physical and chemical properties of the soil are summarized in Table 1. According to the Unified Soil Classification System (USCS), the soil is classified as (CL).The soil consists of 7.54% sand, 52.46% silt and 40% clay as shown in the grain size distribution curve in **Fig. 1**.

3.1.2 The tyre ash material

The tyre ash used was obtained from the burning of used and neglected tyres. They were burnt under normal atmospheric temperature and pressure (Burning air) to obtain the ash. The tyre ash was sieved through sieve No. 200. The sieved ash was immediately kept in air tight containers to prevent pre-hydration during storage or when left in open air. The major oxide compositions of tyre ash were determined in the Department of Chemistry-Science Laboratory, University of Baghdad. The chemical composition of the tyre ash is shown in Table 2.

3.2 Experimental Program

Soil sample was collected from one site with in Missan city ALi- AL-Gharbi region from depth of (1-1.5m). This sample was subjected to testing program, then the all samples were tested at different ratios of tyre ash (2%, 4%, 6%and 8%).

3.2.1. Specific gravity

Specific gravity for the soil studied was determined according to ASTMD-854-00. The results are summarized in the Table 1.

3.2.2. Atterbeger limits

Determination of the liquid limit, plastic limit, and the plasticity index of soil was performed according to test methods given in ASTM D 4318-00. The liquid limit, plastic limit and plasticity index value are summarized in the Table 1.

3.2.3. Grain size distribution

Wet sieving (by water) and hydrometer tests were carried out in accordance with ASTM-D-422-00.The grain size distribution of the sample is shown in **Fig**. **1**. The figure shows that the soil is classified as silty clay according to "ASTM" classification, designated as (CL) according to the Unified soil Classification System, and the percentage of clay is summarized in Table 1.

3.2.4. Moisture content

The moisture content of soil was carried out using ASTM D 2216-05. The sample was kept in the oven at a constant temperature of 100-110°C for a period of 24 hours. Water content of soil value is summarized in Table 1.

3.2.5. Consolidation test

One-dimensional consolidation test was carried out by using the standard odometer to determine the soil compressibility characteristics in accordance with ASTM –D2435-00.

3.2.6. Unconfined compression test

At first, unconfined compression test was carried out on disturbed samples in accordance with ASTM-D-2166-00. Unconfined Compression strength (q_u), undrained shear strength of cohesive soil (Cu), and the relationship between the soil consistency and its unconfined compression strength are according to DAS (2002).

3.2.7. Compaction test

The optimum water content and the maximum dry density of the sample were obtained using the Proctor standard compaction test carried out according to ASTM D698. **Fig. 2** shows the compaction curve obtained and shows optimum water content close to 22% and a maximum dry density of about 1.63kg/m^3.

3.2.8. California bearing ratio test

The California Bearing Ratio (CBR) test is a relatively simple test that is commonly used to obtain an indication of strength of a subgrade soil, sub-base and the base course materials for use in road and airfield pavement design **Liu,** and **Evett, 2003**. The results of the California Bearing Ratio test are summarized later in Table 2. This test is carried out according to ASTM D1883.

4. RESULTS AND DISCUSSION

4.1 Compaction Characteristics

The compaction test was used to determine the influence of stabilizers on maximum dry density (MDD) and optimum moisture content (OMC). The results of the MDD and OMC of soil samples mixed with tyre ash are reported in Table 3. And they are further illustrated in **Fig. 2**. The results show that adding tyre ash increased the OMC and reduced the amount of MDD progressively with the increase of tyre ash addition. Similar behavior was observed by other researcher for lime, volcanic ash, rice husk ash, sugarcane straw ash, lime-natural pozzolana mixture and stabilized soils **Bell, 1996, Hossain, et al., 2007, Eberemu, 2011 and Amu, et al., 2011.** The increase in OMC was due to the additional water required for wetting the large surface area of the fine tyre ash particles. The increase in OMC is also probably due to the additional water held within the flocculent soil structure due to excess water absorbed as a result of the porous property of tyre ash. The decrease in MDD of all treated soft soil was due to the partial replacement of relatively heavy soils with light weight tyre ash (specific gravity 1.92). This decrease in density could also be influenced by increase in porosity of all compacted soil samples due to addition of tyre ash. In addition, the decrease can also result from the flocculation and agglomeration of clay particles, caused by the cation exchange reaction, leading to corresponding increase in volume and decrease in dry density as advanced by **Lees, et al., 1982.** The increase in dry density is an indicator of improvement of soil properties; however, the addition of tyre ash reduced the MDDs. Several researchers **Basha, et al., 2005 and Ola, 1977** found that the change in dry density occurs because of both the particles size and specific gravity of the soil and stabilizer.

4.2 California Bearing Ratio

The California Bearing Ratio (CBR) test is a relatively simple test that is commonly used to obtain an indication of strength of a subgrade soil, sub-base and the base course materials for use in road and airfield pavement design **Liu,** and **Evett, 2003**. The results of the California Bearing Ratio test are shown in Table 4. The CBR values of all the soil samples increased considerably on stabilization with tyre ash shown in **Fig. 3**. This shows that the load bearing capacity of the soil increased with the stabilization mix. The increase in the soaked CBR may be due to the availability of calcium from the ash for the cementations reaction with the silica and iron oxide from the soft soil. Despite the increase in soaked CBR with stabilization, the soaked CBR values of the soils indicate that none can be used for sub-base and base course of roads because the values fall below the 30% and 80% respectively stipulated by **FMWH**, **1997**. The CBR values make the stabilized materials suitable for use as sub grade in road pavement because the value falls within the range (5–11%) specified by **FMWH**, **1997** for sub grade soils. According to **Simon, et al., 1973**, a high reduction in CBR values after soaking indicates that the soil is very sensitive to changes in the moisture content.

4.3 Unconfined Compressive Strength

The results of the unconfined compressive strength (UCS) of the stabilized soils are presented in Table 5. The trends of changes in UCS with various percentages of stabilizers for the clay soil are presented in **Fig. 4**. It is pertinent to note that curing was not necessary for soil samples without tyre ash additive. It can be seen from **Fig. 4** that the addition of tyre ash increased the UCS of the stabilized soft soil samples for the various percentage treated. This could probably

be as a result of the increased pozzolanic reaction with increased tyre ash treatment which results in the formation of calcium silicate hydrates and micro fabric changes which is responsible for increased strength **Kedzi, 1979**. Similar behaviors were also observed by other researcher for lime, volcanic ash, rice husk ash, sugarcane straw ash, lime-natural pozzolana mixture and Lime- rice husk mixture stabilized soils **Bell, 1996, Hossain, et al., 2007, Eberemu, 2011 and Amu, et al., 2011.** These tests presented the effect of tyre ash on the geotechnical characteristics of compacted soft soils derived from migmatite gneiss. On the basis of the tests results, the following conclusions can be drawn. Specific gravity revealed that the soils are inorganic soft soil. The soils are well graded and (CL) according to (UCS). The plasticity index and liquid limit of the soil samples show that the soils are not suitable as base/sub-base materials in road construction because they are above the maximum 12% and 30% values respectively recommended for sub base/base soils. Casagrande chart classification indicated that the soil is of low plasticity and hence compressibility. The compaction results revealed that addition of tyre ash increased the OMC and reduced the amount of MDD with the increase of tyre ash addition. The CBR values of all the soil samples increased considerably on stabilization with tyre ash. The results of the findings show that the geotechnical properties of the stabilized soft soils were significantly improved but still unsuitable for base/sub-base materials in road construction.

4.4 Index Properties

The liquid and plastic limits of tyre ash treated soil decreased and increased respectively with the increase in additive quantity as shown in Table 6, and **Fig. 5**. This shows that the Atterberg limits of the soft soil were improved with a decrease in liquid limit, an increase in plastic limits with a resulting decrease in plasticity index. The liquid limit decreased from38.5to 32.2% with an increase in the tyre ash content from 0 to 8%. This could be attributed to the addition of tyre ash, which has less affinity for water and yielded a decreased liquid limit. The plasticity index decreased from 14.2to 5.5% with increase in the tyre ash content. These effects may be due to the partial replacement of the plastic soil particles by tyre ash fines, which is an abrasive non-plastic material, with consequent reduction in clay content. The plasticity of a soil is controlled by the amount of clay fraction in it; it decreases as the amount of clay fractions decreases **Arora, 2008.** Decrease in plasticity index of a soil shows an improvement in the engineering properties of the soil. This is in agreement with the works of other researchers **Ferguson, 1993, Zia and Fox, 2000, Parsons, and Kneebone, 2005, Basha, et al., 2003.**

4.5 Compression Index

Compression index (Cc) is an important parameter used in geotechnical engineering as it relates to the amount of anticipated consolidation settlement that a soil stratum will experience when introduced to loads that are greater than experienced in the past. The slope of the linear portion of the e-log p curve is designated as the Cc. The variation of compression index with tyre ash content and moisture content relative to optimum moisture content is shown in Table 7, and **Fig. 6**. The Cc generally decreased with increasing tyre ash for up to 8% treatment. Cc ranged from 0.2108–0.0677, at optimum moisture with increasing stabilizer content. The decrease in compression index may be attributed to the formation of pozzolanic products within the pore spaces from physico-chemical changes **Osinubi,** and **Eberemu, 2006**. They may also be attributed to the formation of cementitious bonds between clay particles caused by the addi-

tion of tyre ash. Similar results were obtained by other researchers **Anagnostopoulos, and Stavridakis, 2003, Kazemian, and Huat, 2009**. The settlement of soils is directly related to the compression index which implies that tyre ash can be used to reduce the settlement of soils. Soil structure compacted at the OMC are always flocculated. This results show that the compression index is influenced by the particle state of the soil fabric which is controlled by the moulding water content. **Cássia de BritoGalvão, et al., 2004** observed that addition of lime is effective in improving the compressibility characteristics of tropical soils and also effective in decreasing the potential for collapse of the soils when compacted to densities lower than their maximum dry densities.

4.6 Swelling Index

Variation of swelling index (Cs) with increasing tyre ash content is similar to that of compression index. The variation is shown in Table 7 and **Fig. 7**. Cs ranged from 0.02802–0.01901at the optimum moisture with increasing stabilizer content. **Anagnostopoulos,** and **Stavridakis, 2003** showed that the swell index of soft was also reduced with increasing cement ratio. The variation of swell index with moulding water content relative to optimum moisture content exhibited in Table 7 show that samples compacted at the optimum moisture content have the highest swell index. This may be attributed to water deficiency and random orientation of particles which leads to imbibe of more water and therefore more swelling. This also implies that swell index is influenced by the particle state of the soil fabric which is controlled by the moulding water content. Consequently, the samples at optimum moisture contents will swell less when unloaded because a more compact state of soil is attained when soil is compacted at optimum moisture content.

4.7 Coefficient of Volume Compressibility

The coefficient of volume compressibility (mv) is defined as the volume change per unit increase in effective stress for a unit volume of soil **Craig, 1992**. The volume change expressed in parameter is very useful to estimate the primary consolidation settlement. The variation of coefficient of volume compressibility with tyre ash content is shown in Table 8. The mv generally decreased with increasing the consolidation pressure and tyre ash content in the moulding water contents. This could probably be due to increase in effective stress and pozzolanic reaction taking place within the soil which in turn changed the soil matrix. For instance, at OMC, the values of mv for sample ranged from 2.074– 4.450 m^2/MN, 2.940 – 1.792 m^2/MN, 1.953– 1.396 m^2/MN and 1.094– 1.194 m^2/MN at 10, 20, 40 and 80 N/m^2 loading respectively. **Kazemian,** and **Huat, 2009** also showed that the coefficient of volume compressibility decreased by increasing the consolidation pressure and cement ratio.

The variation of coefficient of mv with different moulding water content in Table 8, and **Fig.8** shows that samples compacted on the dry side OMC have the least mv for all the pressure increments. This can also be attributed to the fabric of the compacted soil **Holtz,** and **Kovacs, 1981**. At the same compacting effort, with increasing water content, the soil fabric becomes increasingly oriented; that is, at dry of optimum, the soils are always flocculated, whereas wet of optimum the fabric becomes more oriented or dispersed. **Arora, 2008** stated that soils with flocculated structure are light in weight, have high void ratio and can resist external forces because of the bond due to attraction between particles hence they have low compressibility and high permeability.

5. CONCLUSIONS

In the present study, a series of tests were performed on soft soil mixed with different percents of tyre ash to investigate the strength and compressibility characteristics of soils stabilized with tyre ash mix. A program of standard laboratory tests carried out on soft clay soil taken from Ali-AL Girbi area in Missan governorate–East of Iraq.

The following conclusions are limited to the material used and test conditions under which the tests were conducted. Based on the results obtained from:

1. The measurements made before and after testing showed that the undrain shear strength in models of footing on soft clay soil improved by tyre ash material, the undrain shear strength is increased by about (1.3 – 14) % due to the implementation of soil stabilization.
2. CBR on compacted soft clay treated with tyre exhibited higher CBR values than compacted untreated soft clay soil.
3. Increased the OMC with the increase of tyre ash addition in compaction test.
4. It was noticed that (the L.L and P.I decreased, while the P.L increased) with the increase of tyre ash addition.
5. The Cc decreased with increase in percentage tyre ash regardless of the moulding water content.
6. The Cc and Cs are increases with increase moulding water content.
7. The Cs decreased with increase in percentage tyre ash irrespective of the mould ing water content.
8. The mv and Cv decreases with increasing tyre ash content and consolidation pressure regardless of the moulding water content.
9. The Cv decreases with increase moulding water content.
10. The soft clay treated with tyre has undraind shear strength higher than untreated soft clay soil.

REFERENCES

- Afolagboye L. O., and Talabi, A. O., 2011, *Consolidation properties of compacted lateritic soil stabilized with tyre ash*. Department of Geology, Faculty of Science, Ekiti State University, Ado-Ekiti, Nigeria

- Afolagboye L. O., and Talabi, A. O., 2014, *Effect of Curing time on unconfined Compressive Strength of lateritic soil stabilized with tyre ash*. Department of Geology, Faculty of Science, Ekiti State University, Ado-Ekiti, Nigeria.

- Akbulut, S., Arasan S. and Kalkan E., 2007, *Modification of clayey soils using scrap tire rubber and synthetic fibers*, Applied Clay Science, 38: 23-32.

- Al-Qayssi, M.R., 2001, *Unreinforced and Reinforced Behavior of Single and Groups of Granular Piles, Ph.D*. Thesis Submitted to the Civil Engineering Department Faculty of the Military Collage of Engineering, Iraq.

- Amu O.O., Ogunniyi S.A., and Oladeji O.O., 2011, *Geotechnical properties of lateritic soil stabilized with sugarcane straw ash,* Am. J. Sci. Ind. Res., 2(2): 323-331.

- Anagnostopoulos A. C., and Stavridakis E. I., 2003, *Influence of sand content on cement and durability of cement-acrylic resin treated soil*. Electron. J. Geotech. Eng. 8: Bundle D.

- Arora K. R., 2008, *Soil mechanics and foundation engineering, standard. Publishers Distributors*, Delhi, pp.118.

- Atkins, H.N., 1980, *Highway Materials, Soil, and Concretes, Reston Publishing Company*, Inc. Reston, Virginia.

- Basha E. A., Hashim R., Mahmud H. B., and Muntohar A. S., 2005, *Stabilization of residual soil with rice husk ash and cement*. Construction and Building Materials. 19:448-453.

- Bell, F. G., 1996, *Lime Stabilization of Clay Minerals and Soils*, Engineering Geology, Vol.42, pp.223–237.

- Bernal, A., C.W., Lovell and R. Salgado, 1996, *Laboratory Study on the Use of tire Shreds and Rubber-Sand in Backfilled and Reinforced Soil Applications*. Publication FHWA/IN/JHRP-96/12. Joint Highway Research Project, Indiana Department of Transportation and Purdue University, West Lafayette, Indiana. doi: 10.5703/1288284313259.

- Brand, E.W., and Brenner, R.P., 1981, *Soft Clay Engineering*, Elsevier Scientific Publishing Company, Amsterdam, pp. 778.

- Broms, B.B., 1987, *Stabilization of soft clay in Southeast Asia*, proceeding 5thInternational Geotechnical Seminar 2-4 Dec. 1987.

- Buringh, P., 1960, *Soils and Soil Conditions in Iraq*, Metherlands by H. Veenman and Zonen N.V., Wageningen.

- Carreon, G. D., 2006, *Stabilization of marginal soils using recycled materials*. These soils Dissertations. Paper 2473.

- Cássia de BritoGalvão T., Elsharief A. and Simões G. F., 2004, *Effects of lime on permeability and compressibility of two tropical residual soils*. J. Environ. Eng-ASCE Vol.130:8.

- Das, B.M., 2002, *Principles of Geotechnical Engineering, fifth edition*, wadsworth group, pp.340.

- Eberemu O. 2011, *Consolidation Properties of Compacted Lateritic Soil Treated with Rice Husk Ash*, Geomaterials, 1, 70-78.
- Ferguson G. 1993, *Use of self-cementing fly ashes as a soil stabilization agent*. ASCE Geotechnical Special Publication No. 36, ASCE, New York.
- FMWH (Federal Ministry of Works and Housing) 1997, *General specifications (roads and bridges)*, vol II, Federal Ministry of Works and Housing, Lagos, Nigeria.
- Ghani, A.N.A., F. Ahmad, R. Hamir and S. Mohd, 2002, *Scrap Tire Based Lightweight Geomaterial for Civil Engineering Works*. In Proceeding of Malaysian Science Technology Congress, Oct. 17-19, Genting Highlands, MALAYSIA.
- Holtz D. R. and Kovacs D. W., 1981, *an introduction to geotechnical engineering, Prentice-Hall,* Inc., Chapter 5, Compaction, pp. l09-165.
- Hossain K. M. A., Lachemi M. and Easa S., 2007, *Stabilized soils for construction applications incorporating.*
- Kazemian S. and Huat B. B. K., 2009, *Compressibility characteristics of fibrous tropical peat with reinforced with cement column*. Electron. J. Geotech. Eng. 14, Bundle C, pp 1-13.
- Kedzi, 1979, *Stabilized Earth Roads*. Elsevier, Amsterdam, pp. 327.
- Liu. and J, Evett. 2003, *Soils and Foundation*, 6th ed. USA: Prentice Hall.
- Misra.A.,Biswas and Upadhyaya,S., 2005, *Physico-mechanical behavior of self-cementing class C Fly ash-clay mixtures*. Fuel, 84(11), 1410-1422
- Ola. S.A., 1977, *Potential of lime stabilization of lateritic soils.* Engineering Geology vol. II, pp 305-317.C.
- Osinubi K. J., and Eberemu A. O., 2006, *Effect of bagasse ash on the strength of stabilized lateritic soil.* Proceedings of 5th Nigerian Material Congress, Abuja, 15-18 November 2006, pp. 214-220.
- Parsons R. L., and Kneebone E. 2005, *Field performance of fly ash stabilized subgrade*, Ground Improvement 9:33-38.
- Rahil F.H., 2007, *Improvement of Soft Clay underneath a Railway Track Model Using Stone Columns Technique*. Ph.D. Thesis, University of Technology, Iraq.

- Rahman M.D.A., 1986, *the potentials of some stabilizers for the use of lateritic soil in construction*, Building and Environment, Vol. 21, pp 57-61.
- Senol, T.B., Edil, M. d., Sazzad Bin-Shafique, H. A., Acosta. and C.H. Benson. 2006, *Soft Subgrades, Stabilization by Using Various Fly Ashes*, Resources Conservation and Recycling, 46, 365-376.
- Walid Z. and Harichane K. 2010, *Effect of Lime and Natural Pozzolana on Dredged Sludge Engineering Properties*, Geotechnical Engineering, vol. 18, pp 589-600.
- Zia N. and Fox P. J., 2000, *engineering properties of loess-fly ash mixtures for road bases*. Transportation Research Record 1717, Transportation Research Board, 49-56.

SYMBOLES

ASTM : American Society for Testing and Materials.

CBR : California Bearing Ratio

C_c : compression index.

CL : clay of Low plasticity

C_s : swelling index.

C_u : undrained shear strength of soil (kN/m^2).

Cv : coefficient of consolidation (mm^2/sec).

FMWH : federal Ministry of Works and Housing

G_S : specific gravity.

L.L : liquid limit

MDD : maximum dry density (g/cm^3).

mv : coefficient of volume change (m^2/MN).

O.M.C : optimum moisture content.

P.I : plasticity index.

P.L : plastic limit

q_u : bearing capacity of soil.

T.S.S : total soluble solids(%).

UCS : unconfined compressive strength

USCS : unified soil classification system.

Table 1. Properties of used soil.

Index Property	Value
Liquid Limit (L.L) (%)	38.5
Plastic limit (P.L) (%)	23.3
Plasticity index (P.I) (%)	15.2
Shrinkage limit (S.L) (%)	14
Activity (At)	0.2
Specific gravity (Gs)	2.75
Gravel (%)(larger than 2mm)	0
Sand(%)(0.06 to 2mm)	7.54
Silt (%)(0.002 to 0.06mm)	52.46
Clay (%)(less than 0.002mm)	40
CBR	3.4
Coefficient of permeability, K(cm/sec)	1.293 *10-8
Unconfined compressive strength, Cu (KN/m2)	19
Natural water content ,W°	17.5
Calcium oxide (CaO) (%)	14.55
SO_3content (%)	0. 2
Total soluable salts % (TSS)	1.53
PH value (%)	7.53

Table 2. Chemical composition of the tyre ash

Oxide	Composition (%)
Silicon oxide (SiO2)	32.33
Aluminum oxide (Al2O3)	3.8
Iron oxide (Fe2O3)	5.878
Calcium oxide (CaO)	21.86
Magnesium (MgO)	1.977
Trioxosulphates (SO3)	1.252
Potassium oxide (K2O)	1.3913
Tin oxide (TiO2)	0.2032
Na2O	1.23
pH	7.41
cL(%)	250
T.S.S(%)	1.02
Gs	1.33
Loss on Ignition (L.O.I)	30.08%

Table 3. Compaction characteristic.

Stabilizer%	MDD(g/cm^3)	OMC %
0	1.63	22.00
2	1.58	23.40
4	1.54	24.50
6	1.53	27.40
8	1.52	27.80

Table 4. Variation of California Bearing Ratio with tyre ash.

Stabilizer %	CBR %
0	3.41
2	3.51
4	4.31
6	5.58
8	9.56
10	9.66

Table 5. Variation of undrained shear Strength with tyre ash.

Stabilizer %	undrained shear Strength(kN/m^2)
0	41
2	55
4	76
6	109
8	122

Table 6. Index properties of soft soils.

Stabilizer (%)	L.L (%)	P.L (%)	P.I (%)	Ac
0	38.5	24.3	14.2	0.2
2	37.6	25	12.6	0.18
4	34.2	25.18	9.02	0.13
6	33.4	25.3	8.1	0.12
8	32.2	26.7	5.5	0.08

Table 7. Compression index and Swelling index of the compacted soil treated with tyre

Stabilizer (%)	Cc	Cs
0	0.2108	0.02802
2	0.2067	0.02564
4	0.1108	0.0237
6	0.0771	0.02085
8	0.06771	0.01901

Table 8. Coefficient of volume compressibility of the compacted soil treated with tyre ash

Tyer Ash / Pressure N/m^2	**mv * 10 $^{-7}$m^2/MN**				
	0%	**2%**	**4%**	**6%**	**8%**
10	4.4503	3.902	3.367	2.502	2.074
20	2.940	2.2740	2.247	2.115	1.792
40	1.953	1. 910	1. 7036	1. 5011	1.396
80	1.194	1.1631	1.1464	1.1317	1.094

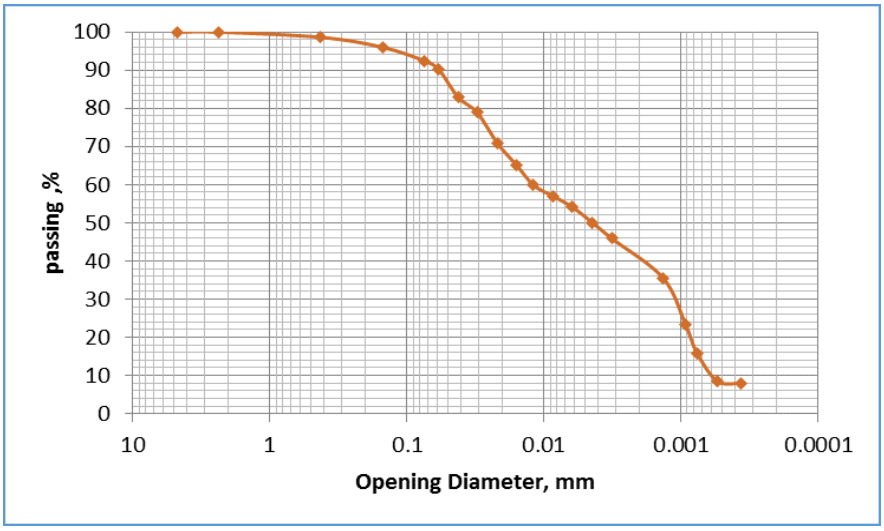

Figure 1 .Grain size distribution curve.

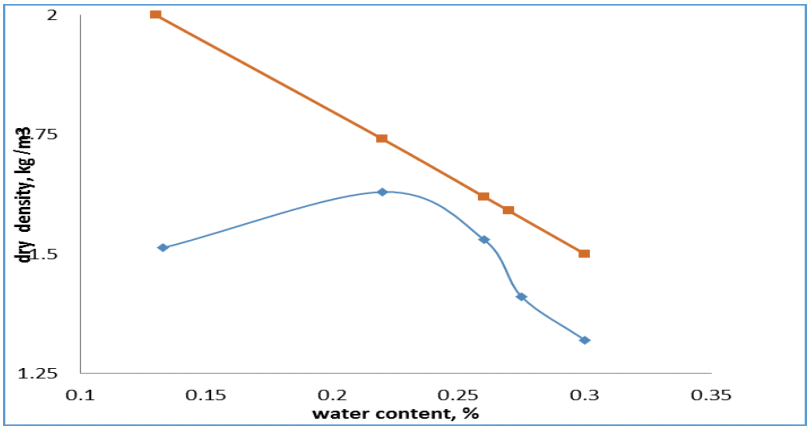

Figure 2. Compaction curve.

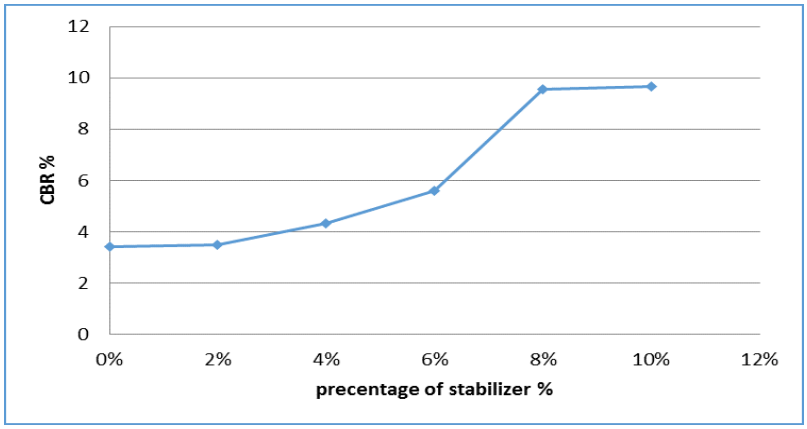

Figure 3. Influence of amount of stabilizer on california bearing ratio.

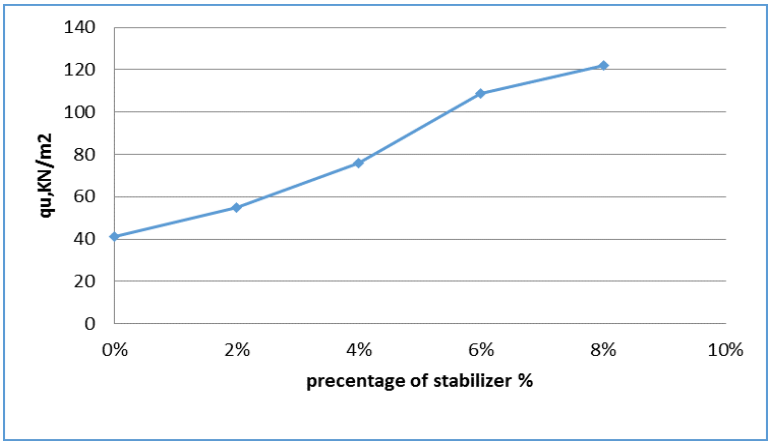

Figure 4. Variation of 2-day unconfined compressive strength with tyre ash content.

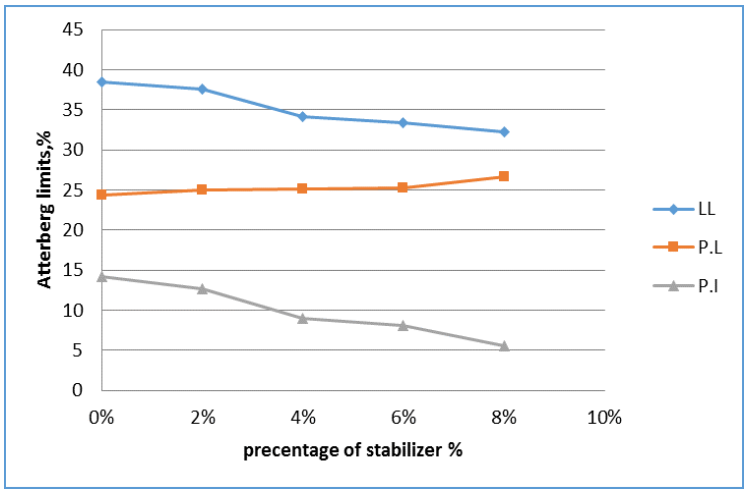

Figure 5. Variation of (L.L, P.L, P.I,) with amount of stabilize.

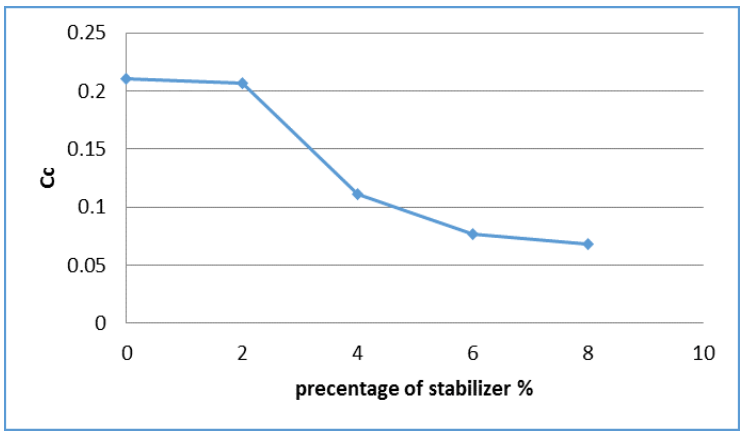

Figure 6. Variation of compression index with amount of stabilizer

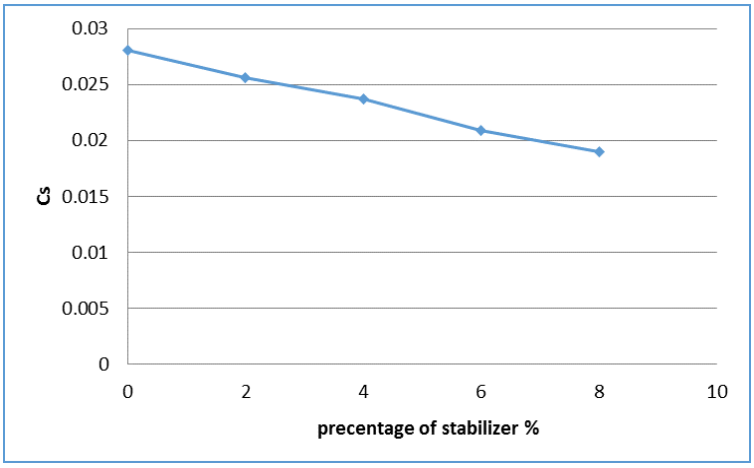

Figure 7. Variation of swelling index with amount of stabilize.

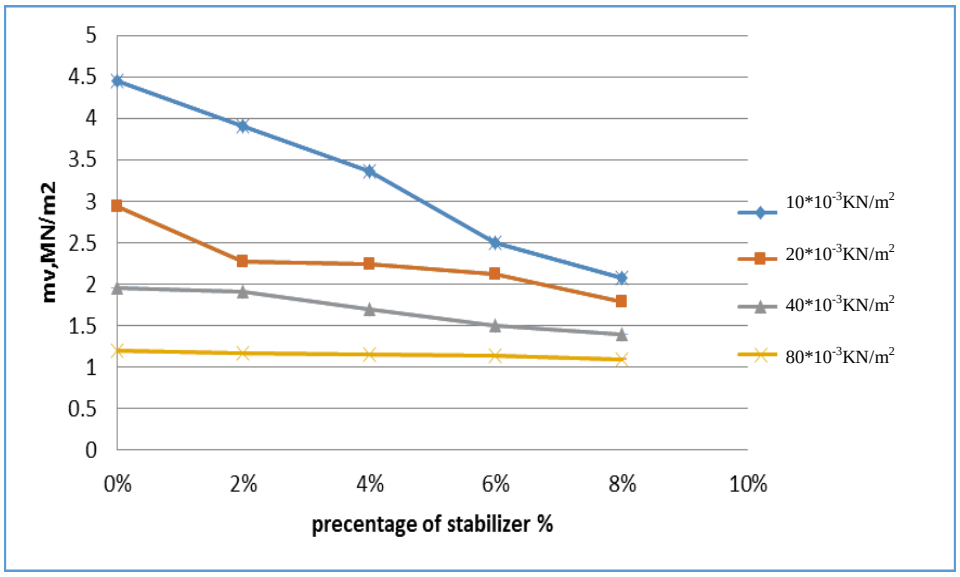

Figure 8. Variation of coefficient of volume compressibility with amount of stabilizer.

Synthesis of Nanozeolite NaA from Pure Source Material Using Sol Gel Method

Najwa Saber Majeed
Assistant Professor Doctor
College of Engineering, University of Baghdad
dr.najwa_saber@yahoo.com

Jwan Taher Majeed
M Sc Student
College of Engineering, University of Baghdad
eng.jwan1@yahoo.com

ABSTRACT

In this work, the nano particles of Na-A zeolite were synthesized by sol –gel method. The samples were characterized by X-ray diffraction (XRD), X-ray Fluorescence (XRF), Surface area and pore volume, Atomic Force Microscope (AFM) and Fourier Transform Infrared Spectroscopy (FTIR). Results show that the nano A zeolite is with average crystal size is 74.77 nm., Si/Al ratio 1.03, BET surface area was 581.211m^2/g and the pore volume for NaA was found equal to 0.355cm^3/g.

Key words: Nanocrystal, nanozeolite, zeolite type NaA, characterization.

تحضيرالنانو زيولايت نوع (NaA) من مصدر المواد النقية بطريقة معاملة الجل حراريا

نجوى صابر مجيد
استاذ مساعد دكتور
كلية الهندسة /جامعه بغداد

جوان طاهر مجيد
طالبة ماجستير
كلية الهندسة /جامعه بغداد

الخلاصة

في هذا العمل تم تحضير زيولايت نوع Na-A بجزيئات نانوية بطريقة معاملة الجل حراريا. تم اختبار خصائص العينات المحضرة بجهاز الاشعة السينية (XRD) وبجهاز المجهر ذو القوة الذرية (AFM) وحساب المساحة السطحية والحجم المسامي بالامتزاز بالنتروجين (BET) وتم حساب نسبة السيلكا الى الالومينا (XRF) والمطياف ذو الاشعة فوق الحمراء(FTIR). واثبتت النتائج فعالية عملية التحضير ونجاحها في الحصول على تركيب نانوي بقياس 74.77نانومتر ونسبة سيلكا الى الومينا 1.03 ومساحة سطحية 581.211 متر^2/ غم وذو حجم فراغي 0.355 سم^3/غم.

الكلمات الرئيسية: النانوية ، النانوزيولايت، زيولايت نوع NaA، التوصيف.

1. INTRODUCTION

Nanoscience is considered as one of the key technological fields of the 21st century, **Olveira et al., 2014**. Nanozeolites are a type of zeolites which have narrow particle size distribution with sizes of less than 100 nm, **Song et al., 2004**. Compared to "ordinary" zeolites of which the particle diameters are of micrometer order, nanozeolites represent very small particle size, reducing the particle size from micrometer to nanometer scale leads to a significant change of material characteristics and their applications in catalysis and adsorption. The number of atoms in the unit cell increases when particle sizes decrease and nanozeolites have large external surface area. The diffusion path length in nanozeolites is shortened as compared to that in the conventional micrometer zeolites, **Song et al., 2004**, **Ngoc et al., 2013**. One of the advantages of nanozeolites is their higher external surface area. The external surface is of vital important in numerous processes, including adsorption and catalysis. Nano-crystalline zeolite is synthesized in many different synthetic methods mostly are: hydrothermal treatments, sol - gel method, and the emulsion method, **Radhi, 2015.**

The sol-gel method is a useful and attractive technique for the preparation of nanosized particles because of its advantages: good stoichiometric control and the production of ultrafine particles with a narrow size distribution in a relatively short processing time at lower temperatures, **Chen, and He, 2001.** One important factor in sol–gel technology is the ageing time allowing the gelation of the sol. It can vary from a few minutes to several weeks, depending on the concentrations in the sol, **Meille, 2006.**

Azizi et al., 2006 prepared NaA nano-zeolite using microwave pretreatment and a hydrothermal method without organic additives. The result showed that the sizes of NaA nanoparticles are in the range of 40 to 90 nm with an average diameter of 60 nm. The specific surface area of the NaA nanozeolite is 97.48 $m^2 g^{-1}$ and the average pore diameter of 2.459 nm.

NaA Nanozeolite was synthesized by the hydrothermal method with different crystallization time (1, 2 and 3 days) at room temperature under stirring. Nanocrystals NaA with crystal sizes ranging from 50 to 120nm were synthesized at room temperature with 3 days aging, without adding any organic additives and external surface of the resulting NaA zeolite was 62.520$m^2 g^{-1}$, **Ghasemi and Younesi, 2011.**

Jawad, 2009 Prepared nano sized particles zeolite Y by sol-gel method the results showed that the pore volume increased as the surface area increased of synthesized nano particles zeolite Y increased with increasing Si /Al ratio.

Rahman et al., 2012 prepared zeolite Y using sol gel method and they obtained highly crystalline and surface area of about 320 m^2/g with pore volume 0.15 cm^3/g.

In this study, a facile method for the preparation of nonocrystalline zeolite NaA is investigated using sol-gel method. Extensive characterization of the final product was done using (XRD), (BET), (XRF), (AFM), and (FTIR).

In this paper, prepared nanozeolite NaA from pure source materials was done using sol-gel method.

2. EXPERIMENTAL WORK

2.1 Synthesis of Nanozeolite NaA

2.1.1 Materials

The chemical Materials used included NaOH (Sigma), sodium aluminate (Kunshan Yalong), sodium silicate (Himedia), and deionized water.

2.1.2 Methods

Nano_Zeolite A was synthesized according to sol-gel method. The preparation involved three major steps, namely: seeding gel, feed stock gel and over all gel. Seeding gel is prepared by adding 4.1 g of sodium hydroxide, 20 g of deionized water and 2.1 g sodium aluminate, **Rahman et al., 2012**, **Al-Tabbakh, 2016**. The mixture was continuously stirred with magnetic stirrer in 50 ml plastic bottle until the mixture became an apparent solution then 20 g of sodium silicate solution was added and stirred moderately for at least 15 min, and then the bottle was capped and the solution is left to age at room temperature for 24hr. The feed stock gel was prepared by adding 131 g of deionized water to 0.14 g sodium hydroxide and 13 g sodium aluminate, stirred in 500 ml plastic beaker until dissolved then 140.5 g of sodium silicate solution was added with stirring vigorously with high shear 4 paddle mixers at 1600 rpm until the gel appears smooth. The overall gel was prepared by mixing the feed stock gel with 16.5g of the seed gel. The seed gel was added slowly under high shear mixing for 40 min at room temperature at 1600 rpm. After that the final gel was transferred to a poly propylene bottle and stored in a water bath at 87°C in a programmable electrical furnace for 24 hours.

The product obtained was filtered using Buckner funnel with the aid of a vacuum pump and repeatedly washed with deionized water until pH reached to 9. The product was dried in an electrical oven for 24 hours at 100°C and then was calcined by the programmable electrical furnace at 500°C for 3 hours. Experimental apparatus is shown in **Fig.1.**

2.1.3 Characterization

XRD analyses were carried out at room temperature using a Shimadzu 6000 (Japan) using CuKα radiation nickel filter (λ= 1.5418A°). Data were collected within the 2Θ range of 2° and 50° with a 2θ step size of 0.02 and a step time of 0.24s per step (40kv and 30mA). The surface area of prepared catalyst was measured by nitrogen physical adsorption at liquid nitrogen temperature at -196 °C using the BET (Brunauer, Emmett, and Teller) method. Pore volume is a measure of the void space in the catalyst. It is measured by nitrogen adsorption BET and expressed in cm^3/g.

The chemical composition of the prepared zeolite was analyzed using XRF technique. The test was conducted by a device of the type SPECTRO XEROS (Germany) by weighing a sample of 3g in powder state and putting in plastic cup of 30mm diameter. Test conducted in inert atmosphere (Helium). Atomic Force Microscope (AFM) is a powerful technique for surface investigation by providing material topology in high resolution. The test was performed by Device (type Angstrom, Scanning Probe Microscope, Advanced Inc, AA 3000, USA), performed for samples by ethanol dispersion to conducted the surface morphology and the particles size.

And FT-IR spectroscopy analysis of zeolites was carried out to study the features their structure by the chemical bonds (functional group) between molecules. This test was done using a Shimadzu FTIR 8400S (Japan) with wave number range (400-4000 cm^{-1}).

3. RESULTS AND DISCUSSION

3.1 X– Ray Diffraction (XRD)

X-ray diffraction was implemented to check the required pattern of NaA nanozeolite and its crystalline. From **Fig.2** X-ray diffraction pattern of the prepared NaA nanozeolite is approximately comparable with the standard. **Table 1** shows a comparison of lattice spacing and angle, between prepared NaA nano-zeolite and standard.

The highly crystalline zeolite is with no amorphous material and the relative intensities of the peaks which are related to the level of zeolite crystallization, **Alrubaye, 2013.**
The relative crystallinity of zeolite was determined by dividing the sum of the peak intensities of the prepared zeolite on the sum of the peak intensities of the standard zeolite and can be expressed mathematically, **Doneliene et al., 2010.** The relative crystallinity is calculated by Eq.(1) and it was found to be equal to 97.6%.

$$Relative\ Crystallinity\ \% = \frac{\sum Intensities\ of\ peaks\ of\ sample}{\sum Intensities\ of\ peaks\ of\ reference\ sample} * 100 \qquad (\mathbf{1})$$

3.2 Surface Area and Pore Volume

The obtained value of surface area of prepared nanozeolite NaA was 581.211m^2/g and the pore volume was found equal to 0.355cm^3/g.

3.3 X- Ray Florescence (XRF)

The chemical composition of the prepared zeolites expressed in weight percent are listed in the **Table (2).** The molar ratio of Si/Al for NaA nanozeolite was equal to 1.03. This result is in a good agreement with the result obtained by, **Ghasemi and Younesi, 2011** which is about 1.071.

3.4 Atomic Force Microscope (AFM)

The surface uniformity of the prepared nanozeolite was studied using Atomic Force Microscope with 408 pixel density. **Fig.3** shows AFM on two-dimensional surface profile while **Fig.4** shows AFM for three dimensional surface profiles.

The particle size distribution for prepared NaA nano_zeolite was obtained as shown in **Fig.5.** This figure shows that the most volume percentage 11% of particle size distribution was at 95 nm and the lowest volume percentage 0.44 % was at 45 and 50 nm. It also shows the prepared zeolite consisted of particles with diameters ranged between 45 - 100 nm. This means that the particles of prepared zeolite are nanometer-sizes and the average particles diameter of NaA nano_zeolite was 74.77nm. This result is in a good agreement with the result obtained by **Ghasemi and Younesi, 2011**.

3.5 Fourier Transform Infrared Spectroscopy (FTIR)

FT-IR spectroscopy analysis of zeolites was carried out to study the features of their structure by the chemical bonds (functional group) between molecules. This test was determined using a Shimadzu FTIR 8400S (Japan) with wave number range (400-4000 cm^{-1}). Samples were prepared by mixing 1wt. % of zeolite and 99% KBr pressed as disk.
Fig.6 illustrates the FTIR spectra of prepared NaA nanozeolite. From this figure it can be observed that, the bands in the region of 983-1030 asymmetric stretching vibrations Si-O in $SiO_4$and Al-O in AlO_4. The band in the region 711-767.62 was symmetric stretching vibrations Si-O-Si. Absorption at about 698 cm^{-1} was assigned to Si – O – Al symmetric stretching where Al in the octahedral coordination. Peaks 1637.54cm^{-1} and 3519.85 cm^{-1} are assigned to the external linkage asymmetrical stretching and internal tetrahedral symmetrical stretching respectively. These results are comparable with the results obtained by many researchers such as **Omisanya et al., 2012, Mozgawa et al., 2011, Alkan et al 2005,** and **Aronne et al., 2002.**

CONCLUSIONS

Nano crystalline NaA zeolite has been prepared successfully using sol-gel method. According to the results obtained from this study, it was found from X-ray that prepared NaA nanozeolite has crystallinity of 97.6% and nearly has the same crystal structure as the standard type A-zeolite with silica to alumina molar ratio 1.03, surface area 581.211m^2/g, the pore volume 0.355cm^3/g and the average particles diameter of NaA nanozeolite was 74.77nm.

REFERENCES

- Al-Tabbakh B., 2016, *Catalytic Reforming of Naphtha Using Novel Prepared Pt Ti / HY Zeolite*, Ph.D. thesis, College of Engineering, Baghdad University .

- Chen, D.H. and He, X.R., 2001, *Synthesis of nickel ferrite nanoparticles by sol-gel method. Materials Research Bulletin*. 36(7), pp.1369-1377.

- Doneliene, J., Vaiciukynienė, D. and Kantautas, A., 2010, *The Influence of Alumosilicate Gel Aging on the Synthesis of NaX Zeolite.* Material Science & Applied Chemistry, (22), pp30-34.

- Meille, V., 2006, *Review on methods to deposit catalysts on structured surfaces*. Applied Catalysis A: General, 315, pp.1-17.

- Ngoc, D.T., Pham, T.H. and Nguyen, K.D.H., 2013, *Synthesis, characterization and application of nanozeolite NaX from Vietnamese kaolin*. Advances in Natural Sciences: Nanoscience and Nanotechnology, 4(4), p.045018.

- Olveira, S., Forster, S.P. and Seeger, S., 2014, *Nanocatalysis: academic discipline and industrial realities*. Journal of Nanotechnology, 2014, pp 1-19.

- Radhi D. B., 2015, *Preparation of Nano ZSM-5 Zeolite by Emulsion Method*, MSC. Thesis, College of Engineering, Baghdad University.

- Rahman M., Awang M. and Youf A., 2012, *Preparation, Characterization and Application of Zeolite Y for Water Filteration*. Astralian Journal of Basic and Applied Science.Vol. 6. - pp. 50-54.

- Song, W., Justice, R.E., Jones, C.A., Grassian, V.H. and Larsen, S.C., 2004, *Synthesis, characterization, and adsorption properties of nanocrystalline ZSM-5*. *Langmuir*, *20*(19), pp.8301-8306.

- Azizi, S.N., Ghasemi, S. and Mikhchian, M., 2016.*Microwave-assisted synthesis of NaA nanozeolite from slag and performance of Ag-doped nanozeolite as an efficient material for determination of hydrogen peroxide*. RSC Advances, 6(57), pp.52058-52066.

- Ghasemi, Z. and Younesi, H., 2011.*Preparation and characterization of nanozeolite NaA from rice husk at room temperature without organic additives*. Journal of Nanomaterials, 2011, p.50.

- Jawad, Y.,2009.*Synthesis and characterization of zeolite nanoparticles catalysis used for N-hexane conversion*, Ph.D. thesis, College of Engineering, Baghdad University.

- Omisanya, N.O., Folayan, C.O., Aku, S.Y. and Adefila, S.S., 2012. *Synthesis and characterisation of zeolite a for adsorption refrigeration application*. Advances in Applied Science Research, 3(6), pp.3746-3754.

- Mozgawa, W., Król, M. and Barczyk, K., 2011. *FT-IR studies of zeolites from different structural groups.* Chemik, 65(7), pp.667-674.

- Alkan, M., Hopa, Ç., Yilmaz, Z. and Güler, H., 2005. *The effect of alkali concentration and solid/liquid ratio on the hydrothermal synthesis of zeolite NaA from natural kaolinite*. Microporous and Mesoporous Materials, 86(1), pp.176-184.

- Aronne, A., Esposito, S., Ferone, C., Pansini, M. and Pernice, P., 2002. *FTIR study of the thermal transformation of barium-exchanged zeolite A to celsian*. Journal of Materials Chemistry, 12(10), pp.3039-3045.

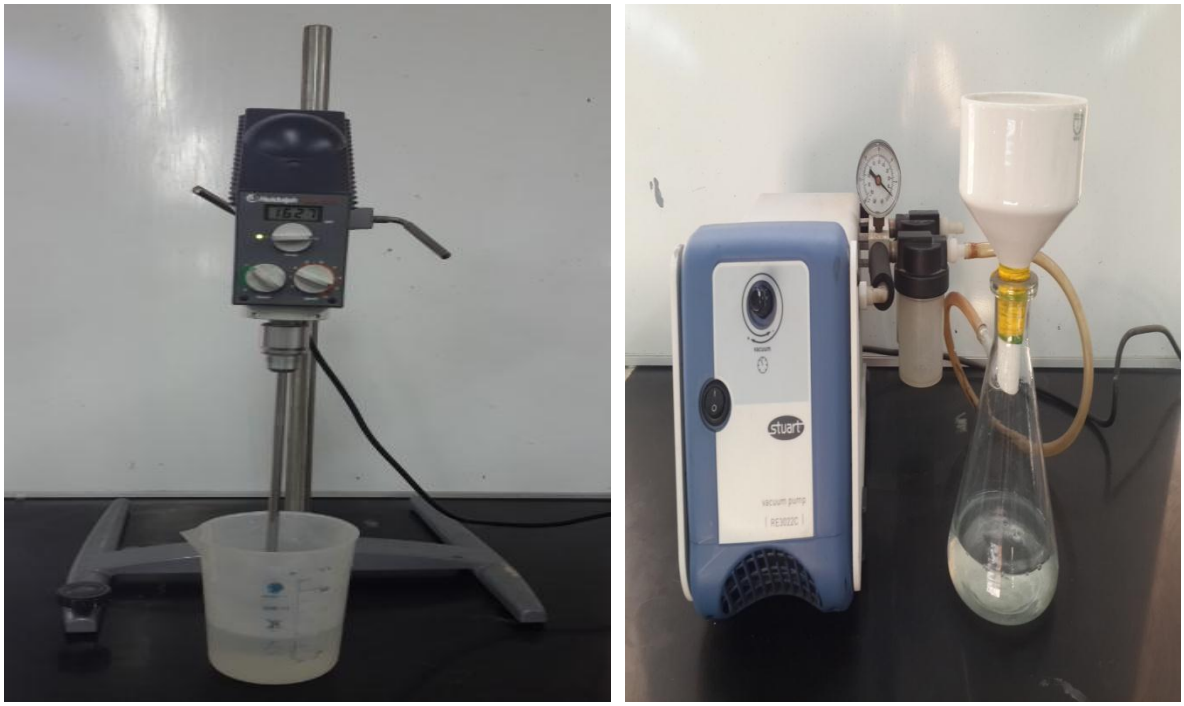

A B

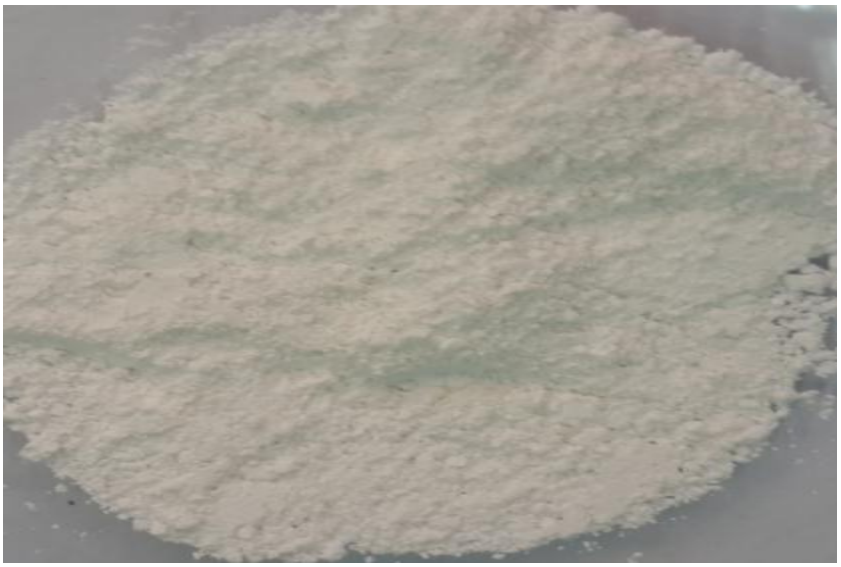

C

Figure 1. Preparation of NaA nano_zeolite:A. mixing of overall gel B. Filtration and washing of final product C. final product.

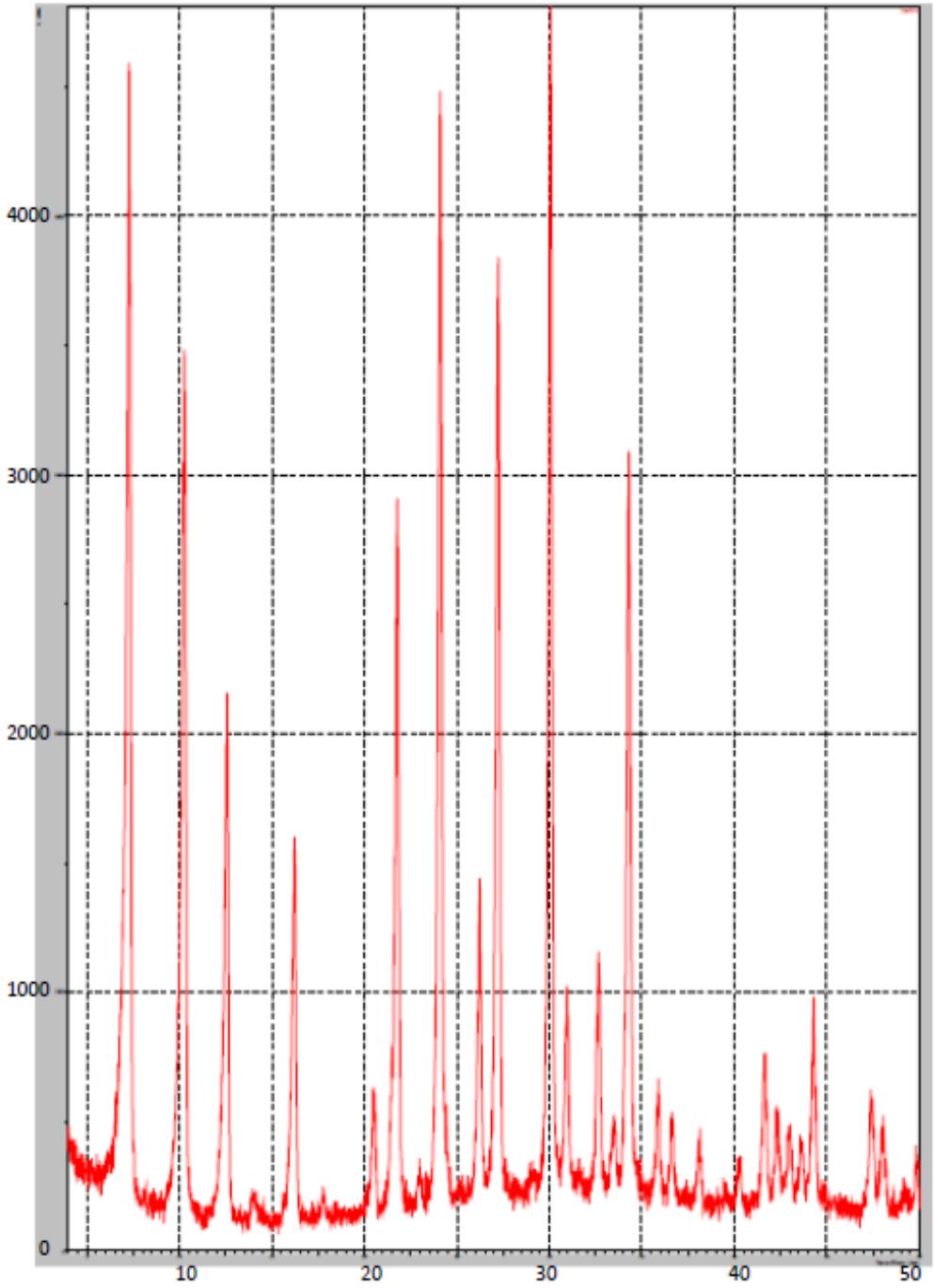

Figure 2. XRD pattern of prepared NaA nano_zeolite.

Table 1. Comparison of lattice spacing and angle, between prepared NaA catalyst and standard A.

Prepared catalyst		Standard of catalyst	
Angle (2Theta)deg	**d, spacing(Å)**	**Angle (2Theta)deg**	**d, spacing(Å)**
7.2010	12.31045	7.18	12.305
10.2015	8.68842	10.17	8.701
12.4623	7.11194	12.46	7.104
16.1316	5.50085	16.11	5.503
22.8617	3.88825	22.85	3.891
23.9898	3.72044	23.99	3.710
25.0672	3.55128	25.07	3.552
27.0990	3.28787	27.11	3.289
30.8190	2.90025	30.83	2.900
31.7103	2.81953	31.70	2.823

Table 2. The chemical composition for the prepared zeolites.

Oxides, wt. %	**Al_2O_3**	**SiO_2**	**Fe_2O_3**	**TiO_2**	**MgO**	**CaO**	**ZnO**
NaA	47.992	30.24	0.2314	0.2346	0.4913	1.8513	0.0063

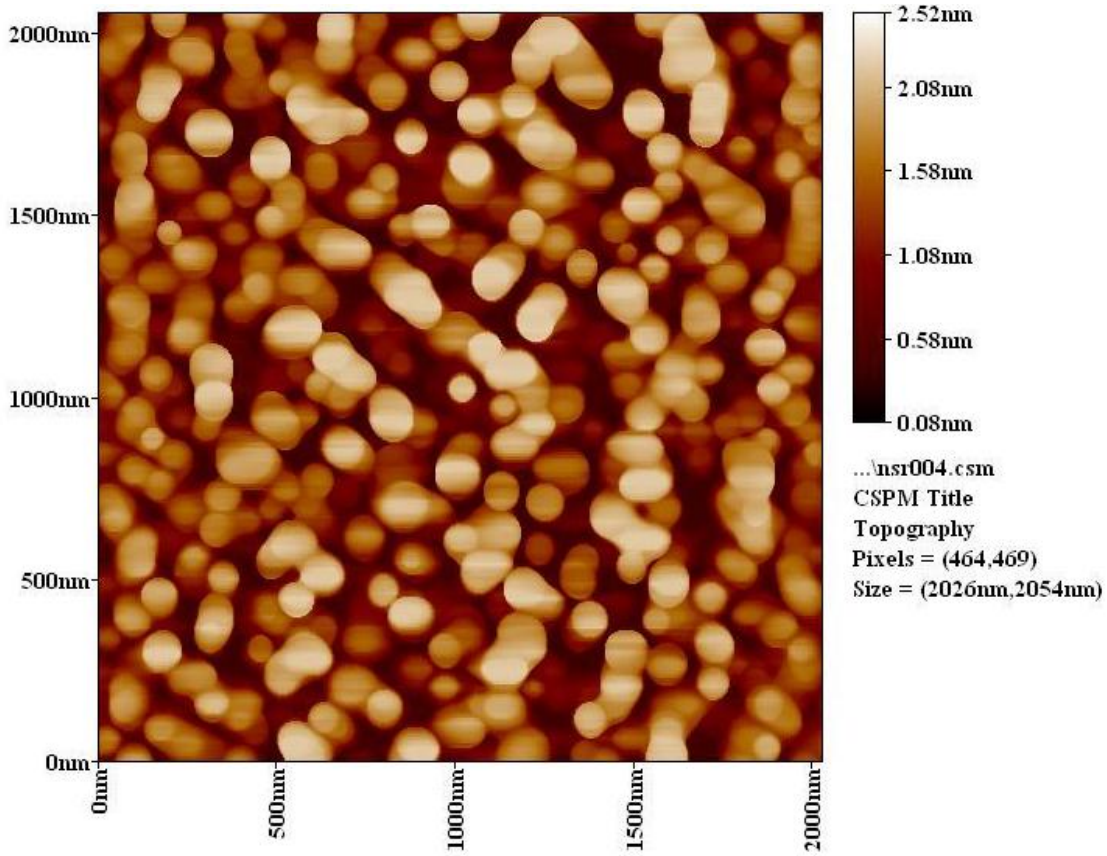

Figure 3. AFM two-dimensional surface profiles for NaA.

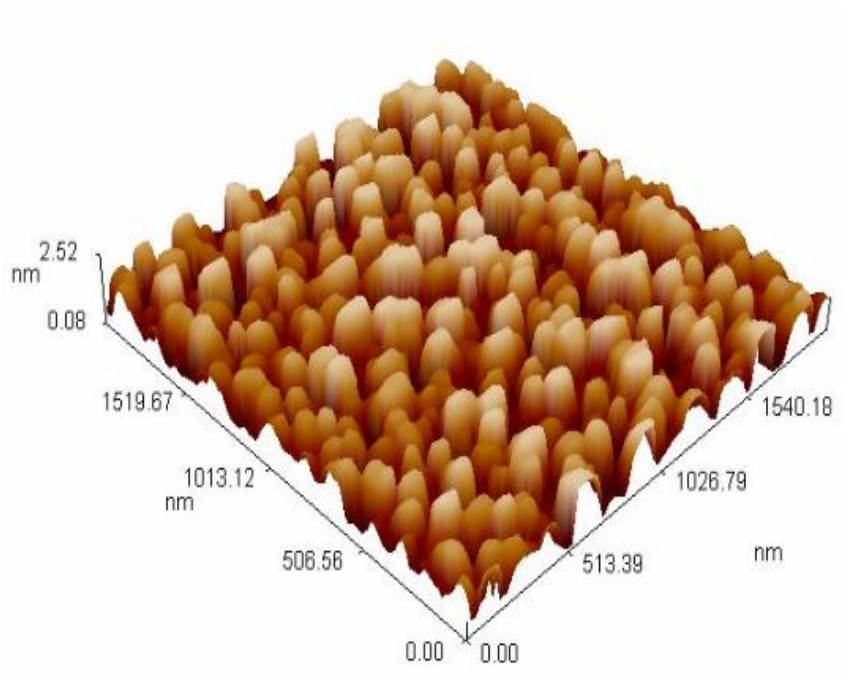

Figure 4. AFM three-dimensional surface profiles for NaA.

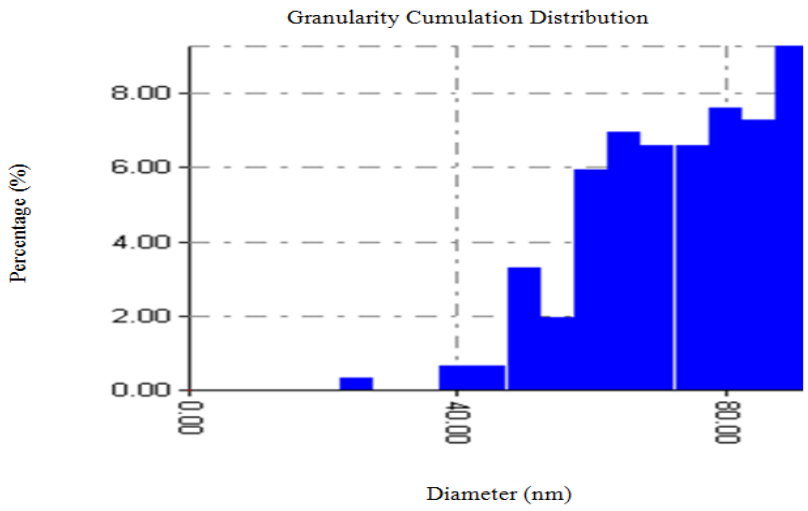

Figure 5. Granularity cumulation distribution for prepared NaA.

Figure 6. FTIR of synthesize nanozeolite NaA.

A Study of Parameters Affecting the Solvent Extraction-Flocculation Process of Used Lubricating Oil

Hussein Qasim Hussein
Assistant Professor, PhD
College of Engineering-University of Baghdad
husseinqassab@yahoo.com

Ali Laith Abdulkarim
Researcher
College of Engineering-University of Baghdad
alilaith.abdulkarim@gmail.com

ABSTRACT

The aim of this study was to investigate the effect of operating variables on, the percentage of removed sludge (PSR) obtained during re-refining of 15W-40 Al-Durra spent lubricant by solvent extraction-flocculation treatment method. Binary solvents were used such as, Heavy Naphtha (H.N.): MEK (N:MEK), H.N. : n-Butanol (N:n-But), and H.N. : Iso-Butanol (N:Iso:But). The studied variables were mixing speed (300-900, rpm), mixing time (15-60, min), and operating temperature (25-40,^{o}C). This study showed that the studied operating variables have effects where, increasing the mixing time up to 45 min for H.N.: MEK, H.N.: n-Butanol and 30 min for H.N.: Iso-Butanol increased the PSR, after that percentage was decreased; increasing the mixing speed for all the studied solvents up to 700 rpm increased the PSR, after that the percentage was decreased, while increasing the operating temperature decreased the PSR for all the solvents. This study has resulted in reasonably accurate multivariate process correlation that relates the removed sludge percentage to the process variables. The determination coefficients (R^2) were significantly high and equal to 0.957, 0.974, and 0.944 for N:MEK, N:n-But, and N:Iso-Butl respectively. The best operating conditions resulted the maximum PSR were (30 min, 900 rpm, 30 ^{o}C), (45 min, 700 rpm, 35 ^{o}C), and (30 min, 700 rpm, 35 ^{o}C) for N:MEK, N:n-But, and N:Iso-Butanol respectively.

Key words: Solvent extraction-flocculation, Used oil re-refining, PSR.

دراسة العوامل المؤثرة على عملية الاستخلاص-التلبد بالمذيبات للزيوت المستهلك

حسين قاسم حسين
أستاذ مساعد, دكتور
كلية الهندسة-جامعة بغداد

علي ليث عبدالكريم
باحث
كلية الهندسة-جامعة بغداد

هذة الدراسة تتضمن دراسة تأثير الظروف التشغيلية على نسبة المواد المتكتلة المزالة خلال عملية معالجة زيت التزيت العراقي (15W-40) باستخدام طريقة الأستخلاص-التلبد بالمذيبات. لهذا الغرض أستخدمت مذيبات ثنائية و هي: النافثا الثقيلة : ميثايل ايثايل كيتون، النافثا الثقيلة : البيوتانول المستمر، بالاضافة الى النافثا الثقيلة : البيوتانول المتفرع. متغيرات العملية كانت سرعة الخلط (15- 60 دقيقة)، مدة الخلط (300-900 دورة)، و درجةحرارة (25-40 درجة مئوية). العملية اظهرت هذة الدراسة بأن الظروف التشغيلية المدروسة لها تأثير على العملية، حيث بزيادة مدة الخلط لغاية 45 دقيقة بالنسبة للنافثا الثقيلة و ميثايل ايثايل كيتون، النافثا الثقيلة و البيوتانول المستمر ازدادت نسبة المواد المتكتلة المزالة، و لغاية 30 دقيقة بالنسبة النافثا الثقيلة و البيوتانول المتفرع، بعدها انخفضت هذة النسبة، و بزيادة سرعة الخلط لغاية 700 دورة/دقيقة ازدادت نسبة المواد المتكتلة المزالة لجميع المذيبات، و بعدها انخفضت هذة النسبة، اما بالنسبة لدرجة الحرارة فأن زيادتها ادت الى انخفاض هذة النسبة لجميع المذيبات. هذة الدراسة انتجت معادلة رياضية تربط بين المواد الصلبة المزالة و متغيرات العملية، معامل الربط للمعادلة المقترحة كان ذو قيمة عالية بشكل ملحوظ، حيث كان 0.957، 0.974، و 0.944

بالنسبة الى النافثا الثقيلة : ميثايل ايثايل كيتون، النافثا الثقيلة : البيوتانول المستمر، و الى النافثا الثقيلة : البيوتانول المتفرع على الترتيب. افضل نسبة من الشوائب المتكتلة أزيلت عند، (30 د، 900 دورة، 30 درجة مئوية)، (45 د، 700 دورة، 35 درجة مئوية)، و (30 د، 700 دورة، 35 درجة مئوية) بالنسبة الى النافثا الثقيلة : ميثايل ايثايل كيتون، النافثا الثقيلة : البيوتانول المستمر، و الى النافثا الثقيلة : البيوتانول المتفرع على الترتيب .

الكلمات الرئيسية: التمثيل الرياضي، الاستخلاص-التلبد بالمذيبات، معالجة زيت التزييت المستهلك، نسبة الشوائب الصلبة المزالة.

1. INTRODUCTION

The increment of energy demand caused the consumption of the lubricating oils to be increased, resulted in yearly increment in the used oil production, beside to disposal issues raised up **Aremu et al., 2015**. Spent lubricating oils have to be recycled due to the presence of highly toxic materials in the oil turning them to highly noxious and carcinogenic such as heavy metals and polycyclic aromatic hydrocarbons (PAHs) **Yang et al., 2013**. Approximately 9 times higher, the crude oil required to produce a specific amount of base oil than that from used oil **Ogbeide, 2010**.

Several techniques were proposed for used oils treatment **Speight, and Exall, 2014**. The eldest acid/clay treatment method produced acidic sludge which is toxic, harm the environment, and difficult to dispose. The acid free vacuum distillation/clay treatment considered an expensive process due to large amount of clay required; besides it produced low yield percentage and quality where, large portion of base oil lost in the clay and relatively high metal content. These two processes are out of service in most of developed countries, and replaced by solvent extraction **Hamad et al., 2005,** and hydrogenation processes **Almutairi et al., 2007**. Hydrogenation treatment method associated with the difficult to control hydrogenation step and the need of catalyst which need to be replaced frequently.

Solvent extraction was preferred over other treatment processes because it solved the problems associated with them and considered a much lower cost than other. Re-refining of used lubricants by solvent extraction-flocculation process mainly associated with two objectives, recovering of base oil and segregating of solid contaminants which are extremely pollutant for the environment. Solvent extraction is a simple process where, the used oil is mixed with an efficient solvent able to flocculate the impurities at an appropriate ratio. The employed solvent is then recovered and can be used again, **Elbashir et al., 2002**.

Statistical modeling of process could have a direct influence on evaluation of the process variables; also result in saving resources and time **Du et al., 2006**. A few attempts were carried out for modeling the treatment of waste lubricants by solvent extraction process each with constricts of its own, such that carried by **Gul et al. 2014**, and **Naqvi et al., 2014**.

The aims of this study are to investigate the effect of operation variables on the PSR for Iraqi used lubricating oil (15W-40) and present them in a mathematical correlation based on the data experimentally found.

2. EXPERIMENTAL WORK

2.1 Materials

The feed to be treated was Al-Duraa (15W-40) used lubricating oil with n-Butanol, iso-Butanol, MEK (analytical grade solvents) and Heavy Naphtha (produced from Al-Duraa Refinery). The properties of the feedstock are indicated in **Table 1.**

2.2 Procedure

In the beginning, determination of the optimum solvent to oil ratio or the critical clarifying ratio (CCR) was carried out by pretreating (settling and heating) the feed. Then the feed was mixed with solvent at different solvent to oil ratio (SOR, 2:1 to 6:1) at, 25±2 ^{o}C, 30 min, mixing time, and 500 rpm, mixing speed, then left for settling at room temperature for 24 hours. After settling time was finished, two layers were formed, the upper one was the extraction solvent and base oil, and the bottom liquid phase was heavier material (contaminants). After separation the upper layer, the lower layer weighted. The wet sludge then was washed with the same used solvent and then dried at 105 ^{o}C for 15 min to remove any remaining solvent and weighted. The percent oil losses (POL) and percentage of sludge removal (PSR) was calculated by using Eq. (1) and Eq. (2) respectively, **Durrani et al., 2012**:

$$POL = \frac{Wwet - Wdry}{Wo}\% \quad (1)$$

$$PSR = \frac{Wdry}{Wo}\% \quad (2)$$

Where:
Wo The initial amount of used oil.
Wwet The wetted sludge.
Wdry The dried sludge.

The studied solvents were binary such as, N:MEK, N:n-But and N:Iso-But; at (20:80), (30:70), and (40:60) ratio of solvent to solvent were investigated. The optimum solvent to used oil ratio which is called the critical clarifying ratio (CCR) was calculated graphically as described by **Elbashir et al., 2002,** for the best binary system composition.

The operation variables were mixing time (15-60, min), mixing speed (300-900, rpm), and operating temperature (25-40, ^{o}C); by using adjustable hot plate magnetic stirrer (Heidolph®) which are able to mix up to 1400 rpm and heat up to 100 ^{o}C. The effect of these variables was investigated at the CCR of solvent to used oil.

3. RESULTS AND DISCUSSIONS

The experimental findings of the best solvent to solvent composition resulted that, the best binary solvent composition was 30:70 for all of the investigated solvents, as indicated in **Table 2**. By comparing the obtained values of the base oil yield, POL, and PSR of the three studied composition of binary solvent, the best binary was selected. 30:70 solvent to solvent ratio resulted in high base oil yield, low POL, and high PSR. At this ratio of solvent to solvent, the CCRs were obtained graphically and were equal to 3.4, 3.8, and 3.7 for N:nBut, N:iso-But, and N:MEK respectively, as indicated in **Fig. 1**. The obtained CCR does not necessary remove the maximum sludge, **Nimir*et al*., 1997.**

The effect of mixing time on sludge removal for the used solvents was shown in **Fig. 2**. For N:MEK, the PSR value increased with increasing the mixing time up to 45 min, this behavior can be attributed to: with increasing the mixing period the contacting between the solvent and used oil, as well as the contact between the

impurities with each other would increase, as a result more of the impurities. Beyond 45 min the PSR decreased, this behavior could be attributed to the flocculated impurities which would be dissociated after 45 min of mixing time. For N:n-But, at 15 min of mixing the PSR was higher than 30 min, after 15 min of mixing the two layers (extracted and raffinate) were not completely separated, that way the PSR was higher than at 30 min, as the POL was higher than at 30 min. After 30 min the PSR increased due to the more mixing time, the more of impurities were flocculated as well as the more of oil lost.

For N:Iso-But, increasing the mixing time up to 30 min increased the PSR, this can be explained as, the increment of mixing time increased the contacting time, and more of impurities flocculated. Increasing the mixing time more up to 45 min made the flocculated impurities to dissociate and the PSR decreased; after 45 min, the increment in the PSR value may be related to that the dispersed impurities before 45 min re-flocculated again. The difference between N:n-But and N:Iso-But can be attributed to the atoms configuration difference between n-Butanol and Iso-Butanol, **Filho et al., 2010**. These results were in agreement with the findings of **Hussein et al., 2014**,

Fig. 3 shows the effect of mixing speed on the sludge removal. As the mixing speed was increased up to 700 rpm, the sludge removal was increased due to increasing of contacting frequency of particles and each other. After 700 rpm high mixing frequency caused to dissociate and/or disperse of solid contaminants, thus the sludge removal percentage was decreased, these results were in agreement with the findings of **Hussein et al., 2014**,

The operating temperature has effect, but not as mixing time and mixing speed as shown in **Fig. 4**. At low temperature (25-30 ^{o}C) the sludge removal was increased, as the temperature increment would increase the affinity as a result the PSR increased; further increment of temperature would increase affinity, as well as the solubility of used oil in solvent **Durrani et al., 2012,** for this reason the percentage of sludge removal was decreased with increasing temperature. These results are in corresponding with the finding of **Durrani et al., 2012**, **Hussein et al., 2014**, and **Aremu et al., 2015**.

The optimized operating conditions were found to be as, (30 min, 900 rpm, 30 ^{o}C) for N:MEK, (45 min, 700 rpm, 35 ^{o}C) for N:n-But, and (30 min, 700 rpm, 35 ^{o}C), for N:Iso-But. The results indicated in **Table 3**, have been obtained at the optimized operating conditions. Decreasing specific gravity value indicates that aromatic compounds and solids have been removed, and lowering of ash content value indicates that dust or oxidation products, or arise from the additives that contain metals have been reduced **Speight and Exall, 2014**. Low value of viscosity index (VI) means that the non-metallic polymeric VI improver, **Kamal and Khan, 2009**. The decrement in the value of the used oil contaminants was in agreement with the finding of, **Kamal and Khan, 2009**, and **Mahmood, 2015**.

4. CORELATION ANALYSIS

The percentage of sludge removal during the extraction-flocculation process nonlinearly changed with the operation variables as indicated in **Fig. 2, 3,** and **4**. It has been indicated by **Naqvi et al. 2014**, that cubic polynomial function efficiently describes such a relation, so a cubic polynomial equation was suggested. The suggested equation variables were eliminated by backward technique. The good fit

indicator to be considered was the determination coefficient. The coefficients of determination R^2 were calculated by Eq. (3), **Naqvi et al., 2010**.

$$R^2 = \frac{SS_{regression}}{SS_{Total}} \quad (3)$$

Where:
R^2 Coefficient of determination.
SS Sum of square.

The best possible polynomial process correlation resulted contains the smallest number of PVs (predicted values) that best describes the variation of the sludge yield against process variables x in a statistically significant manner with high confidence level was the following:

$$\boldsymbol{y = A_o x_1 + A_1 x_1^2 + A_2 x_1^3 + A_3 x_2 + A_4 x_2^2 + A_5 x_1 x_2 + A_6 x_2 x_3 + A_7 x_1^2 x_2^3} \quad (4)$$

Where:
y Percentage of Sludge Removal.
x_1 Mixing Speed.
x_2 Mixing Time (min).
x_3 Operating Temperature (^oC).
A Constant.

Eq. (4) was constrained to the following constraints, $300 \leq x1 \leq 900$ rpm, $15 \leq x2 \leq 60$ min, and $25 \leq x3 \leq 40$ ^oC. All of the results concerning the suggested correlation were obtained by Statistica Software Program. The detailed equation for each of the studied binary solvent can be found in **Table 4**.

The statistical details of the process correlation equation obtained by *Statistica software program* can be found in **Table 5** and **Fig. 5**. In the analysis of variance **Table 5**, the variability amount (8.005657, 33.48974, and 55.27092) is obviously larger than the residual error amount (0.719098, 1.75763, and 6.56869) for N:MEK, N:n-But, and N:iso-but respectively. The significant difference is sufficient to confidently deny the null hypothesis. Besides the P value is less than 0.05; that is, no MLR relationship exists between (y) and the retained PVs **Naqvi et al. 2014**. The R^2 value was equal to 0.957, 0.974, and 0.944 for N:MEK, N:n-But, and N:iso-but respectively indicates that more than 95.7%, 97.4%, and 94.4% of the variation in the calibration response data has been absorbed by the process correlation. These are strong evidences, ensuring that in new circumstances (within the range of the process variable constraints) the correlation will have good predictive capability for percentage of sludge removal.

5. CONCLUSIONS

Solvent extraction-flocculation process operation variables have a direct influence on the percentage of sludge removal. But by using N:MEK, N:n-But, and N:Iso, the specific gravity significantly reduced to less than the virgin base oil value, the TAN value have been recovered to the same value of the virgin base oil, and the

ash content have been reduced by 50%. The studied variables were efficiently represent by a mathematical correlation, which could have a direct impact on the economic considerations as it was used to determine the optimum operating conditions, thus save the time and resources.

6. REFERENCES

- Almutairi, A., Bahzad, D. and Halabi, M. A., A, 2007, *Comparative study on the performance of a catalyst system for the desulfurization of two kinds of atmospheric residues*, Kuwait Export and Eocene residual oils. Catalysis Today, 125, 203.
- Brandenberger, S., Mohr, M., Grob, K. and Neukom, H. P., 2005, *Contribution of unburned lubricating oil and diesel fuel to particulate emission from passenger cars*. Atmospheric Environment. 39, 6985.
- Du, G., Yang, Y., Qiu, W., Lim, S., Pfefferle, L. and Haller, G. L., *2006, Statistical design and modeling of the process of methane partial oxidation using V-MCM-41 catalysts and the prediction of the formaldehyde production".* Applied Catalysis A, vol. 313, no. 1-2, pp. 1 13.
- Durrani H.A., Panhwar M.I. and Kazi R.A., 2011, *Re-Refining of waste lubricating oil by solvent extraction.* Mehran University Research Journal of Eng. & Tech., 30(2), 237- 246.
- Elbashir, N.O., Al-Zahrani, S.M., Abdul Mutalib, M.I., and Abasaeed, A.E., 2002, *A Method of Predicting Effective Solvent Extraction Parameters for Recycling of Used Lubricating Oils.* Journal of Chemical Engineering and Processing, Volume 41, pp. 765-769.
- Filho, J. L. A., Moura, L. G. M., and Ramos, A. C. S. , 2010, *Liquid-liquid extraction and adsorption on solid surfaces applied to used lubricant oils recovery*. Brazilian Journal of Chemical Engineering, Vol. 27, No. 04, pp. 687 – 697.
- Gul, S., Irfan, M., Bilal, H., Atta-ur-rehman, Khan, U., and khan, S., 2014, *Recycling of Used Engine Oil Using Solvent Extraction and Distillation".* J. Engg. and Appl. Sci. Vol. 33 No. 2 July - December.
- Hamad, A., Al-Zubaidy, E., and Fayed, M. E., 2005, *Used lubricating oil recycling using hydrocarbon solvents.* Journal of Environmental Management, 74, 153.
- Hani, F. B., And Al – Wedyan H., 2011, *Regeneration of base-oil from waste- oil under different conditions and variables*. African Journal of Biotechnology, Antje Hansmeier, ISBN: 978 – 90 – 386 – 2264 – 4.
- Hussein, M., Amer, A. A., and Gaberah ,A. S., 2014, *Used lubricating oils re-refining by solvent extraction.* American Journal of Environmental Engineering and Science ; 1(3), pp. 44-50.
- Kamal, A., and Khan, F.,2009, *Effect of extraction and adsorption on re-refining of used lubricating oil.* Oil & Gas Science and Technology, 64 (2), 191-197.
- Kamal, M. A., Naqvi, S. M. D., and Khan, F., *"Optimized liquid-liquid extractive rerefining of spent lubricants"*. The Scientific World Journal Volume 2014, Article ID 458789, 10 pages, (2014).
- Mahmood, S. M., MSc. Thesis, 2015, *Study the effect of different working variables on the re-refining used lubricating oil and reduced the environmental conditions*. University of Al-Nahrain, Chemical Engineering Dep..
- Muhammad Ashraf Kamal, Syed Mumtaz Danish Naqvi, and Fasihullah Khan, 2014, *Optimized Liquid-Liquid Extractive Rerefining of Spent Lubricants*. The Scientific World Journal Volume 2014, Article ID 458789, 10.

- Naqvi, S. M. D., Kamal, M. A., and Khan F., 2010, *Selective homogeneous oxidation system for producing hydroperoxides concentrate: kinetic simulation of catalytic oxidation of gas oils.* Industrial and Engineering Chemistry Research, vol. 49, no. 16, pp. 7210–7226.
- Nimir O.M., AbdulMutalib M.I., and Adnan R., 1997, *Recycling of used lubrication oil bySolvent Extraction – A guideline for Single Solvent Design*. Institute of Technology PETRONAS, 31750 Tronoh, Perak, Malaysia, session B2–4, 420 – 42.
- Ogbeide S.O., 2010, *An Investigation To The Recycling Of Spent Engine Oil.* Journal of Engineering Science and Technology Review , 3(1), 32-35.
- Rauckyte, T., Hargreaves, D. J. and Pawlak, Z., 2005, *Determination of heavy metals and volatile aromatic compounds in used engine oils and sludges".* Fuel, 85, 481.
- Speight, J. G., and Exall, D. I., 2014, *Refining used lubricating oils.* CRC Press, Taylor & Francis Group, Boca Raton, Florida. Ch. 1,2,4 and 7.
- Speight, J. G., and Exall, D. I., 2014, *Refining used lubricating oils.* CRC Press, Taylor & Francis Group, Boca Raton, Florida. Ch. 1,2,4 and 7.
- Yang, X., Chen, L., Xiang, S., Li, L., and Xia, D., 2013 *Regeneration of Waste Lubricant Oil by Extraction−Flocculation Composite Refining*. Ind. Eng. Chem. Res., 52, 12763−12770.
- Yee, F. C., Yunus, R. M., and Sin, T. S., 2002, *New Modeling and Simulation of Used Lubricant Oil Re-refining Process.* 2nd World Engineering Congress, Sarawak, Malaysia, 22-25 July.

Table 1. The properties of the Al-Daura oils.

No.	Specification	Base oil	Virgin oil	Used oil
1	Specific gravity@ 60/60 °F	0.8822	0.8854	0.8933
2	Viscosity, cSt, @ 40°C	65.811	113.6	117.02
3	Viscosity, cSt, @ 100°C	8.656	14.994	15.134
4	Viscosity index	100.6	136.9	134.4
5	Ash wt.%	0.002	0.002	1.051
6	Total acid number (TAN) mg/g.	5.928	2.903	3.584
7	Water wt.%	Nil	Nil	Nil

Table 2. Experimental results of binary solvents at different composition.

		N:MEK			N:n-But			N:Iso-But		
	SOR	Yield	POL	PSR	Yield	POL	PSR	Yield	POL	PSR
40:60	2:1	88.45	13.40	5.57	76.1	24.93	3.83	74.25	21.29	7.11
	3:1	89.71	10.28	3.91	83.7	22.06	3.51	78.27	17.39	3.57
	4:1	95.27	8.825	3.70	86.4	10.44	2.41	78.40	12.81	2.16
	5:1	95.04	5.037	2.99	89.2	7.657	0.58	79.45	10.85	1.13
	6:1	95.52	2.164	2.20	91.3	4.827	0.21	80.52	10.74	0.71

30:70	2:1	92.04	7.62	4.12	89.43	11.65	3.54	92.30	9.19	6.49
	3:1	92.13	7.24	2.95	90.55	9.11	1.00	94.22	9.11	1.41
	4:1	92.57	3.50	1.75	90.60	7.57	0.96	98.38	6.03	0.75
	5:1	93.62	2.75	1.42	91.72	6.16	0.54	98.96	5.62	0.74
	6:1	95.75	2.08	1.04	94.96	4.70	0.12	99.79	5.70	0.46
20:80	2:1	85.48	20.52	1.33	88.56	6.03	4.24	80.19	16.35	6.70
	3:1	88.97	15.70	0.92	88.47	4.37	0.96	92.55	11.03	5.20
	4:1	89.09	4.79	1.00	88.68	4.29	0.71	94.30	8.07	4.12
	5:1	89.68	4.04	0.71	89.76	3.87	0.69	94.63	6.82	3.99
	6:1	90.67	3.37	0.37	91.14	3.33	0.33	95.50	6.45	3.91

Table 3. The Properties of used oil and recovered base oil at the optimized conditions.

Properties	Used oil	Recovered base oil		
		N:MEK	N:n-But	N:Iso-But
Specific gravity at 15°C g/cm^3	0.8934	0.8785	0.8802	0.8803
Viscosity at 40 ^{o}C ,cSt	117.02	26.293	44.893	26.982
Viscosity at 100 ^{o}C, cSt	15.134	5.048	7.197	5.096
Viscosity index (VI)	134.4	120.5	121.2	118.2
Ash content (wt%)	1.0511	0.8051	0.6070	0.5767
Water Content	Nil	Nil	Nil	Nil
Total acid number (mg KOH/g oil)	3.5839	1.9702	2.8542	2.1786
Yield (%)	-	86.25	87.75	88.88
POL (%)	-	4.54	8.46	3.62
PSR (%)	-	2.54	5.63	6.12

Table 4. The binary solvent mathematical correlations.

Solvent	Correlation	R^2
N:MEK	$y = 0.0396\,x_1 - 5.98E-5\,x_1^2 + 4.5E-8\,x_1^3 - 1.0578\,x_2 + 0.0282\,x_2^2 + 4.44E-4\,x_1x_2 - 0.002\,x_2x_3 - 1.025E-9\,A_7x_1^2x_2^3$	0.957
N:n-But	$y = -0.0911\,x_1 + 0.0003\,x_1^2 - 1.5E-7\,x_1^3 + 0.261\,x_2 + 0.013\,x_2^2 - 0.0012\,x_1x_2 + 0.0016\,x_2x_3 - 5.13E-10\,x_1^2x_2^3$	0.974
N:iso-But	$y = -0.1871\,x_1 + 0.0004\,x_1^2 - 2.82E-7\,x_1^3 + 3.8279\,x_2 - 0.0771\,x_2^2 - 0.0018\,x_1x_2 - 0.0072\,x_2x_3 + 2.58E-9\,x_1^2x_2^3$	0.944

Table 5. Analyses of variance and goodness of fit of the correlation with using binary solvents.

Heavy Naphtha : MEK (N:MEK)				
	SS	DF	MS	P-value
Regression	64.04525	8.00	8.005657	0.0169
Residual	2.87639	4.00	0.719098	
Total	66.92164	12.00		
Heavy Naphtha : n-But (N:n-But)				
	SS	DF	MS	P-value
Regression	267.9179	8.00	33.48974	0.0062
Residual	7.0305	4.00	1.75763	
Total	274.9485	12.00		
Heavy Naphtha : iso-But (N:iso-But)				
	SS	DF	MS	P-value
Regression	442.1674	8.00	55.27092	0.0281
Residual	26.2748	4.00	6.56869	
Total	468.4421	12.00		

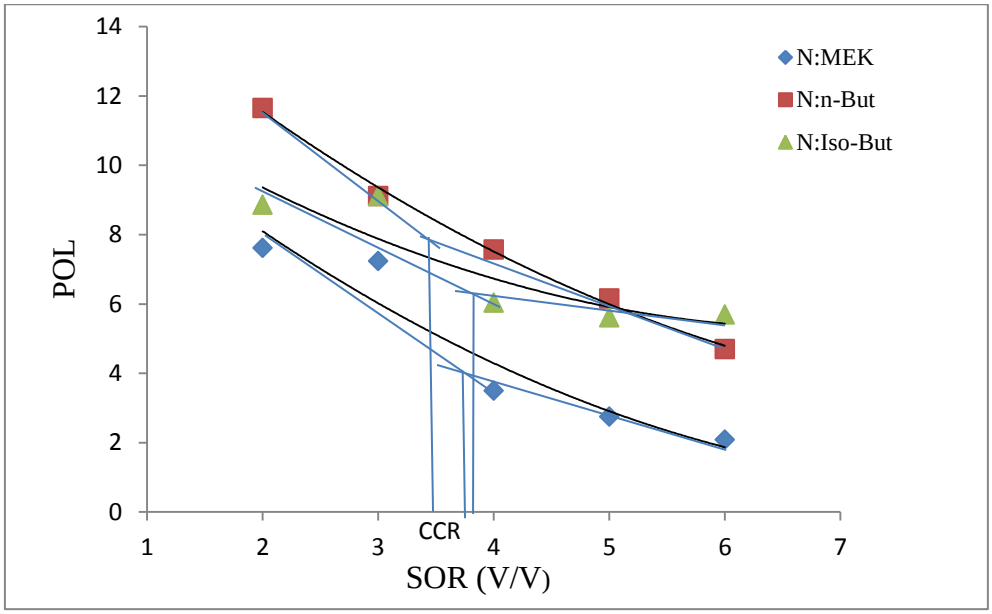

Figure 1. Graphical determination of the critical clarifying ratio (CCR) based on percentage of oil loss (POL).

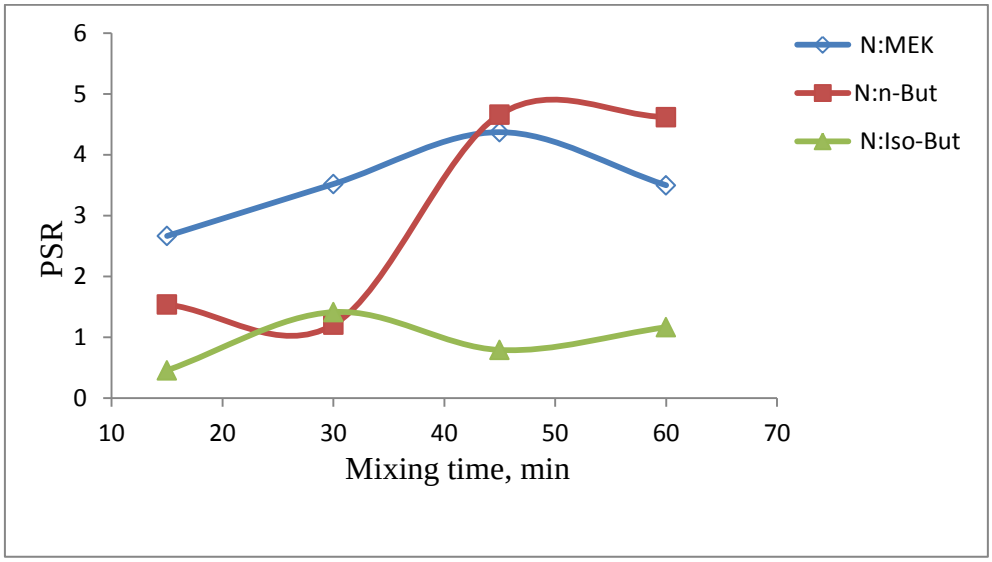

Figure 2. The effect of mixing time on the percentage of sludge removal (PSR).

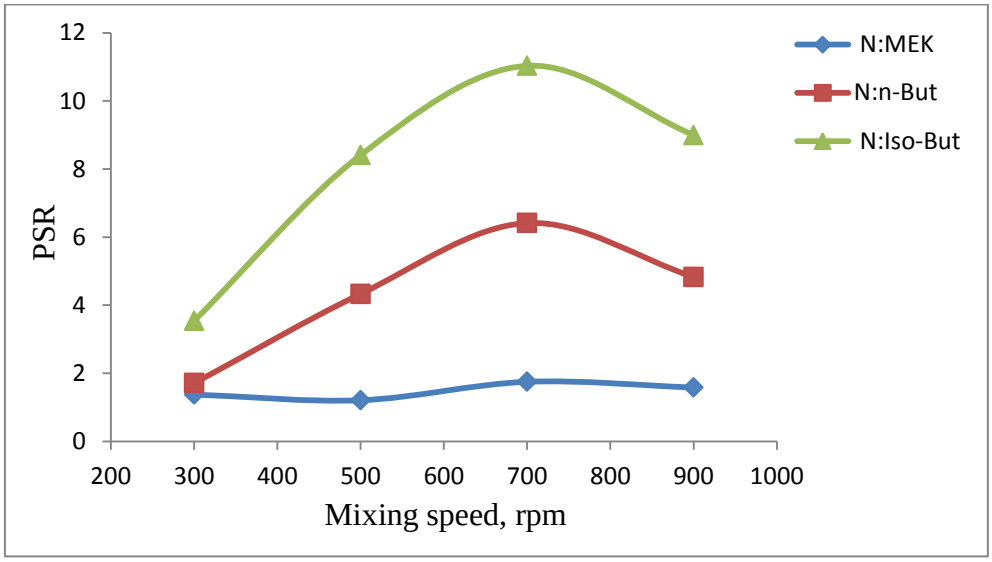

Figure 3. The effect of mixing speed on the percentage of sludge removal (PSR).

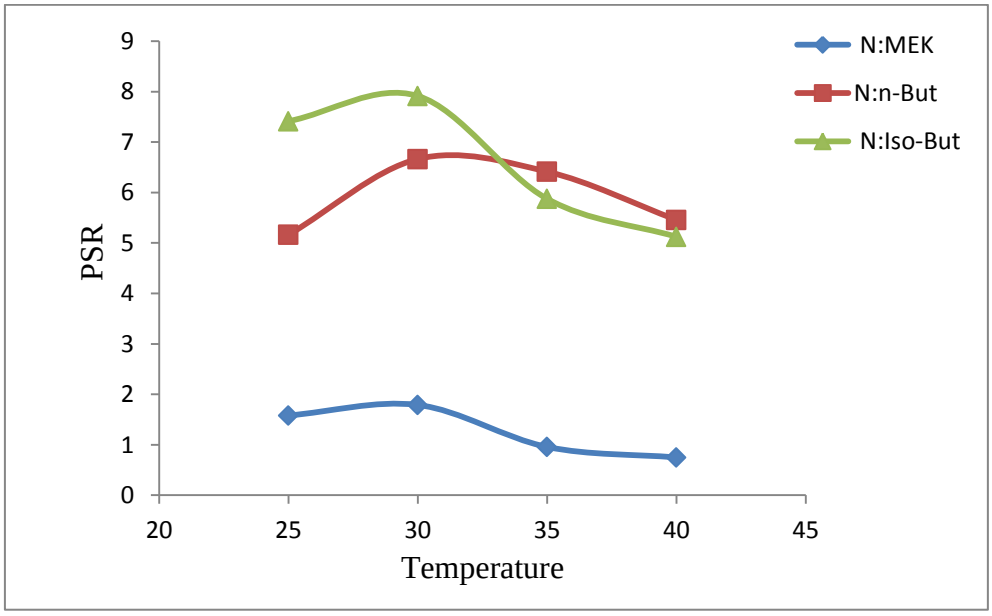

Figure 4. The effect of operating temperature on the percentage of sludge removal (PSR).

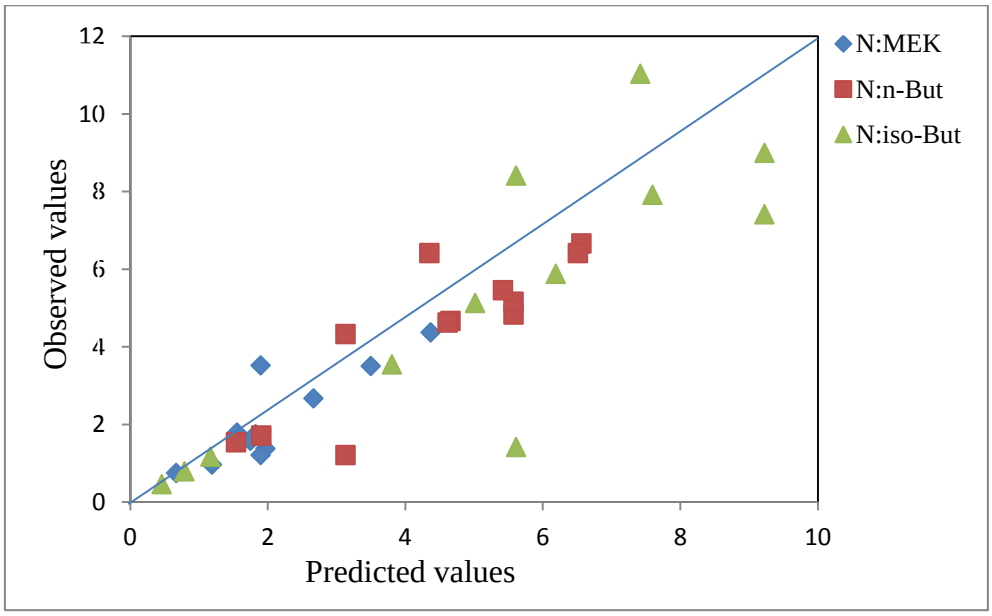

Fig 5. The observed versus predicted values of the PSR.

Design and Implementation of Classical Sliding Mode Controller for Ball and Plate System

Marwa Mohammed Alwan
MSc Student
Control and Systems Eng. Dep.
University of Technology, Baghdad- Iraq
marwa.aldalbozi@gmail.com

Dr. Laith Jasim Saud
Assistant Professor
Control and Systems Eng. Dep.
University of Technology, Baghdad- Iraq
laithjasim15@yahoo.com

ABSTRACT

Ball and Plate (B&P) system is a benchmark system in the control engineering field that has been used to verify many control methods. In this paper the design of a sliding mode controller has been investigated and verified in real-time via implementation on a real ball and plate system hardware. The mathematical model has been derived and the necessary parameters have been measured. The sliding mode controller has been designed based on the obtained mathematical model. The resulting controller has been implemented using the Arduino Mega 2560 and a ball and plate system built completely from scratch. The Arduino has been programmed by the Arduino support target for Simulink. Three test signals has been used for verification purposes, namely: single point stabilizing, circular trajectory tracking, and square trajectory tracking. The results obtained have shown that sliding mode controller is able to follow the desired test signals with low error.

Keywords: Ball and Plate, Sliding Mode Controller, Arduino.

تصميم وتنفيذ متحكم منزلق كلاسيكي لنظام الكرة ولوحة

مروة محمد علوان
طالبة ماجستير
قسم هندسة السيطرة و النظم
الجامعة التكنولوجية، بغداد-العراق

د. ليث جاسم سعود
أستاذ مساعد
قسم هندسة السيطرة و النظم
الجامعة التكنولوجية، بغداد-العراق

الخلاصة

الكرة واللوحة هو نظام قياسي في مجال هندسة التحكم حيث تم استخدامه للتحقق من العديد من طرق السيطرة. في هذه الورقة تم تصميم متحكم انزلاق كلاسيكي والتحقق من ادائه في الوقت الحقيقي من خلال استخدامه في نظام حقيقي للكرة و اللوحة. تم في هذا البحث اشتقاق النموذج الرياضي للمنظومة مع قياس المعلمات الضرورية. وقد تم تصميم متحكم انزلاق كلاسيكي على أساس النموذج الرياضي الذي تم الحصول عليه. وقد تم تنفيذ المتحكم الناتج باستخدام "اردوينو ميجا 2560" ونظام الكرة واللوحة حيث تم بناء هذا النظام بالكامل من الصفر. تمت برمجة "اردوينو" من خلال برنامج Simulink. وقد استخدمت ثلاث إشارات اختبار لأغراض التحقق، وهي: الاستقرار في نقطة واحدة ، وتتبع مسار دائري، وتتبع مسار مربع. وقد أظهرت النتائج أن متحكم الانزلاق قادر على اتباع إشارات الاختبار المطلوبة مع خطأ منخفض.

الكلمات الرئيسية: الكرة و اللوحة، متحكم الانزلاق، اردوينو.

1. INTRODUCTION

The ball and plate (B&P) system shown in **Fig. 1** is a promoted version of the traditional ball and beam control problem. The problem consists of a plate which its inclination can be manipulated in two perpendicular directions. The goal is to carry the ball moving on the plate to a desired position, that is to control a freely rolling ball in a specific position or moving it on a trajectory on the plate. The B&P apparatus is a two dimensional electromechanical device which can be further categorized as nonlinear, multivariable (with two inputs and two outputs) and unstable system. Furthermore, the system is under-actuated, as it possesses more degrees of freedom than the number of available actuators. Thus, the fact that the ball‘s motion is indirectly controlled by changing the plate inclination in two orthogonal directions is quite an interesting challenge to consider. B&P system has a direct application in robotic manipulation of round objects. When it comes to indirect applications, the system can present many challenges and opportunities as an educational tool to university students studying control systems engineering.

Unlike other educational models, the B&P system has several interesting features for the study of unstable and nonlinear systems. Firstly, models like Magnetic Levitation, Inverted Pendulum and Ball and Beam are all one-dimensional. The degree of freedom (DOF) for Magnetic Levitation is one, for Inverted Pendulum and Ball and Beam is two. The B&P system has four DOF, i.e., with two independent motions of the ball about the plane of the plate and another two motions of the combined ball and plate inclinations (rotations) about the fixed pivot at the center of the plate. Secondly, the B&P system offers an opportunity to study trajectory tracking problems in addition to the stability problems that is the only subject that could be studied in the remaining educational models mentioned.

The ball and plate system has been studied and controlled in several control methods that ranged from linear control technique for optimal, intelligent, and nonlinear control. Some of the recent available researches on the ball and plate system are reviewed in this section.

In Linear controllers field: **Jadlovská, et al., 2009** have designed PD, PID and proportional sum derivative (PSD) controllers for trajectory tracking of the ball and plate system. The result showed that the PD controller is much better than the PID controller with a relatively small overshoot. **Ghiasi, and Jafari, 2012** have designed an optimal robust ($H\infty$) controller for the ball and the plate system. The ($H\infty$) controller has been designed based on lower fractional transformation structure with multiplication uncertainty. The authors didn’t show the transfer function of the ($H\infty$) controller nor the (γ) parameter which is an essential part of determining if the control system is robust or not. **Zeeshan, et al., 2012** have focused on the hardware implementation of the ball and plate with a cost effective design. They have used an array of eleven by eleven phototransistors to get ball position. This method gives a direct discrete position of the ball, but with low resolution. This required precise placement of laser sensors and the phototransistors. Two DC motors, one on top of the others was used to move the plate. A standard PID controller is used to implement position tracking. **Galvan-colmenares, et al., 2014** have proposed a duel PD controller to solve the ball and plate regulation problem. A novel model for a ball a plate has been developed in the form of robot manipulator equations. The authors used the model for the stability test and to design dual nonlinear compensator for nonlinearities cancellation. According to their results the PD controller with compensator gave better results when compared with PD without compensator. **Singh, and Saxena, 2015** have designed a PD controller for trajectory tracking problem of the ball and plate system. The PD controller was used in a cascaded control scheme, where an inner PD controller was used to control the plate dynamics and the outer PD controller was used to control the ball dynamics. The gains of PD controllers have been tuned by PSO.

In Intelligent controllers field: **Wang, et al., 2008** have designed a trajectory tracking controller for the ball and plate system. The control system consists of a double loop structure. The inner loop has a servo controller, while the outer loop has a position regulator. The external loop was a single rule fuzzy logic controller with position, velocity and acceleration as inputs and plate angle as output. **Dong, et al., 2009** have designed a GA Fuzzy Neural Network Controller (GA-FNNC) for the stabilization problem of ball and plate system. The controller consists of 5 layers. The first layer is the input linguistic layer which is the error and change of error. The second layer represents the membership functions. The third layer are the rules. The fourth layer is to make rules unitary. The fifth layer is the output layer. GA is used to find the optimal weights of the Neural Network. **Han, et al., 2012** have designed aneural network PID controller (PIDNN) to solve trajectory tracking problem of ball and plate system. Two PIDNN were used, one for each axis. A differential evaluation PSO (DEPSO) has been used to train PIDNN weight online. **Pattanapong, and Deelertpaiboon, 2013** have designed a Fuzzy PD controller with with an adaptive integral action for stabilization and trajectory tracking of the ball and plate system.

In Sliding mode field: **Park, and Lee, 2003** have used an industrial robot manipulator as an actuator to change the plate's angle. It has been assumed the motion of the ball and plate is slow enough to neglect the dynamics of industrial robot. A classical sliding mode controller is used for trajectory tracking purpose, it has performed well with tracking and was robust to uncertainty.

Liu, et al., 2009 have designed a sliding mode controller for the ball and plate system. Two scenarios have been used to deal with the uncertainties. In the first scenario, an upper and lower bound has been assumed on the uncertain items and disturbances. In the second scenario, an observer has been used to estimate it. The later scenario gave a better response in terms of tracking and disturbance rejection when compared to the first one. Debono and Bugeja **Debono, and Bugeja, 2015** have designed integral sliding mode and state feedback controllers for the ball and plate system. An upper bound on the disturbance and uncertain items has been assumed in simulation. In the practical implementation, the integral sliding mode controller has been able to track a sinusoidal signal with magnitude of ±0.11m and frequency of 3Hz. **Negash, and Singh, 2015** have used a sliding mode controller with fuzzy logic to control the ball and plate system. A double loop structure has been used to control the ball position. The sliding mode controller was used in the outer loop to stabilize the ball. A linear compensator based on Diophantine equation was used in the inner loop to control the x and y axis motors. The sliding mode chattering has been reduced by using fuzzy logic.

2. THE MATHMATICAL MODEL

Before any controller design, it is important to obtain a mathematical model for the system to be controlled which is a closest approximation of its true behavior. The system can then be analyzed, and controller can be designed to meet the required performance. The ball and plate system equations is given by **Negash, and Singh, 2015**:

$$\left(m+\frac{J_B}{R^2}\right)\ddot{x}-mx\left(\dot{\theta}_x\right)^2-my\dot{\theta}_x\dot{\theta}_y=mg\sin\theta_x \tag{1}$$

$$\left(m+\frac{J_B}{R^2}\right)\ddot{y}-my\left(\dot{\theta}_y\right)^2-mx\dot{\theta}_x\dot{\theta}_y=mg\sin\theta_y \tag{2}$$

$$(mx^2 + J_B + J_{P_x})\ddot{\theta}_x + 2mx\dot{x} + mxy\ddot{\theta}_y + m(\dot{x}y + x\dot{y})\dot{\theta}_y = \tau_{\theta_x} - mgx\cos\theta_x \quad (3)$$

$$\left(my^2 + J_B + J_{P_y}\right)\ddot{\theta}_x + 2my\dot{y}\dot{\theta}_y + mxy\ddot{\theta}_x + m(\dot{x}y + x\dot{y})\dot{\theta} = \tau_{\theta_y} - mgycos\,\theta_y \quad (4)$$

The schematic diagram of the ball and plate system that these equations describe is given in **Fig. 2**, while, the nomenclature is given in **Table 1** and the parameters' values are shown in **Table 2**. Eq. (1) and Eq. (2) describe the ball motion on the plate, and they tell that the acceleration of the ball movement depends on the angles and the angular velocity of the plate inclination. Eq. (3) and Eq. (4) tell how the plate inclination dynamics is influenced by the external driving forces. The system can be simplified with the following assumptions:

1. If the system inputs are considered as θ_x and θ_y instead of the torque moments $\tau_{\theta_x}$and τ_{θ_y}, where the plate is assumed to move to the specified angles instantaneously, then the equations (3) and (4) could be dropped out.
2. In the steady state, the plate should be in the horizontal position where both inclination angles are equal to zero. If one assumes that the angle do not change much, say ±30°, the sine function can be replaced by its argument.

Based on these basic assumptions and by substituting the moment of inertia of the ball, $J_B = \frac{2}{5}mR^2$ into Eq. (1) and Eq. (2), two ordinary differential equations are obtained.

$$\ddot{x} = B\theta_x + \delta_x \quad (5)$$

$$\ddot{y} = B\theta_y + \delta_y \quad (6)$$

Where $B = \frac{5}{7}g$, $\delta_x = mx\left(\dot{\theta}_x\right)^2 + my\dot{\theta}_x\dot{\theta}_y$, and $\delta_y = my\left(\dot{\theta}_y\right)^2 + mx\dot{\theta}_x\dot{\theta}_y$

3. CLASSICAL SLIDING MODE CONTROL, Utkin, et al., 2009

Consider a nonlinear dynamical system described by

$$\dot{x} = f(x) + g(x)u + h(t,x) \quad (7)$$

Where $x \in \mathbf{R}^n$ is the state vector, $u \in \mathbf{R}^m$ is the control vector, $(x) \in \mathbf{R}^n$, $g(x) \in \mathbf{R}^{n\times m}$ are generally nonlinear functions, and $h(x) \in \mathbf{R}^n$ is the uncertainties and disturbances. The task is to design a function of states called sliding function and a state-feedback control law $u\left(x(t)\right)$ That will drive the state towards the sliding surface (reaching phase), see **Fig. 3**, and then slide it to origin $x = [0 \quad 0 \quad ... \quad 0 \quad]^T$ (sliding phase). If the states are considered as the difference between some physical states and desired trajectories, then a tracking behavior can be ensured if the states return to origin. The design of sliding mode controller requires:

I. Selecting a manifold or sliding surface in such a way that makes the system follow a desirable performance when the trajectory subjected to the sliding manifold.
II. Finding a feedback control law that makes the system trajectory hits the sliding surface and stays on it.

The surface function $s(x)$ is designed to resemble the distance of the states x to the sliding surface. The value of $s(x)$ must not equal "0" when that state is away from the sliding surface, and equals "0" when the state is on the sliding surface. The control law of the sliding mode controller will switch its value based on the sign of this distance. So, the sliding mode

controller will always try to direct the states towards the sliding surface where *s(x)* = 0. Since the controller is not a continuous one, the time to reach the surface is finite, and any trajectory hits the surface will slide along it to the origin *x* = 0.

To make the system states satisfy $s(x) = 0$, the following conditions are required:

I. Reaching $s(x) = 0$ has to be ensured from any initial condition.
II. Once $s(x) = 0$ is reached, the control action has to be able to maintain it.

Based on that lets consider the following Lyapunov function candidate:

$$V\big(S(x)\big) = \frac{1}{2}S^T(x)S(x) = \frac{1}{2}\|S(x)\|_2^2 \tag{8}$$

Where $\|.\|$ is Euclidean norm, i.e., $\|S(x)\|_2$ is the distance to the manifold where $S(x) = 0$. A sliding mode will exist when the sufficiency condition $\frac{dV}{dt} < 0$ is satisfied (where; $\frac{dV}{dt} = \frac{dV}{dS} \times \frac{dS}{dt}$). This condition is also known as the reachability condition. As an example, when a scalar system is considered (with $n = 1$ in Eq. (7)), to achieve $s\frac{dS}{dt} < 0$ the feedback control law $u(x)$ is designed so that s and $\frac{dS}{dt}$ have opposite signs. That is;

1. $u(x)$ makes $\frac{dS}{dt}$ negative when $s(x)$ is positive.
2. $u(x)$ makes $\frac{dS}{dt}$ positive when is $s(x)$ is negative.

So for the system given in Eq. (7) and the Lyapunov function candidate given in Eq. (8) we have:

$$\dot{V}(s) = s\dot{s} \tag{9}$$

according to existence and reachability condition

$$s\dot{s} < 0 \tag{10}$$

The time derivative of the surface function $S(x)$ is given by:

$$\begin{aligned}\dot{s}\,(x) &= \frac{\partial s}{\partial x}\dot{x} = \frac{\partial s}{\partial x}\{f(x) + g(x)u + h(t,x)\} \\ &= \frac{\partial s}{\partial x}f(x) + \frac{\partial s}{\partial x}g(x)u + \frac{\partial s}{\partial x}h(t,x)\end{aligned} \tag{11}$$

Thus, the responsibility of the control action is to keep the states directed toward the surface, hence $u(t)$ is given by

$$u(t) = -\left\{\frac{\partial s}{\partial x}g(x)\right\}^{-1}\left(\frac{\partial s}{\partial x}f(x) + k_d sign\big(s(x)\big)\right) \tag{12}$$

Where; k_d is the switching gain that usually compensates for the uncertainties and the disturbances in case their upper bounds are known. By substituting Eq. (12) in Eq. (11):

$$\dot{s} = \frac{\partial s}{\partial x} h(t,x) - k_d sign\big(s(x)\big)$$
$$\dot{s} = -sign\big(s(x)\big)\left(k_d - \frac{\partial s}{\partial x} h(t,x) sign\big(s(x)\big)\right) \tag{13}$$

By choosing k_d as Eq. (14) states, the condition Eq. (10) can be ensured.

$$k_d > \left|\frac{\partial s}{\partial x} h(t,x) sign\big(s(x)\big) + \eta\right| \tag{14}$$

Where η is a small positive design scalar. The condition in Eq. (10) becomes;

$$s\dot{s} \leq -\eta|S| \tag{15}$$

From mathematical point of view, the differential equation Eq. (7) can no longer be solved because the input signal is no longer unique. One method to solve Eq. (7) that was suggested by **C. Edwards, and S. K. Spurgeon, 1998** is the method of equivalent control. The equivalent control is the required control action to maintain the sliding motion and is derived by equating Eq. (11) to zero without considering the uncertainty $h(t,x)$.

$$0 = \frac{\partial s}{\partial x} f(x) + \frac{\partial s}{\partial x} g(x) u_{eq}$$
$$u_{eq} = -\left\{\frac{\partial s}{\partial x} g(x)\right\}^{-1} \frac{\partial s}{\partial x} f(x) \ \ \forall x \tag{16}$$

In fact, the equivalent control is the low frequency component of the switching signal, or in other words, low pass filtering the infinitely fast switching control input. In general, Eq. (16) would not itself induce a sliding motion and it does often form part of the overall control law, as shown in the first term of Eq. (12). However, despite the fact that the Eq. (16) and the first term of Eq. (12) is identical, their interpretation is different. Where the equivalent control gives a continuous interpretation of the total control signal, the first term of Eq. (12) should be seen as an approximation of the required signal to maintain sliding mode.

The classical sliding mode controller design for the ball and plate system is given below:

Returning to the Eq. (5), the design for x axis is as following:

$$\ddot{x} = B\,(\sin(u) + \delta_x) \tag{17}$$

$$s = \dot{e} + \lambda e \tag{18}$$

Where:

$$e = x - x_d \tag{19}$$

$$\dot{e} = \dot{x} - \dot{x}_d \tag{20}$$

$$\ddot{e} = \ddot{x} - \ddot{x}_d \tag{21}$$

$$\dot{s} = \ddot{e} + \lambda \dot{e} \tag{22}$$

With substituting Eq. (21) in Eq. (22):

$$\dot{s} = \ddot{x} - \ddot{x}_d + \lambda \dot{e} \tag{23}$$

$$\dot{s} = B\,(\sin(u) + \delta_x) - \ddot{x}_d + \lambda \dot{e} \tag{24}$$

$$s\,\dot{s} = s(B\,(\sin(u) + \delta_x) - \ddot{x}_d + \lambda \dot{e}) \tag{25}$$

$$u = \sin^{-1}\left[\frac{1}{B}\left(\ddot{x}_d - \lambda \dot{e} - k\,sgn(s)\right)\right] \tag{26}$$

$$s\,\dot{s} = s(-k\,sgn(s) + \delta_x) \tag{27}$$

$$s\,\dot{s} = -k|s| + s\delta_x \tag{28}$$

$$s\,\dot{s} \leq -k|s|[k - |\delta_x|] \tag{29}$$

$$k \geq |\delta_x| \tag{30}$$

$$\therefore u = \sin^{-1}\left[\frac{1}{B}\left(\ddot{x}_d - \lambda \dot{e} - k\,sgn(s)\right)\right]\ with\ k \geq |\delta_x| \tag{31}$$

Where: λ is the slope of the sliding surface. The same procedure is repeated to design the controller for the y axis by using Eq. (6). In both controllers, a saturation function is used instead of "signum" to reduce chattering.

4. BALL AND PLATE HARDWARE

The ball and plate hardware consists of several components that are working together in harmony to accomplish the central task of ball stabilizing and trajectory tracking. The system can be divided into two parts: mechanical system and electrical system. In mechanical system the physical structure of the ball and plate is presented which consists of the plate, joints, linkage... etc. The electrical components consist of the microcontroller, touch screen, motors...etc.

The mechanical system represents the physical structure of the ball and plate system in which several components are present. A comprehensive view of the system with the components being apart is shown in **Fig. 4**. The structure consists of a plate made from Acrylic in which the touch screen will be fitted inside. This plate sits on central pillar which goes inside a universal joint this makes the plate able to tilt in two perpendicular directions. Two braces are attached to the plate to deliver the movement of the two servo motors to the plate via linkages. The linkages will transmit the motor movement from the servo arm to the braces, each linkage has a ball joint end to enhance the movement. The whole structure is fitted on a wood made base. The description of each component in **Fig. 4** is shown in **Table 3**.

The electrical system is responsible for ball position sensing and plate moving and controlling. It consists of a touch screen, servo motors, Arduino MEGA, DC-DC converter, and power supply. A resistive touch screen works by applying a voltage across a resistor network, see **Fig. 5**, and measuring the change in resistance at a given point on the matrix where a screen is touched by an input stylus, pen, or finger. The 5-wire touch screen panel works by applying a voltage at the corners of the bottom resistive layer and measuring the vertical or horizontal resistive network with the wiper, or 5th wire which is embedded in the top sheet. The servo

motor is a titanium gear D-940TW, which is part of Hitec's D-Series with high-resolution and high-speed technology. The response time is 0.07 sec/60° at no load when supplied with 7.5V. The Arduino Mega 2560 is a microcontroller board that is used to implement the sliding mode controller, and it has been programmed in Simulink software. An adjustable step-down module DC-DC converter is used to step down a 12V to 7.5V, which is necessary for the servo motors. The DC-DC converter used is the LM2596. A PC power supply unit is used to power up the motors. This power supply provides 12V which is stepped down to 7.5V and then delivered to the motors.

The electrical schematic diagram is shown in **Fig. 6**. The touch screen is connected to the C-Port of the Ardunio Mega which is represented by pins A0-A4. The servo Motor X is connected to D7 PWM pin, and the servo Motor Y is connected to D8 PWM pin.

Fig. 7 shows the real construction of the ball and plate system. The Arduino Mega is connected to a laptop PC through the USB port. This connection is necessary to plot various signals such as the ball position, the error, and so on. The software on the PC is Simulink which is used to plot signals only. The control algorithm runs inside Arduino with the help of Simulink support for embedded hardware add-one. This add-one will convert a Simulink file into C-code and write it directly to the Arduino program memory so the code runs independently of the PC.

The rest of this paper is organized as follows. Section 2 introduces the mathematical model of the ball and plate system. Classical Sliding Mode theory and controller design for trajectory tracking is presented in Section 3. The Ball and Plate system hardware is described in section 4. Implementation and results are shown in section 5.

5. IMPLEMENTATION AND RESULTS

The implementation Simulink file consist of three parts. The first part is shown in **Fig. 8** which contains the touch screen block and the range converter block that converts the position signal from integer to meter. The discrete derivative is used to get the ball velocity from the position. The obtained signals enter to Kalman filter to reduce noise. The second part is given in **Fig. 9**, the first block represents the reference signals. The equations of the circular path case or the square path case, or the point case, are represented inside this block. The sliding mode controller block, **Fig. 10**, contains the classical sliding mode controller equations. The 180/pi block will convert the signal from radian to degree. The saturation block will limit the angle to +/-10 °. The range converter will convert the range from (-45 ° to +45 °) to (0 ° to 180 °) because the servo motor range is 0 ° to 180 °. The third part is shown in **Fig. 11**, this part is responsible for sending signals via serial port. The signals are multiplied by 10000 or 1000 to convert them into integers.

The classical PD controller is used to compare the results with the Sliding Mode (SM) controller. The PD parameters are Kp=0.5 and Kd=0.2. A low pass filter with a cutoff frequency of 1.5 Hz is used in the derivative action of the PD controller to reduce the noise amplification by the differentiation.

Fig. 12 to **Fig. 16** are the results for tracking a circular trajectory. The ball follows the desired trajectory with high amount of error when PD controller is used. It can be notice form **Fig. 14** the ball is rotating on an oval shape lies outside of the desired trajectory. The SM was able to make the ball follow the desired trajectory with low error. The control action of PD controller is smoother than that of SM because SM suffers from the chattering effect.

Fig. 17 to **Fig. 21** are the results for tracking a square trajectory. In this case, the PD controller was faster than the SM as the rising time in PD is smaller than that in SM as shown in **Fig. 18** and **Fig.19**. Although PD is faster, but it suffers from high error, especially at the square corners where the response has high overshoot. In **Fig. 19** it can be noticed the SM trajectory is

closer to the desired and the corners are mores stable. The control action in PD reached the saturation limit $\pm 10°$ at the corners, while in SM, the control action is kept less than $\pm 4°$.

Fig. 22 to **Fig. 26** are the results for stabilizing the ball at a fixed position on the plate. In the single point stabilizing, the PD had the advantage of starting at a point closer to the origin as shown in **Fig. 22** to **Fig. 24**. Despite that, the SM still has a better stabilization. It can be noticed from **Fig. 22** that the ball has a high overshoot in x axis while in SM there is no overshoot. The steady state error in PD is higher than that in SM. The PD is faster in terms of reaching a point near the origin, but it will move around that point rather than heads towards the origin. The control action in SM has a lot of oscillation, again this is due to the chattering phenomenal. A chattering reduction was used with the three cases (circular, square, and single point), the chattering reduction method will reduce the chattering but will not eliminate it.

In overall, the SM controller was able to follow a circular trajectory, square trajectory and a single point stabilizing with a low amount of error and overshoot. The PD controller seems to have a faster rising time, but with a high overshoot and steady state error which is not acceptable in control engineering point of view.

6. CONCLUSTIONS

In this work, the ball and plate system has been studied and explained. In the experimental work of the ball and plate system, one of the problems was how to connect the mechanical linkage to the plate in a way to make it free to rotate. 3D parts has been designed and 3D printed to act as a hinge attached to the plate from one side and the linkage is free to rotate form the other side. A high speed servo motors have been used to execute the controller commands as fast as possible. The controller commands are the plate angles. It has been noticed that the servo motors suffers from chattering when it move to an angle. To reduce this chattering, a ferromagnetic ring has been used to reduce noise in the servo cable which causes the chattering. The used touch screen provides the ball position, but it does not provide its velocity. The ball velocity is important since it is an essential part of the controller algorithm. By differentiating the ball position, the velocity is obtained, but the problem is that it is contaminated with a high amount of noise. To solve this issue, Kalman filter has been used to filter out the position and velocity signals.

The classical sliding mode controller was able to stabilize the ball and also make it follow desired trajectories. The sliding mode controller showed a significant improvement in response over the classical PD controller. To reduce chattering effect, a boundary layer chattering reduction method has been used. Without this chattering reduction, the implementation would be impossible because the servo motors will damage.

REFERENCES

- C. Edwards and S. K. Spurgeon, 1998. *Sliding Mode Control: Theory and Applications 1st ed.*, CRC Press.

- Debono, D. and Bugeja, M., 2015. *Application of Sliding Mode Control to the Ball and Plate Problem.* In 12th International Conference on Informatics in Control, Automation and Robotics (ICINCO). PP. 412–419.

- Dong, X., Zhang, Z., and Tao, J., 2009 *Design of fuzzy neural network controller optimized by GA for ball and plate system.* In 6th International Conference on Fuzzy Systems and Knowledge Discovery, FSKD. PP. 81–85.

- Galvan-colmenares, S., Galvan-colmenares, S., Moreno-armendáriz, M.,Rubio, J.,Ortíz-rodriguez, F.,Yu, W., and Aguilar-ibáñez, C. 2014. *Dual PD Control Regulation with Nonlinear Compensation for a Ball and Plate System.* Mathematical Problems in Engineering, Vol. 2014, No. 1, PP.1–10.

- Ghiasi, A.R. and Jafari, H., 2012. *Optimal Robust Controller Design for the Ball and Plate System.* In The 9th International Conference on Electronics Computer and Computation ICECCO-2012, At Ankara, Turkey. PP. 1–4.

- Han, K., Tian, Y., Kong, Y., Li, J., and Zhang, Y., 2012. *Tracking control of ball and plate system using a improved PSO on-line training PID neural network.* 2012 IEEE International Conference on Mechatronics and Automation, ICMA 2012, PP.2297–2302.

- Jadlovská, A., Jajčišin, Š., and Lonščák R., 2009. *Modelling and PID Control Design of Nonlinear Educationl Model Ball & Plate.* In 17th International Conference on Process Control. PP. 475–483.

- Liu, D., Tian, Y., and Duan, H., 2009. *Ball and Plate Control System based on sliding mode control with uncertain items observe compensation.* In Proceedings of 2009 IEEE International Conference on Intelligent Computing and Intelligent Systems, ICIS 2009. PP. 216–221.

- Negash, A. and Singh, N.P., 2015. *Position Control and Tracking of Ball and Plate System Using Fuzzy Sliding Mode Controller.* In Afro-European Conf. for Advances in Intelligent Systems and Computing. PP. 147–161.

- Park, J.H. and Lee, Y.J., 2003. *Robust visual servoing for motion control of the ball on a plate.* Mechatronics, Vol. 13 No. 7, PP.723–738.

- Pattanapong, Y. and Deelertpaiboon, C., 2013. *Ball and plate position control based on fuzzy logic with adaptive integral control action.* In 2013 IEEE International Conference on Mechatronics and Automation, IEEE ICMA 2013, PP.1513–1517.

- Singh, D. and Saxena, P., 2015. *Trajectory Control of a Ball in a Ball and Plate System Using Cascaded PD Controllers Tuned by PSO.* In Proceedings of Fourth International Conference on Soft Computing for Problem Solving, Advances in Intelligent Systems and Computing. PP. 53–65.

- Utkin, V., Guldner, J., and Shi, J., 2009. *Sliding mode control in electro-mechanical systems 2nd ed.*,CRC Press.

- Wang, H., Tian, Y., Ding, C., Gu, Q., and Guo, F., 2008. *Output regulation of the ball and plate system with a nonlinear velocity observer.* In Proceedings of the World Congress on Intelligent Control and Automation (WCICA). PP. 2164–2169.

- Zeeshan, A., Nauman, N., and Khan, M.J., 2012. *Design Control and Implementation of*

a Ball on Plate Balancing System. In Proceedings of 2012 9th International Bhurban Conference on Applied Sciences & Technology (IBCAST) Islamabad-Pakistan, PP. 22–26.

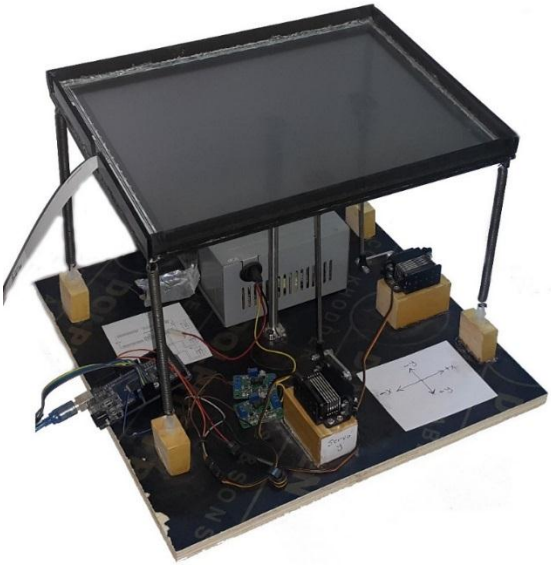

Figure 1. The Ball and Plate system.

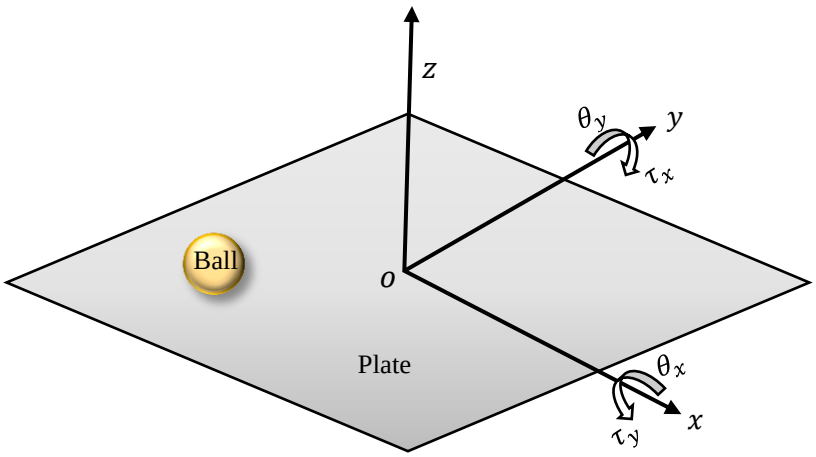

Figure 2. A schematic diagram of the ball and plate system.

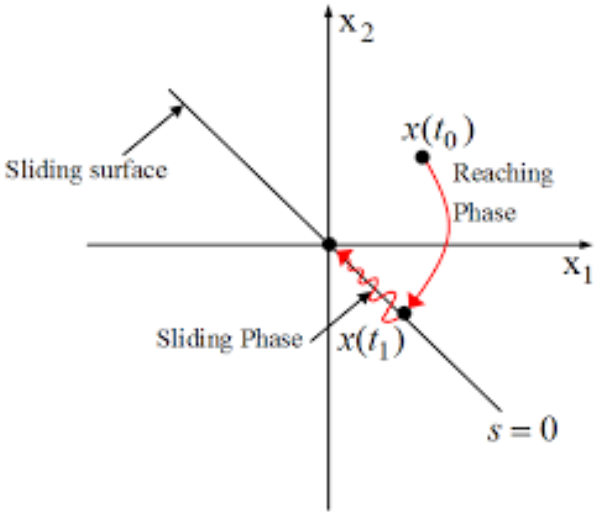

Figure 3. Phase plane response of an SMC system.

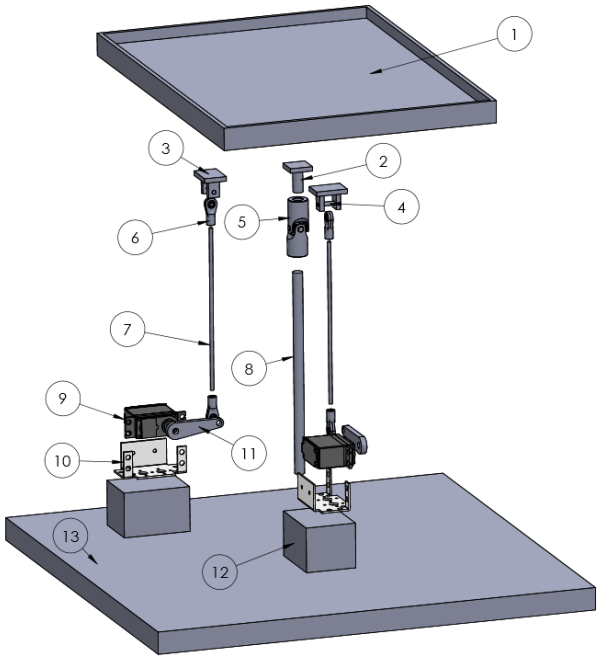

Figure 4. The Ball and Plate system Structure.

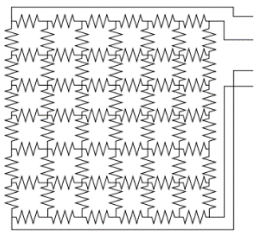

Figure 5. The five wire touch screen resistor network.

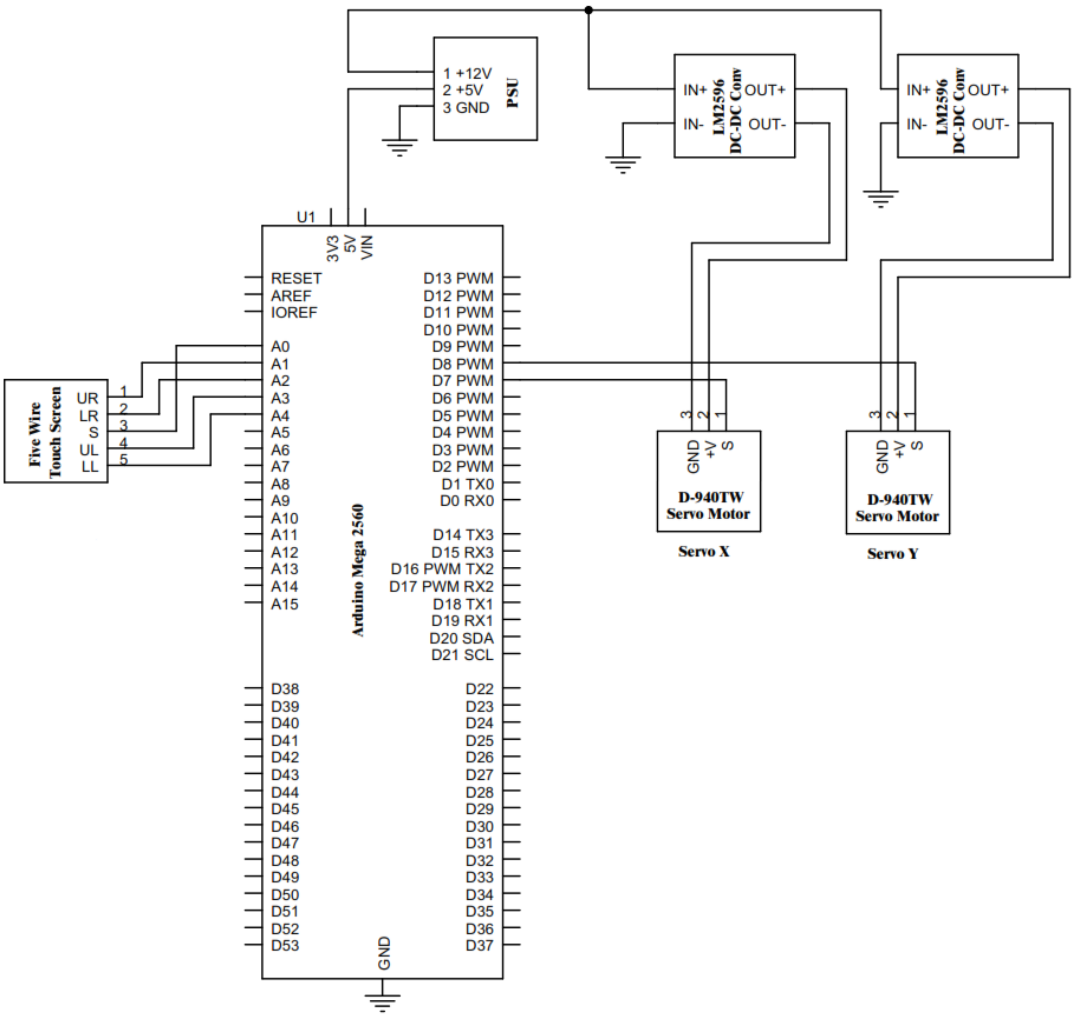

Figure 6. Electrical schematic.

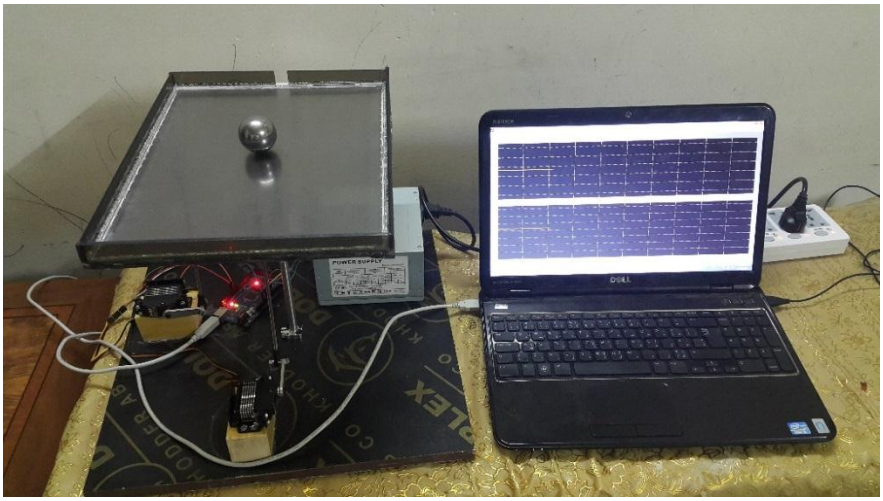

Figure 7. The real construction of the ball and plate system.

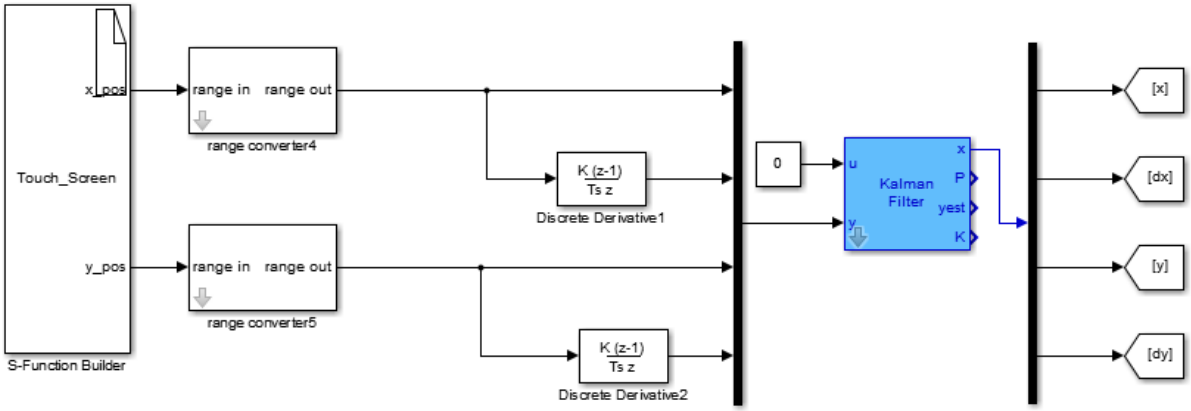

Figure 8. The first part of the Simulink file.

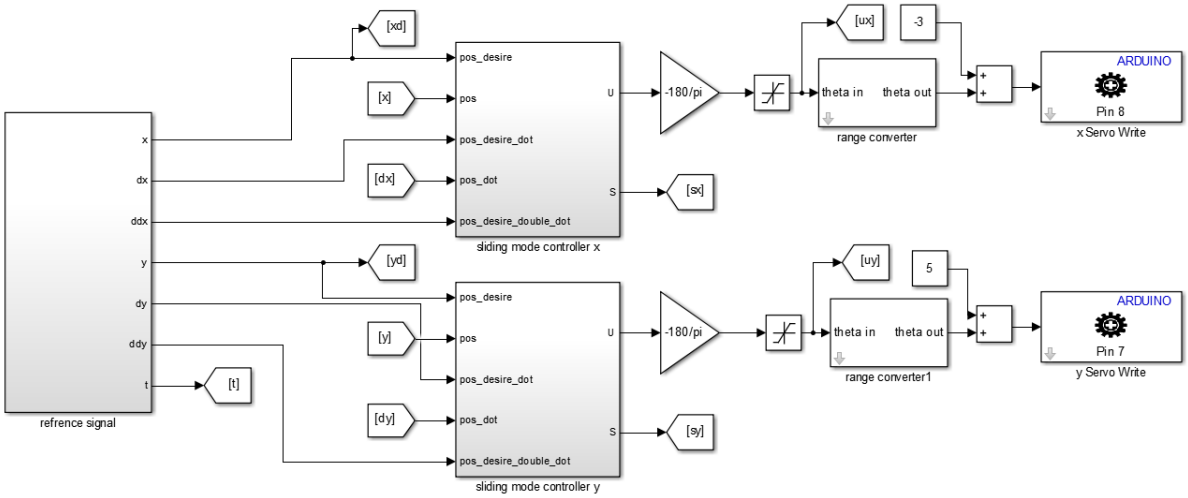

Figure 9. The second part of the Simulink file.

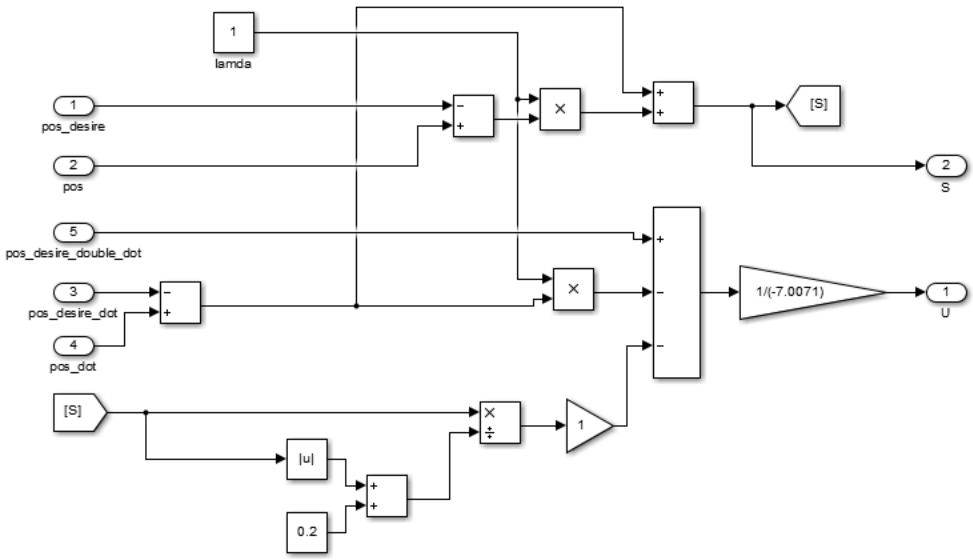

Figure 10. The sliding mode controller.

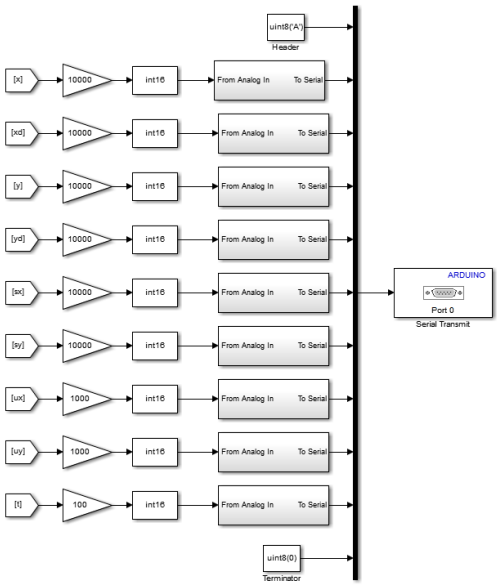

Figure 11. The third part of the Simulink file.

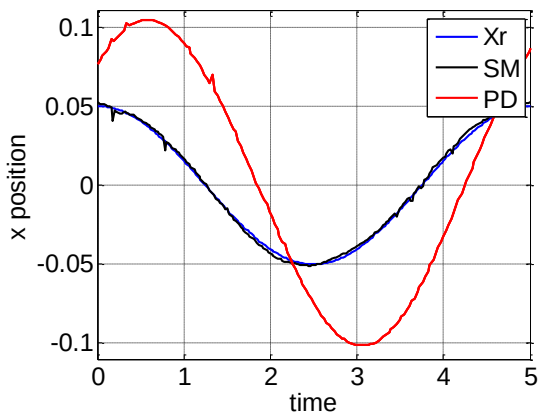

Figure 12. The X axis signal (for circular path).

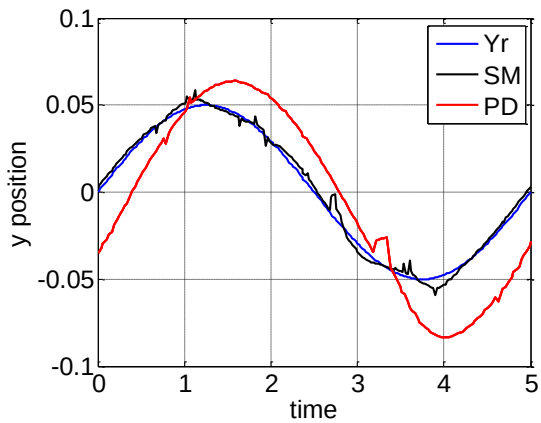

Figure 13. The Y axis signal (for circular path).

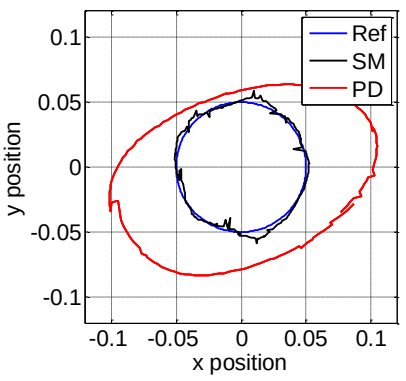

Figure 14. The circular path.

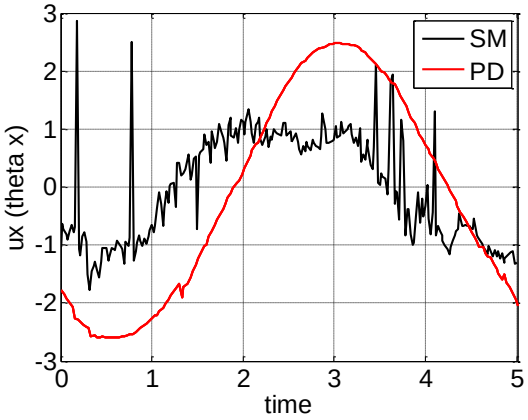

Figure 15. The control action for X axis (for circular path).

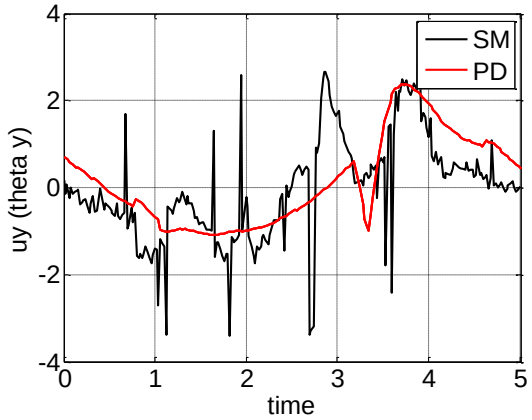

Figure 16. The control action for Y axis (for circular path).

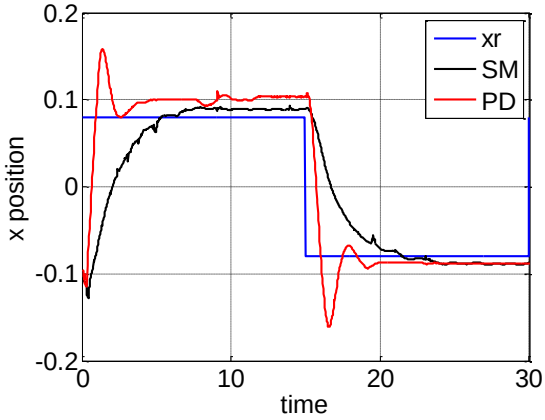

Figure 17. The X axis signal (for square path).

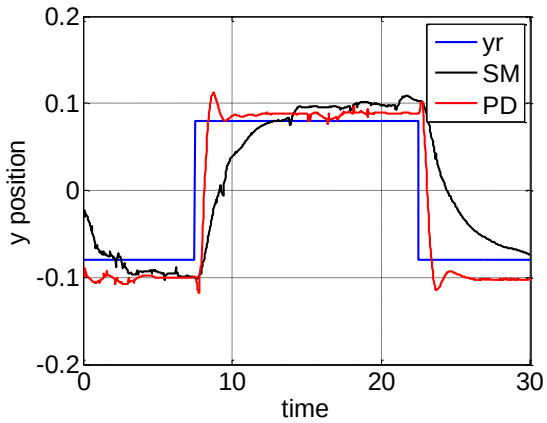

Figure 18. The Y axis signal (for square path).

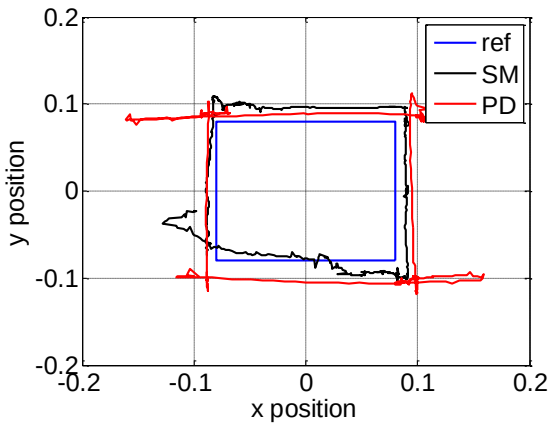

Figure 19. The square path.

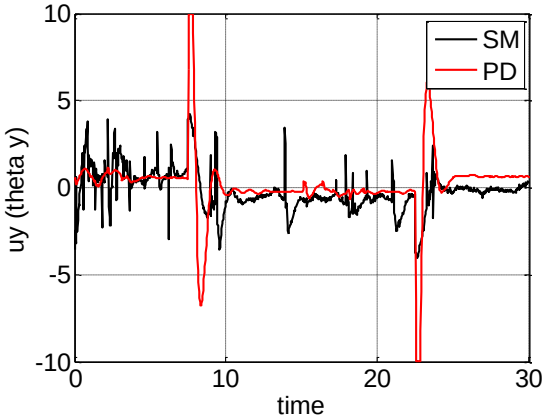

Figure 20. The control action for X axis (for square path).

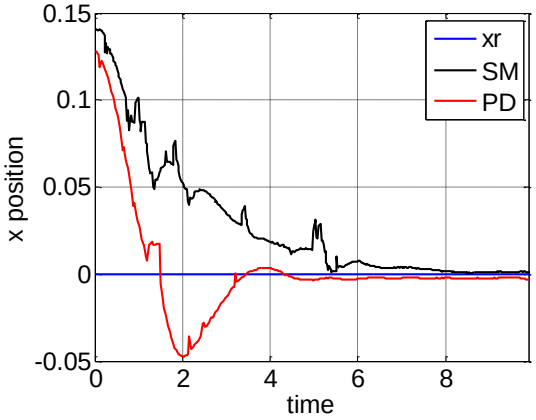

Figure 21. The control action for Y axis (for square path).

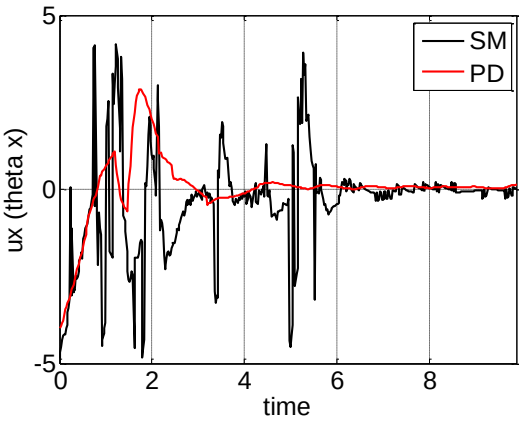

Figure 22. The X axis signal (for single point).

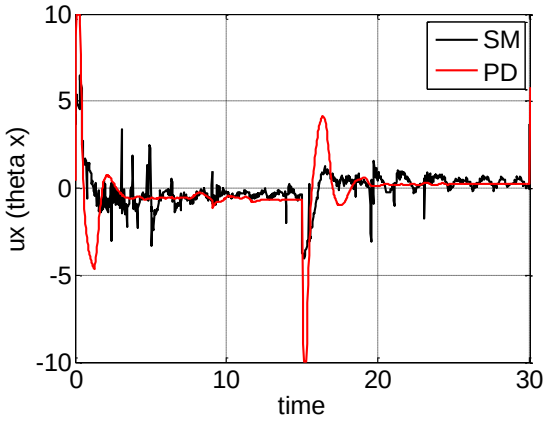

Figure 23. The Y axis signal (for single point).

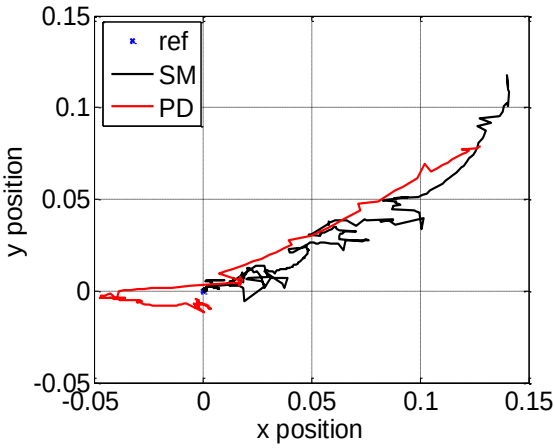

Figure 24. The point position

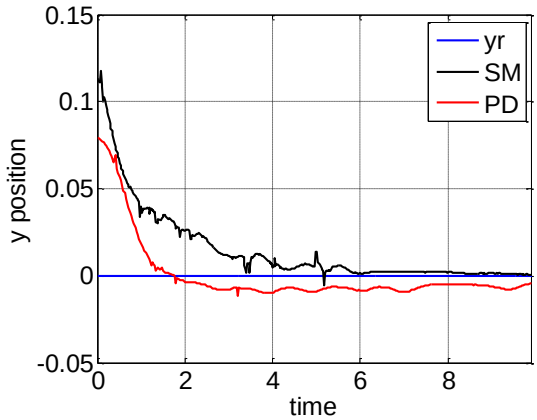

Figure 25. The control action for X axis (for single point).

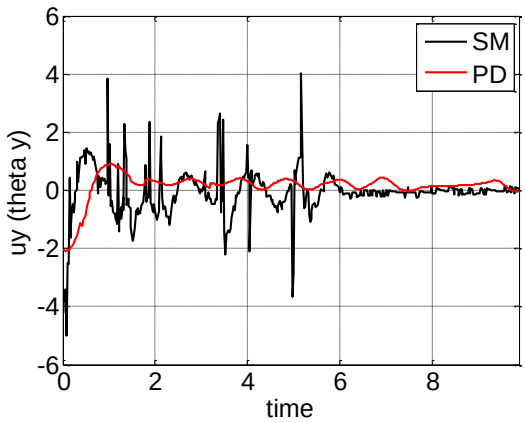

Figure 26. The control action for Y axis (for single point).

Table 1. The ball and plate nomenclature.

Name	Unit	Description
m	kg	Mass of the ball
R	m	Radius of the ball
x	m	Ball position along x-axis
y	m	Ball position along y-axis
$\dot{x}$	m/s	Velocity along x-axis
$\ddot{x}$	m/s^2	Acceleration along x-axis
$\dot{y}$	m/s	Velocity along y-axis
$\ddot{y}$	m/s^2	Acceleration along y-axis
θ_x	rad	Plate deflection angle about x-axis
$\dot{\theta}_x$	rad/sec	Plate deflection angular velocity about x-axis
θ_y	rad	Plate deflection angular about y-axis
$\dot{\theta}_y$	rad/sec	Plate deflection angular velocity about y-axis
τ_{θ_x}	Nm	Torque exerted on the plate in x-axis direction
τ_{θ_y}	Nm	Torque exerted on the plate in y-axis direction

Table 2. The parameters' values.

Parameter	Descriptions	Valu	Unit
m	Ball mass	0.11	Kg
R	Ball radius	0.02	m
g	Gravitational Acceleration	9.81	m/s2
B	Constant	7.007	-

Table 3. A description of the system structure components of **Fig. 4.**

No.	Description	No	Description
1	Plate made from Acrylic with four sides	8	Central shaft
2	Central pillar	9	Servo motor
3	Brace	10	Servo motor bracket
4	Brace screw	11	Servo arm
5	Universal joint	12	Servo motor base made from wood
6	Ball joint linkage	13	The structure base made from wood
7	Linkage threaded rod		

The Effect of Cyclic Bending Loads on Crack Growth in Pipes for Inclined and Transverse Cracks with or Without Internal Pulsing Pressure

Dr.Fathi Alshamma
Assistant Professor
College Of Engineering-University Of Baghdad
E-mail : fathi_alshamma@yahoo.com

Shwan Abdulmuhsin Zainalaabdeen
Senior Engineer In State Company For Oil Projects
(SCOP) - Ministry Of Oil
E-mail : shwanabdulmuhsin@gmail.com

ABSTRACT

In the present research a new test rig has been proposed to be suitable for different cyclic loads such as cyclic bending, cyclic torsion, proportional and non proportional loads. In this work the efforts were concentrated on the cyclic bending loads concerning cracked pipes with or without internal pulsing pressure to study crack propagation in small bore pipes (up to 1") for transverse or inclined cracks. The rig simulates the real service conditions under different stresses by means the least dangerous case will be suggested, so the experiments were considered for copper pipe, and the results have been tabulated and drawn to demonstrate the crack growth behavior as well as to justify the outcomes practically, consequently the durability of this new rig has been confirmed with new concluded facts.

Key words: cyclic bending load, copper pipe, crack growth

تأثير احمال الحني الدورية على نمو الشق في الانابيب التي فيها شقوق مائلة او العرضية بوجود او عدم وجود الضغط النبضي الداخلي

الدكتور : فتحي الشماع
أستاذ مساعد
كلية الهندسة - جامعة بغداد

الطالب : شوان عبد المحسن زين العابدين
مهندس أقدم في شركة المشاريع النفطية
وزارة النفط

الخلاصة

هذه الدراسة تقترح جهاز مستحدث بحيث يكون ملائم لتسليط انواع حمل عديدة مثل احمال الحني الدورية واحمال اللي الدورية والاحمال التناسبية والغير تناسبية الدورية ، لكن في هذه الدراسة تم التركيز على احمال الحني الدورية لعينات من الانابيب فيها شق بدائي بوجود او عدم وجود ضغط نبضي داخلي لدراسة نمو الشق في الانابيب ذات القياسات الصغيرة (الى قياس(1) بوصة) للشقوق العرضية اوالشقوق المائلة والتي تحاكي واقع الحال لانواع مختلفة من الاجهادات بحيث يتم اقتراح الحالة الأكثر أمانا. لذا تمت التجربة على أنابيب النحاس ومن ثم جدولة ورسم النتائج الخاصة بنمو الشق لتوضيح تصرف هذا الشق وتبريرهذه النتائج بصورة عملية لاثبات متانة هذا الجهاز المستحدث والحصول على حقائق واستنتاجات جديدة .

1. INTRODUCTION:

There are many mechanical components that are subjected to cyclic loads that lead to damage such as crack that may propagate till final rupture. Pipes are one of the such components that are used in several industrial units like oil field, plumbing, air conditioning and refrigeration…..etc., and for this reason a new test rig has been designed and manufactured to investigate a crack growth for different stress ratio (R). This new rig is suitable to test the pipe under proportional cyclic loads , non proportional cyclic loads, bending cyclic loads and torsion cyclic loads with a little bit changes in some simple parts according to each case but in this study the efforts have been concentrated on the cyclic bending loads, a little consideration will show that the pipes that are used in real service conditions might be defected already due to shipment or sharp tool marks that cause transverse or inclined crack which may not be observed, so the dangerous state of pipe behavior will be estimated under different loads before rupture , in other words , diagnosis of the metal state seriousness as soon as possible , taking into account that the crack growth direction (θ_c) might be examined for each state, adding to this that the test rig designed to simulate the real service of pipes and the used specimens have the same dimensions in actual practice to monitor the behavior of crack growth in pipes, so the main goal of this research is to verify the results of this new rig to be reliable as a useful device .

Pavlou D.G. 2000 focused on the direction of mixed mode crack propagation for inclined crack in plate (which was included already in the specimen before test commencement), so the main conclusion demonstrates the clockwise direction of crack initiation angle as well as mode that had been considered only for crack growth prediction. **Robertson S.W. and et al, 2006** investigated crack growth properties of the super elastic alloys and a sample which cut from Nitinol tube with different orientation as a compact tension specimen (new test samples) that is used under cyclic uniaxial load as well as different orientation had been discussed. **Boljanovic Slobodanka and Maksimovic Stevan, 2014** sstudied mixed mode crack propagation in plate specimen with two holes regarding crack path and life estimation, so good agreement was observed between experiments and finite elements work.

1Generally there is no standard rig for cyclic load experiments, therefore, researchers build a rig that meets their requirements, noting that the results of two different test rigs are hard to compare, **Pauw J.De, et al, 2011.** In this study an increasing of crack length due to cyclic loads has been observed against number of cycles and the transverse crack and its inclination effect has been considered also for copper pipes as a type of multiaxial cyclic stress case due to force analyzing that caused mixed mode case, and the state of art concept had been studied for another specimen that gathers an applied remote stresses and internal pulsing pressure as an overload state. Cyclic load test rig is based on two main issues, the first is the configuration of a test specimen and the second is an increasing the functionalities, **Pauw J.De, et al, 2011**. So in this study the specimen configuration has been illustrated accordingly.

Carful tests for several material were studied via previous works regarding crack growth data that ranged within the regime (from about 10^{-4} to 10^{-2} mm/cycles), **Ragab, A. and Bayoumi, S., 1998**. Other opinions were ranged between (10^{-6} and 10^{-3} mm/cycles), **Vethe, S. 2012,** and these results for the specimens under cyclic tension loads, so it is obvious that the results near 10^{-4} refers to the slow crack growth as well as a very good toughness of the material and any crack growth data within same range represent a bonus of the rig outcomes.

A little consideration will show that the crack growth were non uniform at both sides and the phenomena had been observed by **Rozumek Dariusz and et al**. **2008**. As well as the change of growth is a property of the material microstructure itself and this change might be observed in the same specimen at both sides as stated also by **Hos Y. and Vormwald M. 2015**.

2. EXPERIMENT WORK:

The new manufactured rig consists of rig base (0.6x60x105)cm , electrical motor (1.5 HP) and the power transmitted via pulleys and belts to the crank shaft that transmitted this power to the specimen via action shaft where the oscillation of the specimen was equal to around 1800 rpm, so the process was governed by control system . Pumping system equipped also to introduce an internal pulsing pressure with 1800 rpm as in **Fig.1**. It is worth mentioning that the procedure includes several steps and as indicated here under:

1. The crack had been introduced in pipes and the crack was partly through toward an inside portion, as in **Fig.2**. In other word the crack already was existent and after test commencement the crack grew due to cyclic load.

2. The specimen settled in the rig and the limitation pads arranged in such away the displacement was equal to (3.25 mm) that checked and measured again during the test by mechanical and digital caliper.

3. After several minutes of a test commencement the crack grew toward inside a pipe (i.e. through the thickness), thereafter a crack initiation was observed on the specimen surface such that the crack lengths have been recorded as the following tables, to be investigated and clarified by drawing (a) against (N). It is worth mentioning also that the rig was turned off each period according to crack growth rate to be possible an observation of crack lengths increment.

4. The displacement substituted in the following formulas, **Hearn , E. J. , 1981.** to find out the load and the direct stress .

$$(load)w = \frac{3EIx}{l^3} \tag{1}$$

$$(direct\ stress)\sigma = \frac{My}{I} = \frac{(wl)y}{I} \tag{2}$$

5. In case of internal pulsing pressure the air media entered via specimen upper hold and the pump turned on that synchronized with turning on the electrical motor, so the pressure was equal to (1 Mpa) which represents small value comparing with applied remote stress to demonstrate the clear difference of crack growth behavior due to internal pressure, so the hoop stress was estimated to be equaled to (8 Mpa) by using the following formula, **Hearn, E. J., 1981.**

$$\sigma_h = \frac{PD}{2t} \tag{3}$$

Noting that the dimension of all specimens were 180 mm (gauge length), 12.6mm (outside diameter) and 0.7mm (wall thickness), so all specimens were classified as thin pipe, and the

copper pipe was tested in laboratory to find out mechanical and chemical properties that indicated in **Table 1.**

For displacement (x) = 3.25 mm the applied remote stress was equal to(219.77 Mpa), i.e. around 91% of $\sigma_{y.p.}$ to accelerate the test as much as possible in such away the crack monitored carefully.

Three cases of specimens have been considered, the first was pre cracked specimen (i.e. the crack introduced before test commencement) with transverse crack length (2a) equal to 6.48 mm, the second was similar to the first specimen with hoop stress equal to 8 Mpa, and the third was pre cracked specimen where the crack (2a) was inclined by 30^0 to get clear reading regarding(θ_c) and crack length was equal to 6.48 mm also, so these three different specimens were considered to demonstrate the less dangerous state.

2.1. Specimen (1)

After (around 32.5) minutes of the test commencement, the crack completely grew through the thickness and after around 0.5 minutes the crack initiation has been observed on the specimen surface such that the crack lengths have been recorded as indicated in **Table 2**.

2.2. Specimen (2)

After (around 27.5) minutes of the test commencement , the crack completely grew through the thickness and after around 0.5 minutes the crack initiation has been observed on the specimen surface such that the crack lengths have been recorded as indicated in **Table 3**.

2.3. Specimen (3)

After (around 18.5) minutes of the test commencement, the crack completely grew through the thickness and after around 0.5 minutes the crack initiation has been observed on the specimen surface such that the crack lengths have been recorded as indicated in **Table 4**.

The experiments were analyzed to verify the durability of the new test rig to illustrate new facts about a damage models and as indicated here under:

1. Regarding the above mentioned crack growth data for specimen (1) under cyclic bending loads that affect the element by the same way of the cyclic tension loads the outcomes was equaled to around 10^{-4} (i.e. within the same acceptable regime), adding to this that the crack path was approximately perpendicular to the applied remote tensile stress in this case, **Qian , J. and Fatemi A. , 1996,** as seen in **Fig.3**.
2. Regarding the specimen (2), hoop stress equal to 8 Mpa that was implemented to accelerate crack growth as overload case that was considered besides to the external cyclic bending load which was equal to 219.77 Mpa, noting that the existence of the internal pulsing pressure must be more dangerous because the overload increment even though the hoop stress tend to close the crack for a particular period.

3. Regarding specimen (3) the crack initiated in the clockwise direction and at angle was equal to 58^0 due to mixed mode existent, however, the direction of crack growth for this specimen under cyclic load and monotonic load is approximately the same**, Pavlou D.G. 2000**, and according to special curves that proposed by **H.V. Lakshminarayana and M.V.V. Murthy, 1976**, and regarding to the specified constant β the following formulas had been considered to find out stress intensity factor (SIF) of (mode I) and (mode II) from the special curves which is suitable with studied case .

$$\beta^2 = \frac{a^2}{8rt}[12(1-\vartheta^2]^{0.5} \quad (4)$$

$$\frac{K_I^{(m)}}{\sigma\sqrt{a}}=1.2 \quad (5)$$

$$\frac{K_{II}^{(m)}}{\sigma\sqrt{a}}=0.35 \quad (6)$$

$$\frac{K_I^{(b)}}{\sigma\sqrt{a}}= - 0.12 \quad (7)$$

$$\frac{K_{II}^{(b)}}{\sigma\sqrt{a}}=1.25 \quad (8)$$

$$K_I^{eff}=K_I^{(m)} + 0.5K_I^{(b)} = K_I \quad (9)$$

$$K_{II}^{eff}=K_{II}^{(m)} + 0.5K_{II}^{(b)} = K_{II} \quad (10)$$

Via two main formulas the direction of crack growth regarding the line of crack that were defined with positive value in counter clockwise direction and the reverse is also true,so θ_C were estimated either by the following formula that used by, **Blazic, M. et al, 2014**.

$$\theta_C = 2tan^{-1}\left(\frac{K_I}{4K_{II}} - \frac{1}{4}\sqrt{\left(\frac{K_I}{K_{II}}\right)^2 + 8}\right) \text{ for } K_{II} > 0 \quad (11)$$

Or by using this hereunder formula that used by**, Vethe, S. June 2012**.

$$\theta_C = -arccos\left(\frac{2K_{II}^2+K_I\sqrt{K_I^2+8K_{II}^2}}{K_I^2+9K_{II}^2}\right) \quad (12)$$

Where the durability of this new rig has been verified again via the result of specimen with inclined crack .

4. RESULTS AND DISCUSSION:

Based on the received data that monitored from experiments for different scenarios that are indicated in **Table 5**, several important figures have been established to be discussed accordingly.

Regarding **Fig.4** the differences between two cracks at left hand side (LHS) and right hand side (RHS) was less with respect to specimen (2) for overall curves, in the other hand the difference was more regarding specimen (1), so the internal pulsing pressure made a convergence between LHS and RHS curves due to the fact that the hoop stress try to close the crack from 30 minutes to 48 minutes and this action led to crack growth deceleration up to a point for this period and the cracks at both sides of specimens has enough time to grow closely, while the more divergence had been observed for the case of transvers crack without internal pulsing pressure among these three specimens where the change of growth is a property of the material microstructure itself and this change might be observed in the same specimen at both sides as demonstrated by **HosY. and Vormwald M. 2015,** so it is normal phenomena, a little consideration will show that the first reading of initial crack increment (which is very short compared with other reading) was not clear and classified as threshold stage and this is common problem.

Regarding **Fig.5** the cracks at LHS and RHS, the initiation of crack propagation observed clearly and earlier for specimen (3) compared with other specimens due to shear existence beside direct stress which resulted from crack inclination. In the same context the crack initiated for the case of transverse crack with internal pulsing pressure earlier than the case of the transverse crack without internal pulsing pressure, but the crack lengths increment due to cyclic load was more in the case of the pressure existence compared with other specimens despite the crack deceleration for particular period (from 30 to 48 minutes) thereafter the crack grew dramatically. In the other hand the increment of crack lengths in the case of inclined crack was less among these three specimens where the effect of opening mode decreased where this mode represent the most effective mode for crack growth comparing with other well-known modes (shearing mode and tearing mode).

The direction of the crack angle that grew in the specimen (1) and (2) to be approximately perpendicular to the applied tensile load due to bending, and the direction of crack initiation of specimen (3) was estimated according to eq.11 and eq.12 to be verified. A little consideration will show that θ_C will be observed due to crack inclination thereafter the crack grew in the direction to be approximately perpendicular to the applied bending load and this is normal phenomena that is observed in previous similar cases. This I shown in **Table6.**

5. CONCLUSIONS

1. In spite of implementation 91% of $\sigma_{y.p.}$ concerning specimen (1), the crack grew slowly to be equal to about 10^{-4} mm/cycles due to the fact of the high toughness for this type of copper pipe.

2. Despite crack initiation of specimen (3) earlier than other specimens, this case of inclined crack represents the least dangerous state, and the case of transverse crack with internal pulsing pressure represents the most dangerous state among other specimens.
3. Concerning the case of inclined crack, it will be more sensible to use the equation (12) to guess the crack direction because the error between experimental and analytical part was around 0. 97 %.
4. The durability of the new test rig has been confirmed according to above mentioned outcomes to illustrate the compatibly between previous opinions and actual practice.

REFERENCES:

- Blazic , M. et al , 2014, *Determination Of Fatigue Crack Growth Trajectory And Residual Life Under Mixed Modes* , Journal of Mechanical Engineering, 250-254.

-Boljanovic Slobodanka and Maksimovic Stevan , 2014**,** *Mixed mode crack growth simulation with / without overloads* , International Journal of Fatigue 67 (2014) 183-190.

- Lakshminarayana , H.V. and Murthy , M.V.V, august 1976 *On Stresses Around An Arbitrarily Oriented Crack In Cylindrical Shell* , international journal of fracture, Vol. 12 , No. 4.

- Hearn , E. J. , 1981, *An Introduction To The Mechanics Of Elastic And Plastic Deformation Of Solids And Structural Components* ; Mechanics Of Materials UK .

-HosY. and Vormwald M. 2015 , *Measurement And Simulation Of Crack Growth Rate And Direction Under Non Proportional Loadings* , IGF- ESIS 34.14 .

- Pavlou D.G. 2000 , *Approximate Prediction Of Mixed Mode Fatigue Crack Growth* Technological institute of Halkidas , Greece .

- Pauw J.De, et al , 2011 , *Review And Classification Of Fretting Fatigue Test Rigs* , sustainable construction and design , Belgium .

- Qian , J. and Fatemi A. , 1996 , *Mixed Mode Fatigue Crack Growth : A Literature Review* , Engineering Fracture Mechanics , Vol. 55, No. 6, pp. 969-990.

- Ragab , A. and Bayoumi, S. , 1998 , *Engineering Solid Mechanics* , CRC

- Robertson S.W.2004 , et al , 2006 , *Cyclic Fatigue Of Nitinol* , ASM international.

- Rozumek Dariusz and et al , 2008 ,*Fatigue Crack Growth Rate In Non Proportional Bending With Torsion Loading* , 17th European conference ,Czech Republic .

- Vethe , S. June 2012 , *Numerical Simulation Of Fatigue Crack Growth* , M.Sc. dissertation .

NOMENCLATURE :

a=crack length (mm)

β = specified constant from which the stress intensity factor will be found according to each mode

σ =direct stress (Mpa)

σ_h =hoop stress (Mpa)

D=Inside diameter(m)

E=young modulus (Gpa)

I=moment of inertia (m^4)

$K_I^{(m)}$ = membrane stress intensity factor for mode I (Mpa$\sqrt{m)}$

$K_{II}^{(m)}$ = membrane stress intensity factor for mode II (Mpa$\sqrt{m)}$

$K_I^{(b)}$ = bending stress intensity factor for mode I (Mpa$\sqrt{m)}$

$K_{II}^{(b)}$ = bending stress intensity factor for mode II (Mpa$\sqrt{m)}$

K_I^{eff} = K_I = effective stress intensity factor for mode I (Mpa$\sqrt{m)}$

K_{II}^{eff} = K_{II} = effective stress intensity factor for mode II (Mpa$\sqrt{m)}$

l=gauge length(m)

M=bending moment (N.m)

N=number of cycles (r.p.m.)

P=Internal pulsing pressure (Mpa)

r=mean radius ($\frac{Outside\ diameter-t}{2}$)$(m)$

R= stress ratio ($\frac{\sigma_{min}}{\sigma_{max}}$)

SIF= stress intensity factor (Mpa$\sqrt{m)}$

t=Wall thickness (m)

θ_c = angle of crack growth according to crack line(degree)

w=required load to cause a displacement (N)

ϑ = poisons ratio =0.33

x=linear displacement (m)

y=$\frac{\text{Outside diameter}}{2}$ (m)

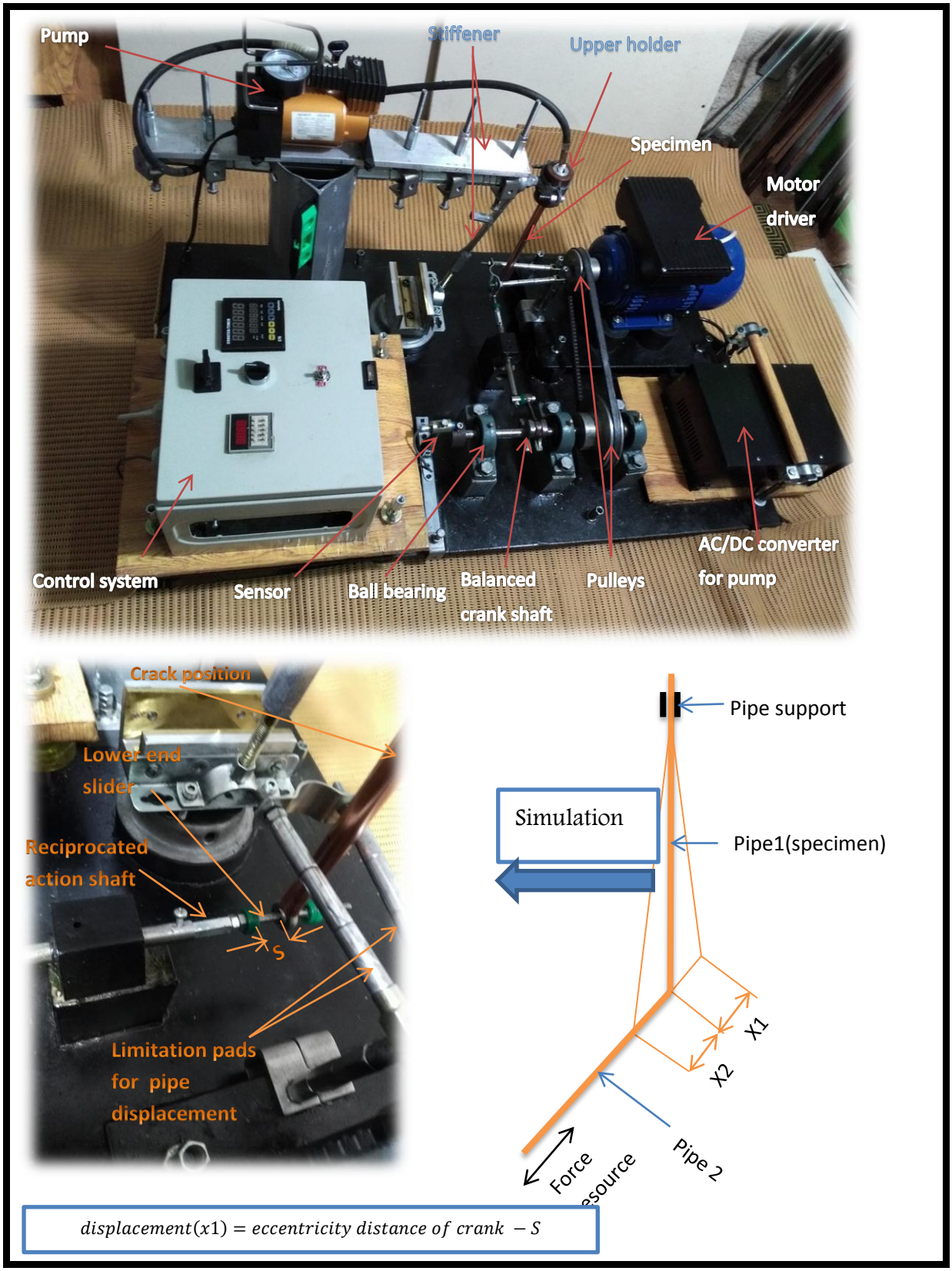

Figure 1. New test rig with its simulation form.

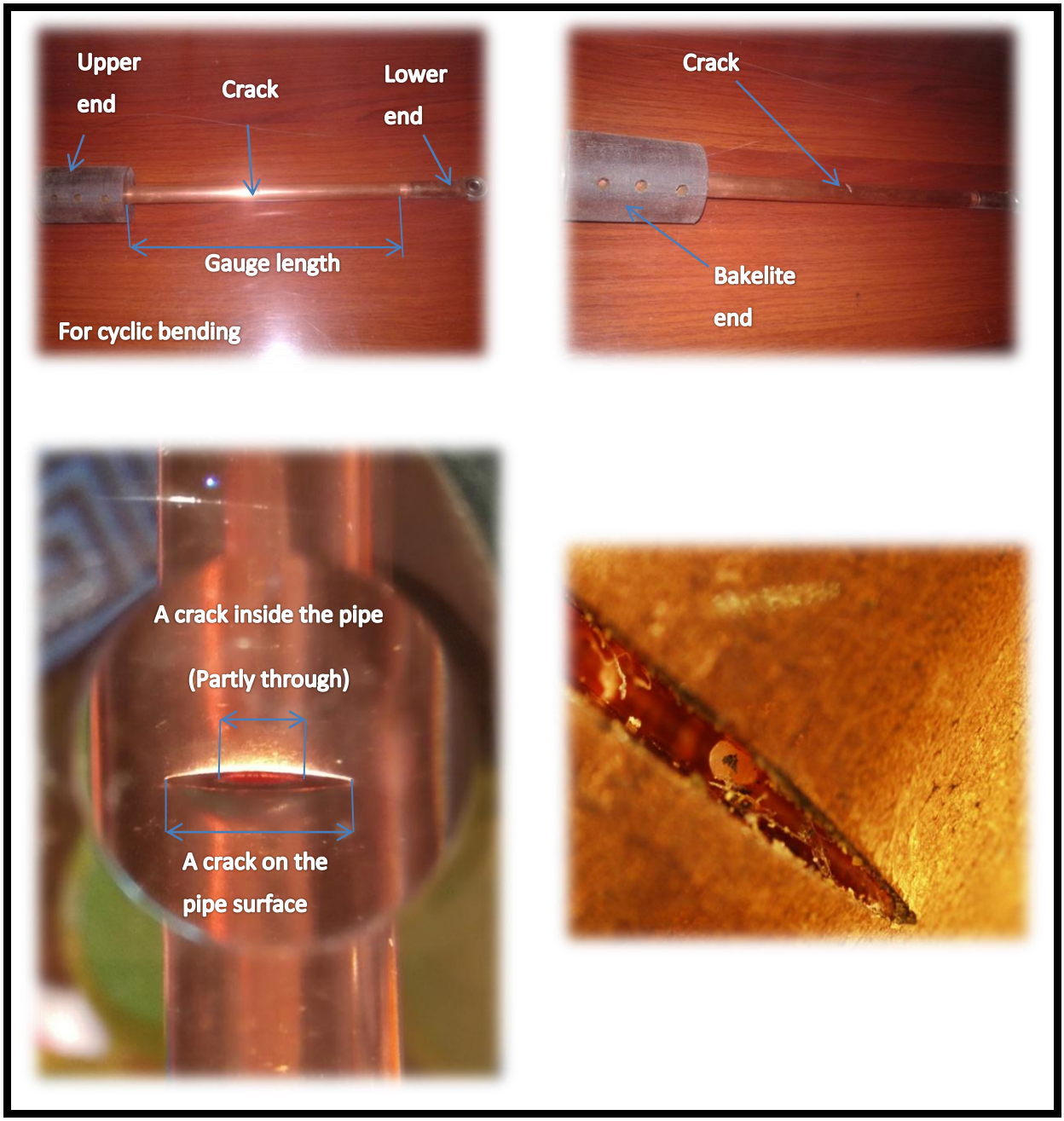

Figure 2. Specimen shape.

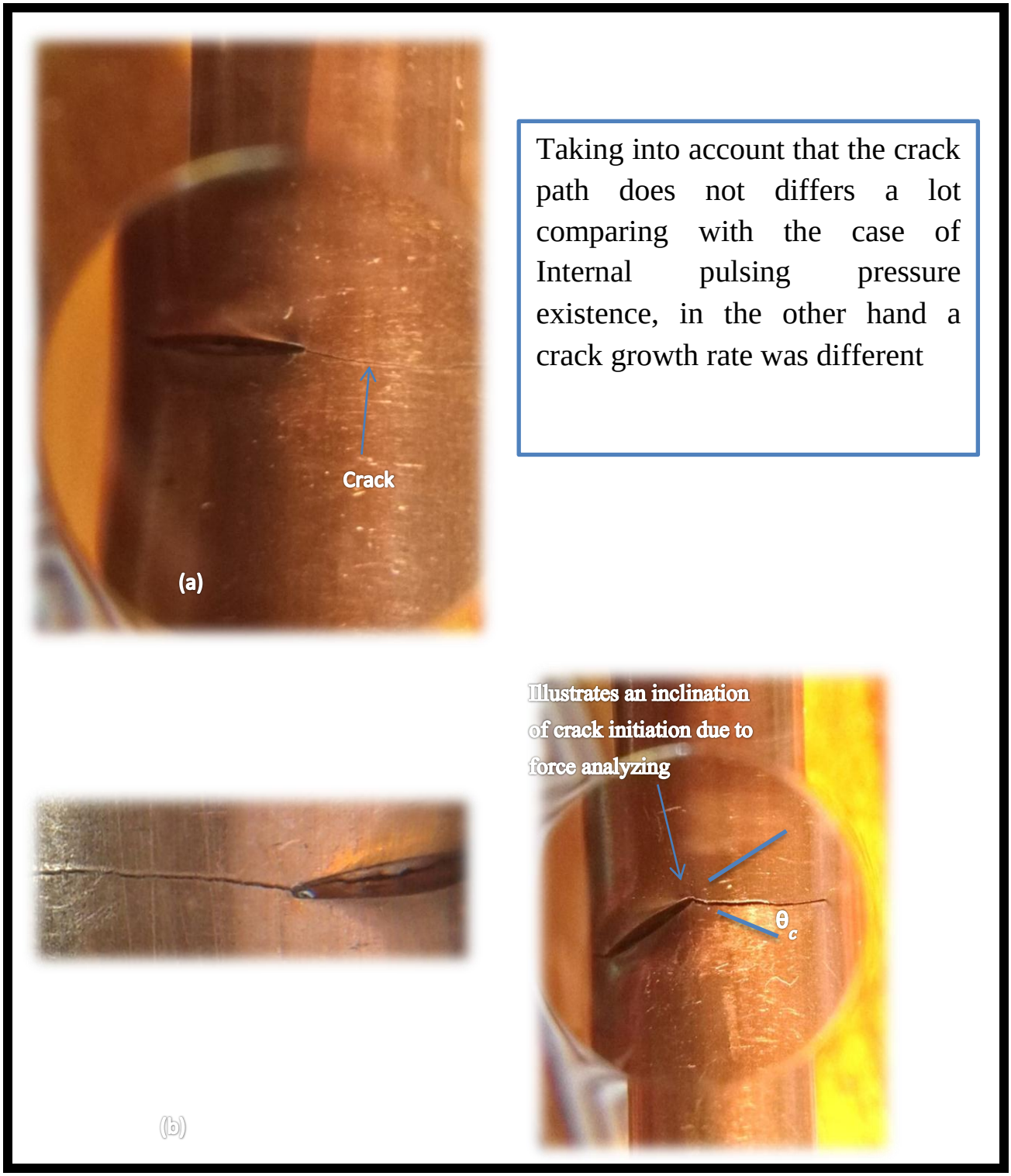

Figure3. Illustration of crack growth

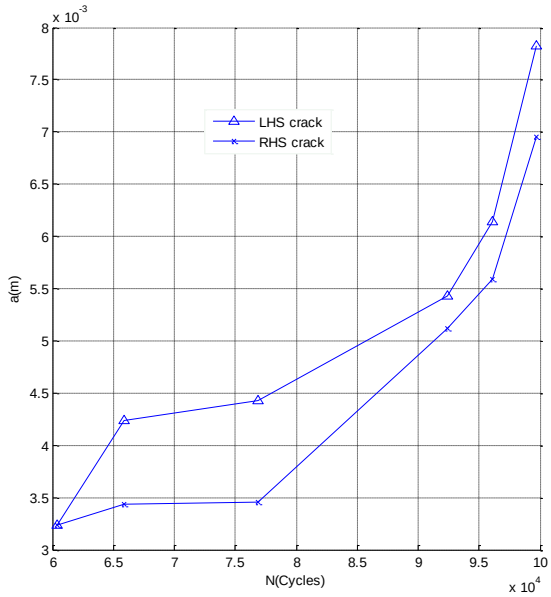

Specimen (1)

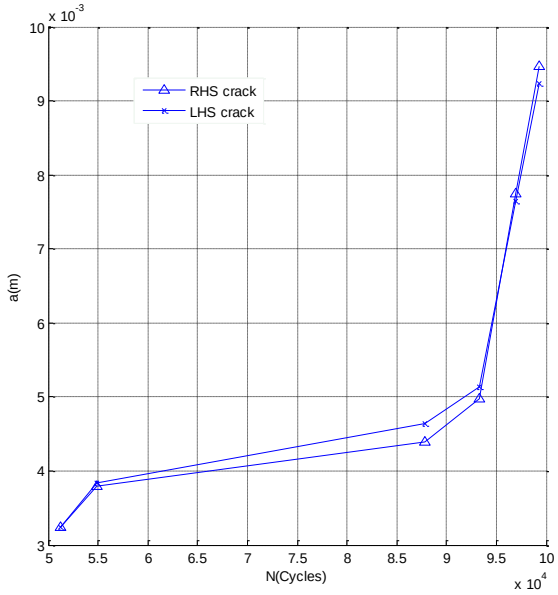

Specimen (2)

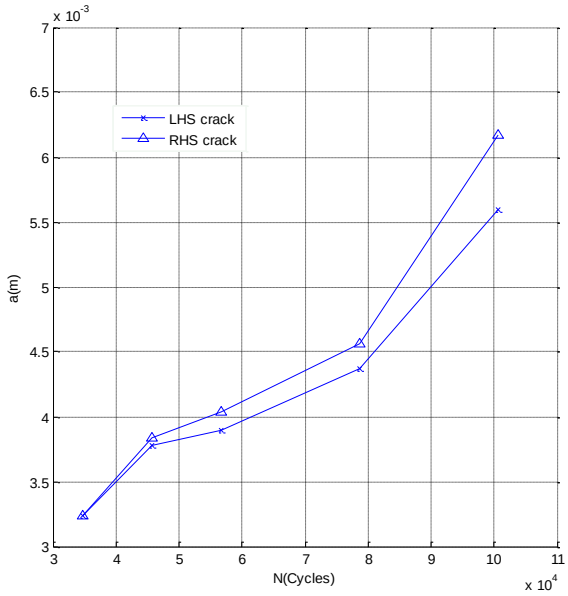

Specimen (3)

Figure4. Illustration of LHS crack and RHS crack growth in specimen (1), specimen (2) and specimen (3)

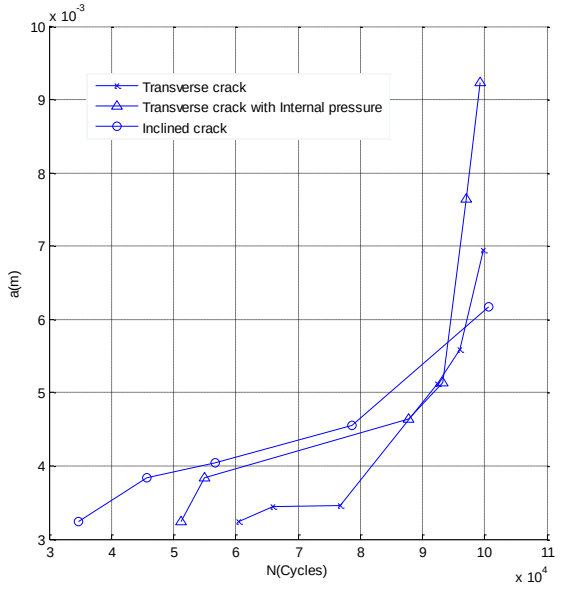

LHS crack for three specimens

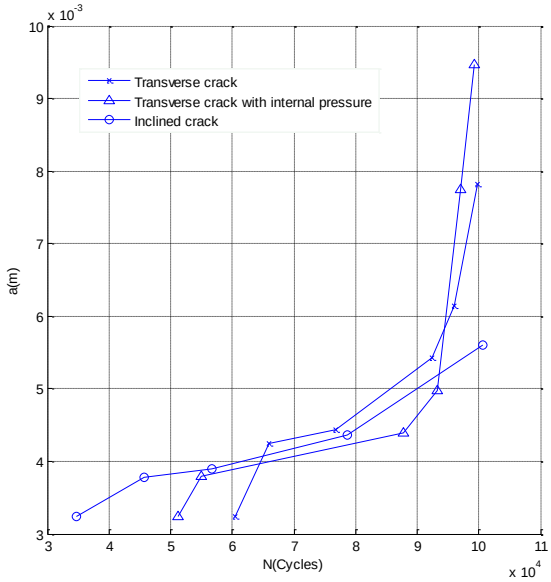

RHS crack for three specimens

Figure5. Illustration of comparison between LHS crack growth and RHS crack growth in three specimens

Table1. Mechanical and chemical properties

Mechanical properties			
Yield point stress (Mpa) , $\sigma_{y.p.}$	Ultimate stress (Mpa) , $\sigma_{ult.}$	Young modulus (Gpa) , E	Plane strain toughness , K_{IC}
240	269.5	115.93	90

Chemical properties				
Zn%	Pb%	P%	Fe%	Al%
0.0062	0.0205	0.0376	0.0127	0.0221
S%	Ni%	Bi%	Sb%	Cu%
0.0116	0.0052	0.0147	0.114	≈99

Table2. Specimen (1)

G.L.=180 mm

Disp.=3.25 mm

2a=6.48 mm

N=1830 r.p.m.

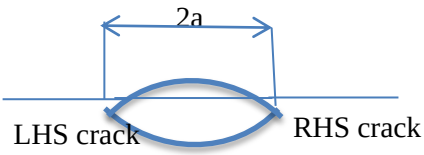

LHS Crack length (m) x10^{-3}	$\frac{da}{dN}$ (LHS)	RHS Crack length (m) x10^{-3}	$\frac{da}{dN}$(RHS)	The required time for crack growth
1	-	0.2	-	After 3 minutes(i.e. from 33 minutes to 36 minutes)
1.19	$\frac{1.19-1}{(6*1830)}$	0.22	$\frac{0.22-0.2}{(6*1830)}$	After 6 minutes (i.e. from 36 minutes to 42 minutes)
2.19	$\frac{2.19-1.19}{(8.5*1830)}$	1.88	$\frac{1.88-0.22}{(8.5*1830)}$	After 8.5 minutes (i.e. from 42 minutes to 50.5 minutes)
2.9	$\frac{2.9-2.19}{(2*1830)}$	2.35	$\frac{2.35-1.88}{(2*1830)}$	After 2 minutes (i.e. from 50.5 minutes to 52.5 minutes)
4.58	$\frac{4.58-2.9}{(2*1830)}$	3.71	$\frac{3.71-2.35}{(2*1830)}$	After 2 minutes (i.e. from 52.5 minutes to 54.5 minutes)
-	Av.=1.83 *10^{-4}	-	Av.=1.52*10^{-4}	-

Table3. Specimen (2)

G.L.=180 mm

Disp.=3.25 mm

2a=6.48 mm

N=1830 r.p.m.

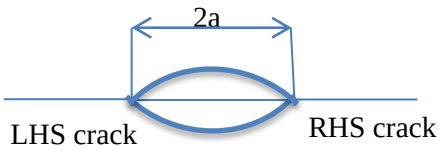

(With Internal pulsing Pressure)

LHS Crack length (m) x10^{-3}	$\frac{da}{dN}$ (LHS)	RHS Crack length (m) x10^{-3}	$\frac{da}{dN}$(RHS)	The required time for crack growth
0.55	-	0.6	-	After 2 minutes(i.e. from 28 minutes to 30 minutes)
1.16	$\frac{1.16-0.55}{(18*1830)}$	1.4	$\frac{1.4-0.6}{(18*1830)}$	After 18 minutes (i.e. from 30 minutes to 48 minutes)
1.74	$\frac{1.74-1.16}{(3*1830)}$	1.9	$\frac{1.9-1.4}{(3*1830)}$	After 3minutes (i.e. from 48 minutes to 51 minutes)
4.5	$\frac{4.5-1.74}{(2*1830)}$	4.41	$\frac{4.41-1.9}{(2*1830)}$	After 2 minutes (i.e. from 51 minutes to 53 minutes)
6.23	$\frac{6.23-4.5}{(1.25*1830)}$	5.99	$\frac{5.99-4.41}{(1.25*1830)}$	After 1.25 minutes (i.e. from 53minutes to 54.25 minutes)
-	Av. = 4.08*10^{-4}	-	Av.= 3.72*10^{-4}	-

Table4. Specimen (3)

G.L.=180 mm

Disp.=3.25 mm

2a=6.48 mm

N=1830 r.p.m

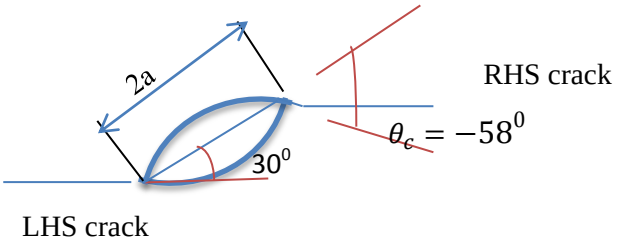

LHS Crack length (m) x10^{-3}	$\frac{da}{dN}$ (LHS)	RHS Crack length (m) x10^{-3}	$\frac{da}{dN}$(RHS)	The required time for crack growth
0.54	-	0.6	-	After 6 minutes(i.e. from 19 minutes to 25 minutes)
0.66	$\frac{0.66-0.54}{(6*1830)}$	0.8	$\frac{0.8-0.6}{(6*1830)}$	After 6 minutes (i.e. from 25 minutes to 31 minutes)
1.13	$\frac{1.13-0.66}{(12*1830)}$	1.32	$\frac{1.32-0.8}{(12*1830)}$	After 12 minutes (i.e. from 31 minutes to 43 minutes)
2.36	$\frac{2.36-1.13}{(12*1830)}$	2.93	$\frac{2.93-1.32}{(12*1830)}$	After 12 minutes (i.e. from 43 minutes to 55 minutes)
-	Av. =2.94*10^{-5}	-	Av. =3.83*10^{-5}	-

Table5. Proposed scenarios

No.	Remote applied load	Crack inclination	Internal pulsing pressure effect
(1)	cyclic bending load	transvers crack(0^0)	without Internal pulsing pressure
(2)	cyclic bending load	transvers crack(0^0)	with Internal pulsing pressure
(3)	cyclic bending load	inclined crack(30^0)	without Internal pulsing pressure

Table6. Comparison between θ_C experimental and θ_C analytical

Equations	θ_C experimental	θ_C analytical	Error %
Eq. (11)	-58	-50.61^0	14.6
Eq. (12)	-58	-57.44^0	0. 97

السياسات العمرانية في الحرم الجامعي
دراسة تحليلية لسياسة التخطيط العمراني في حرم جامعة الكوفة

طالب حميد الطالب
استاذ – قسم هندسة العمارة
كلية الهندسة–جامعة بغداد

زمن عودة عمران
كلية الهندسة– جامعة بغداد
قسم هندسة العمارة

الخلاصة

الحُرُم الجامعية كأي كيان مادي ديناميكي، عرضة للتَغير المستمر في مراحل مختلفة تمليها فترات النمو والتطور والتغيّر، سواء بتطور المشاريع المتنوعة القائمة منها او استحداث الجديدة، وقد يؤثر ذلك سلباًعلى الشعور والاحساس القوي(Strong sense) بالتنظيم الوظيفي والشكلي والاستدلال بمسالك الطرق وتجانس البيئة الحضرية للحرم الجامعي كنتيجة لهذا التطور، فأصبحت غالبية البيئات الحضرية الجامعية المعاصرة تعاني من مشاكل جمة، ولعل ابرز تلك المشاكل تلك التي تكمن في فقدان عملية الترابط بين اجزاء المنظومة البيئية الكلية.

وتجسدت مشكلة البحث بـ "الحاجة المعرفية الى توضيح اثر السياسة الفكرية والتنفيذية في تحقيق الترابط والتنظيم الوظيفي والفضائي لعناصر البيئة الحضرية الجامعية وفي مراحل النمو والتغير المستقبلي"، واستهدف البحث "ابراز ودراسة السياسة العمرانية في الحرم الجامعي بمقوماتها الفكرية والتنفيذية، فضلا عن توضيح دور السياسة التنفيذية في تطبيق الفكر" ، وصيغت فرضية البحث بالاتي " تؤثر السياسة العمرانية بمقوماتها (الفكرية والتنفيذية)على عملية تنظيم وتجانس البيئة الحضرية الجامعية وبما يجعلها متكيفة مع التغيرات المستقبلية" ، وتم اختيار حرم جامعة الكوفة لتمثل حقلاً تجريبياً للبحث.

الكلمات الرئيسية : – التخطيط العمراني– الحرم الجامعي– السياسات التنفيذية.

Construction Policies on Campus
An Analytical Study of the Policy of Construction Planning on Kufa Campus

Prof. Talib Hamid Altalib
College of Engineering - University of Baghdad

Zaman OUDA Aljaberi
College of Engineering-University of Baghdad
E-mail:archzaman24@gmail.com

ABSTRACT

University Campuses, as any lively physical entity, is subject to continuous variation due to growth, development and change. This reality covers the existing or futuristic additives or additions, consecutively these changes may have a strong sensation of disorientation as a result of formatic changes in buildings, or in movement paths.

And it epitomized the research problem to "the need for knowledge to clarify the impact of intellectual and executive policy in achieving coherence, functional and space organization of the elements

of the university urban environment and in the stages of future growth and change," the search targeted "to highlight the study of constraction politics on campus Bmqomadtha intellectual and executive , as well as clarify the role of the executive policy in the application of thought, "and formulated the hypothesis search " urban policy affect Bmqomadtha (intellectual and executive) on the process of organizing and homogeneity of the university urban environment to make them adapted to future changes, "the University of Kufa it was chosen as the campus to represent the experimental field of research.

Key Word: Construction Planning, Campus, Executive policy

1-المقدمة

يعد التخطيط العمراني على مستوياته المختلفة في البيئات الحضرية، من ابرز المهام والمواضيع التي تشغل اهتمام المصممين والمخططين الحضريين، ومن المجالات العلمية والعملية التي تلعب دوراً فاعلاً في تطور وتنمية الانسان والمكان، واحدى الادوات الهامة للوصول بالتنمية الشاملة الى المستويات الطموحة، من خلال البرامج والسياسات ومشاريع التنمية المهتمة بجيل الحاضر والمستقبل في جوانب البيئة المختلفة العمرانية والاجتماعية والاقتصادية.

وكنتيجة لتفاعل الانسان بطريقة خاطئة مع بيئته المحيطة تولّدت العديد من الاشكالات البيئية والاجتماعية والسياسية والاقتصادية، لذا اصبح الاهتمام بالبيئة العمرانية من المواضيع المهمة، والبيئة الجامعية واحدة من تلك البيئات الحضرية التي تمثل احد قطاعات المدينة المهمة وجزءاً حضرياً منها، وقد شهد الحرم الجامعي خلال العقود المنصرمة تنمية واسعة في شتى المجالات وصولا الى تنمية شاملة متوازنة للانسان والمكان على حد سواء، وكان للتخطيط العمراني دورا فاعلا في تلك المؤسسة.

2-التخطيط العمراني: يعتبر التخطيط العمراني المجال الاكثر إلماماً وفاعلية في الاشارة الى اساليب معالجة المشكلات القائمة في المجمعات الحضرية ووضع الأطر المستقبلية لتطويرها، يؤكد الشهري* ذلك من خلال طرح الدراسات التنظيمية لنمو وتطور كل جزء من المدينة وتحديد اتجاه ومناطق التوسع والنمو بفعالياتها المختلفة. واشار ايضا الى إن عملية التخطيط العمراني بمراحلها الأربعة: التفهم Understanding, والتصميمDesign ثم التنفيذ Implementation والتقييم والمتابعةEvaluation and Control ، تمثل عملية موازية لما يسمى" بعملية التنمية العمرانية الشاملة"، والتي تشمل أنشطة للكثير من المتخصصين كالمعماريين والمخططين العمرانيين ومصممي البيئة والمهندسين والاجتماعيين والجغرافيين والاقتصاديين والإداريين والسياسيين وغيرهم، وهم جميعاً مشاركين لازمين لإعداد تخطيط المدينة، **الشهري،2006.**

3-الحرم الجامعي ومراحل التطور في اوائل القرن العشرين: يمثل الحرم الجامعي المكان الذي يتجسد فيه الفن الانساني Human Art في صناعة المكان، فهو نتاج فني من خلال التكوين الكلي للمنشات والاعمال النحتية والمشاهد الخارجية والفضاءات العامة، ويمثل ايضا المكان الذي يتم فيه ربط احدث الافكار التصميمية والتقنيات المبتكرة بمهمة التطوير والتنمية، وهو محط بناء العلاقات والجسور مع المجتمع، فالمنشات الموجودة تساعد على فهم التواصل مع المجتمع والمثاليات الفنية، **Edwards,2000**. ان الحرم الجامعي يمثل مجموع البيئة المادية بما في ذلك جميع المباني وفضاءات المشهد الخارجي، وهذا المزيج بين المباني والفضاءات الخارجية وبين وظائف تلك المباني كمؤسسة او منظمة باكملها، يعطي هوية مميزة وتشكل مكاناً رئيساً في الذاكرة الجماعية للمؤسسة، **Yang,2007**. في اوائل القرن العشرين تعالت الاصوات المعمارية الناقدة لتخطيط

*د.فائز سعد الشهري، استاذ بقسم التخطيط الحضري والاقليمي ،كلية العمارة والتخطيط ،جامعة الملك فيصل

وتصميم الحرم الجامعي، ففي عام 1903 أنتُقد تصميم الحرم الجامعي التقليدي في امريكا الذي لم يحترم العلاقات، ويفتقد للوحدة بين المباني، ودعت كثير من الاراء الى ضرورة تحقيق الانسجام والوحدة بين الابنية الجامعية في تخطيط الحرم الجامعي والتاكيد على علاقة الكل بالجزء. وفي عام 1909، برز نمو الذوق في العمارة Growth of Taste ، من خلال الدعوة الى تحقيق التماسك والالتحام لمكونات الحرم الجامعي التي من الاوجب أن تحقق نفس السياق او الطراز، ومن جانب اخر فقد أُعتِمد مبدأ المجموعات في التصميم Group Plan من خلال تقسيم المخطط الافقي الى انماط معينة تبعا لشكل الموقع مثل النمط المغلق او المفتوح او الطولي او التركيب غير المتماثل، مع اهمية تنسيق الفضاءات الثانوية لغرض تحقيق التدرج والهرمية في تصميم الجامعات، **Turnel,1984.**

4-التجارب المعمارية لمباني الحرم الجامعي- النصف الاول من القرن العشرين: بدأت مباني التعليم الجامعي بالتطور وظهرت بشكل واضح من خلال اعمال رواد العمارة الحديثة، ويمكن استقراء بعض من اعمالهم وكالاتي:

أ- **Mies Van DerRoh:** عين المعماري ميس فان دوره كاستشاري لمشروع اضافة مباني جامعية لمعهد التكنولوجيا بالينوي Illinois Institute of Technology الذي انشأ في 1892، حيث صمم مبنى جديد للمعهد في 1938(وهو اول تجربة له في تخطيط الابنية الجامعية)، عكس فيه الاتجاه الجديد المفتوح واعتمد التصميم مبدأ التماثل حول المحاور وهو ما انُتقِد عليه من قبل مخططي الجامعات كونه غير مرن وتقليدي، لكنه اعتمد فيما بعد كنسق تصميمي لمباني الجامعات، وجسد المصمم افكاره من حيث اهتمامه بالتفاصيل ووضوحية الصورة ، فضلا عن المحافظة على النسب، كما ان التصميم تميز ببساطته في استخدام الحديد الظاهر في الانشاء والزجاج في الواجهات، شكل(1). **Turnel,1984.**

ب- **Walter Gropius** : صمم المعماري Walter Gropius مباني الدراسات العليا في جامعة هارفارد، بعد تعيينه رئيس قسم الدراسات العليا في الجامعة 1937، واعتمد التصميم على ثمان وحدات من المباني التي كونت بتشكيلها فراغات غير منتظمة ومتدرجة ينساب كل منها في الاخر، تعطي احساسا بالحركة، مكونا بذلك انماط تشكيلية مغلقة ومفتوحة. هذا التصميم عكس الفكر العقلاني للمصمم المتميز بوضوح الصورة وبساطة المواد المستخدمة وانسيابية الحركة، شكل(2). **Dober,1996.**

5-التجارب المعمارية لمباني الحرم الجامعي- النصف الثاني للقرن العشرين:ازدادت مباني الجامعات في الحرم الجامعي نتيجة لزيادة عدد الطلاب والاقبال الشديد على التعليم بعد الحرب العالمية الثانية، واصبحت الجامعة تعبر عن الرقي اضافة الى دورها في تغطية الحاجة من العمال المتعلمين لدعم نمو الاقتصاد، ونتيجة لذلك فان الجامعات الجديدة استمرت بالنشوء والتاسيس والجامعات القائمة وسّعت لتلبية الاعداد المتزايدة للطلاب، فعلى سبيل المثال في بريطانيا وحدها بنيت مالايقل عن ستة جامعات خلال عام 1960, **Hashimshony ,2007.** ومن اعمال المعماريين في فترة النصف الثاني من القرن العشرين والتي عبرت عن الافكار والنظريات الحديثة :

أ- **المعمار Le Corbusier في جامعة هارفارد:** صمم المعماري لوكوربوزيه المركز الفني في جامعة هارفارد سنة1960، وانطلقت افكاره في تصميم المبنى من ممرات الحركة الخاصة بالمشاة حول المبنى حيث يقطع المبنى طريقا منحدرا يرتبط بشارعين مهمين ويحقق كفاءة وانسيابية عالية لحركة الطلاب والمشاة، واعتبرت هذه الفترة منطلقا لفكر تصميمي جديد للجامعات وذلك من خلال تبني ممرات حركة المشاة كدافع اساسي في تشكيل الحرم الجامعي، شكل(3)،**Turnel,1984 .**

ب- **المعمار William في جامعة Irvine بكاليفورنيا:** نتيجة لزيادة الاقبال والتوجه نحو التعليم العالي، اصبحت الجامعات تواجه مشكلة تضاعف اعداد الطلبة وزيادتها، مما جعل منها جامعات عملاقة Mega Universities، ولحل هذه المشكلة العددية طرح المعماري William L.Pereira مبدأ جديد يتعلق بتقسيم المباني التعليمية وفصلها، حيث صمم المعمار في عام 1963 ست وحدات او مجموعات من المباني كل منها ينتمي الى نظام تعليمي متخصص، تنفصل هذه المباني عن بعضها بمنطقة خضراء، كما ان الحرم الجامعي محاط بطريق دائري مما يدل على تشابه الفكر التصميمي مع افكار المدينة الحدائقية، شكل(4)، **Turnel,1984.** وفي عام 1996 اقترح المعمار Richard Dober نظرية عامة لربط العمارة بالحرم الجامعي، حيث ذكر فيها النهج التصميمي للحرم الجامعي، اما تصميم مبنى واحد او مجموعة مباني ضمن الحرم وهو ما عبر عنه بمستوى الوحدة Micro Scale Design ،اي طراز المبنى وصفاته المنعكسة على الواجهات والمخططات والتفاصيل والمواد المستخدمة، وكذلك وضوح الوظيفة وعكسها على المبنى معماريا،او تصميم جزء حضري متكامل او قطاع ضمن الحرم وبوحدة وظيفية وبصرية معبرا عنه بالمستوى الشاملMacro Scale Design وصولا لفكر تصميمي يخلق صورة وهوية مميزة للحرم الجامعي من خلال الاسلوب الانشائي لصنع المكان، **Dober,1996.**

ان القيم الحقيقية لما تناولته التجارب السابقة للمباني الجامعية تكمن بالاعتماد المتلائم والمتكافئ بين هذه الافكار والطروحات المتنوعة وبشكل متداخل ومتكامل وبما يحقق عملية التنظيم التخطيطي والتصميمي للحرم الجامعي، حيث اتفق المختصين من حيث المبدأ باعتماد الفكر الفلسفي ومايترتب عليه من اعتبارات تصميمية اساسية ومقومات القيم المكانية والزمانية (الاجتماعية والثقافية والتاريخية (مؤثرات محلية)، ويمكن اعتبار هذه المبادئ والمفاهيم التنظيمية ادوات تصميمية مرنة يمكن اعتمادها من قبل المخطط والمصمم هذا من جانب، ومن جانب اخر فأن هناك مؤثرات ومتغيرات لها دور فعال في ابراز وطرح السياسة الفكرية والفلسفية واخراجها الى الواقع بطريقة معينة، اما ان تعزز الجانب الايجابي للعملية التصميمية او قد تقوده الى نتائج سلبية معاكسة، الا وهو الجانب التنفيذي. وانطلاقا مما سبق، يعتمد البحث ان اليات تحقيق بيئة حضرية جامعية منتظمة يكون من خلال (المستوى الفكري الفلسفي والمستوى التنفيذي) للوصول الى اليات تنظيمية للبيئة الحضرية الجامعية، شكل (5).

6- اليات تحقيق بيئة حضرية جامعية منتظمة

6-1 المستوى الاول- الجانب الفكري والفلسفي: ان التعامل مع منظومة متكاملة من عناصر ومقومات البيئة الحضرية الجامعية بطريقة تحافظ على تجانس الصورة الكلية ويجعلها اكثر تصورا وادراكا، هو الدور الذي يحاول المخطط والمصمم تحقيقه، باعتبار ان هذه البيئة تمثل كيانا متكونا من اجزاء وعناصر وعلاقات رابطة بينها على المستوى الشكلي والوظيفي والفضائي. وسيتناول البحث المستويات التنظيمية للحرم الجامعي كالاتي:

6-1-1 المستوى التخطيطي الشامل Macro Scale Concept (الفلسفة التخطيطية والتصميمية للبيئة الجامعية) : ان تخطيط الحرم الجامعي يتشابه مع تخطيط وتصميم المدينة، حتى انه يمكن اعتبار الجامعة هي مدينة صغيرة داخل مدينة اكبر رغم وجود بعض الاختلافات بينهما مثل الاحتياجات الوظيفية المحدودة للجامعة وامكانية الاستجابة للتغيرات المستقبلية، وبالمقارنة مع المدينة، فان التغيرات داخل الحرم الجامعي متكررة وذات معدل سريع وهذه احدى السمات الاساسية بالتخطيط الجامعي، **عز الدين، 1993.** ان التخطيط المتكامل والمثالي، يكون من خلال خلق استراتيجيات تخطيطية متكاملة تتطلب مرونة

وحرية في كل فضاء ولكل وقت، فالتخطيط يهدف بالاساس الى تأطير العملية الحياتية التي تجري داخل الحرم الجامعي، **Campos,2012**.

6-1-2 المستويات التخطيطية للحرم الجامعي Planning Levels of The Campus

ان معالجة كل متطلبات التخطيط والتصميم الخاصة بالمجمع التعليمي الحضري يكون من خلال تحقيق التكامل والتوازن بين المستويات التخطيطية للحرم الجامعي، والذي سيتناوله البحث من خلال المستويات التخطيطية المتكاملة الاتية لضمان نجاحه :

أ-التخطيط الشامل لاستعمال الاراضي Comprehensive land Use Planning : هذا المستوى من التخطيط يشمل مختلف عناصر الارض والبنى التحتية والتنمية القائمة واستراتيجية التخطيط المستقبلي، والاتجاه العام لتطوير الحرم الجامعي من خلال المخطط الشامل لاستخدام الارض وياتي بنفس السياق والطرق المتبعة في مخططات التنمية الشاملة للاستخدام الوظيفي لمدينة معينة.

ب-تخطيط القطاعات District Planning: والتي يظهر من خلالها الحرم الجامعي كقطاعات متنوعة من خلال تقارب المستويات الوظيفية(مثل العلوم والهندسة، السكن، الالعاب والترفيه).

ج-تخطيط الموقع Site Plan : ان تحديد مواقع المباني الجامعية ضمن المخطط الاساس هي واحدة من اهم اعمال تخطيط الحرم الجامعي، كما يجب ان تاخذ بعين الاعتبار معايير هامة عديدة، منها مايلي :

- المطابقة مع مخطط استخدام الاراضي والحرم الجامعي وتخطيط القطاعات .
- تعزيز العلاقات المادية(الفيزياوية) مع البرامج الاكاديمية ذات الصلة .
- احترام العلاقات الوظيفية للبرامج والانشطة الاخرى .
- تلبية متطلبات الوصول للمشاة والدراجات والمركبات والخدمات .
- تسهيل استخدام الموقع للغرض الحالي مع السماحللاستخدامات البديلة المستقبلية، **Neuman ,2013** .

ان أختيار الموضع الاكثر منطقية للمباني الجديدة يتطلب تحقيق العلاقات المتميزة مع البيئة المحيطة بشكل كامل، من خلال انسجام المباني وتوجيهها وتنظيم حركة الطلبة والسيارات والمداخل، وان تسهم في اغناء الخصائص الرمزية والجمالية، اضافة الى اسهامها في عدم تفكيك وتشظي البيئة المحيطة، كما اكد على ضرورة الاخذ بنظر الاعتبار علاقة المبنى بالمخطط العام للموقع، **الجميلي،2012**.

ومن هنا يتضح ان اختيار المواقع الملائمة للمباني الجامعية ينبغي ان تخضع الى تحليل موضوعي وفقاً للمخطط الشامل للحرم الجامعي، فضلاً عن اهمية احترام المبادئ الاساسية للفكرة التصميمية وعدم انتهاكها باختيار مواقع يمكن ان تسبب في حصول خروقات تصميمية وتخطيطية تفقدها هويتها، وبذلك تُعزز التوافقية مع المساحات المفتوحة لا ان يتجاهلها، ان اي اضافة فيزياوية في الحرم الجامعي من شأنه ان يغير من التكوينات الشكلية للفضاءات المفتوحة، وهنا يبرز ابداع المخطط او المصمم في جعل الجديد جزءا متوافقاً مع الكل الشامل.

6-1-3 علاقة الحرم الجامعي بالمدينة: ان المدن والحُرُم الجامعية تتفاعل مع بعضها بعلاقة جوهرية من خلال تأثير كل منهم على التطورات، ووفقاً لذلك فان هذه الرؤية الحالية والمستقبلية للحرم الجامعي متعلقة بسياقها الحضري الاجتماعي والثقافي والاقتصادي وسيستمر التشابك والتداخل ليس اجتماعياً فحسب بل فيزيائياً (مادياً) مع الاحياء المحيطة بها وبالتالي فان المناطق الحضرية للحرم الجامعي هو جانب له صلة بتحديد انواع العلاقات الفيزيائية (المادية) مع بنية المدينة. ويمكن تحديد نوعين من الجامعات وفقا لموقعها:

- الجامعات الكلاسيكية داخل المدينة Classical Inner City Campuses
- الجامعات في المناطق الريفية Green Field Campuses

وهناك نوعين من الجامعات داخل المدينة والتي تحدد انواع العلاقات الاجتماعية :

- الرسمي Formal : والذي يتم فصلها فيزيائياً (مادياً) عن البيئة الحضرية وتمتلك الطابع المحافظ .
- غير الرسميInformal **:** والذي يشير الى المجمعات التعليمية(الحرم الجامعي) في وسط المدينة مع فرصة مثمرة للتقاطع الثقافي، ووفق الاراء ووجهات النظر للمعنيين بالموضوع فان كل المجمعات يمكن ان تكون مناسبة لسياقات محددة ولكن لاينبغي تجنب العزلة او المجمعات العشوائية، شكل(6).**Flavia,2013.**

ان اختيار موقع الجامعة يؤثر في بنيوية الجامعة وفي طبيعة المكونات والفضاءات الموجودة داخل الجامعة، كذلك فان إستراتيجية وأهداف الجامعة ورسالتها، لها ايضا تأثير كبير في نوعية الخدمات والعناصر المكونة لمدينة الجامعة، فلو كانت الجامعة تسعى إلى ان تكون مركزا للتنمية للبيئة الحضرية المحيطة بها فهي بحاجة إلى مكونات أكثر مما لو كانت مؤسسة تعليمية فقط. فطبيعة النهج التعليمي وعلاقته بالتطورات التقنية واستثمار التعليم (من خلال ربطه بالصناعة او التجارة)، يحتاج لبيئة ومقومات خاصة.

4-1-6 الانماط الحضرية التخطيطية الجامعات:يمكن تحديد الانماط الحضرية لبنية الحرم الجامعي اعتمادا على نوعية الهيكل الداخلي للجامعة وخصائص العناصر المكونة لها والفضاءات وعلاقاتها مع المحيط، فضلا عن طبيعة استجابة الجامعة وتكيفها مع التحديات التي تواجهها، حيث يمكن تقسيم البنية الداخلية لمجمع الحرم الجامعي الى ستة انواع، وهي بدورها ايضا تقسم الى انواع فرعية، يوضحها شكل (7) :

1. الشبكي: ويقوم على نسيج خطي وتتألف من تقاطع مجموعتين من الخطوط المتوازية ويمكن ان تكون بانواع :

- شبكي بشكل عام حيث يمكن ان تكون مجموعات الخطوط المتوازية قائمة الزوايا او منحرفة والمساحات المتكونة هي متوازي اضلاع.
- شبكي قائم الزوايا: حيث تكون مجموعات الخطوط المتوازية بزوايا قائمة او عمودية والمساحات المتكونة هي مستطيلات .
- شبكة Grid : تكون مجموعات الخطوط المتوازية هي دائما قائمة الزاوية والمسافات بينها متساوية والمساحات المتكونة هي مربعات.

2. الخطي Linear : يتم ترتيب الهيكل الداخلي على طول محور طولي.
3. المركزي Central: التكوين مرتب حول نقطة واحدة مركزية او اكثر.
4. متعددة المراكز Multi-central: مجموعة التركيبات تكون مختلفة المركز وتم تطويرها لمساحات اكبر مما نتج عنها مراكز بعيدة .
5. الشعاعي Radial : يتم ترتيب التصميم بشكل سلسلة من انصاف اقطار متقاربة حول نقطة مركزية.
6. العضوي Organic: يكون الهيكل مشابه للاشكال العضوية او النظام التركيبي وهو مستوحى من الاشكال الناشئة من الطبيعة
7. هندسي غير منتظم Irregular geometries التكوين يعتمد على ترتيبات غير نظامية تتحدى النماذج الهندسية المنتظمة **Campos,2014.**

من التصنيفات السابقة تتضح انماط البنية المادية للحرم الجامعي المتنوعة والمتغيرة وفقا للمقتضيات الزمانية والمكانية وتلبية

للمتغيرات الاجتماعية والاقتصادية والسياسية، ويعتمد اختيار النمط الشكلي على الرؤى والسياسة المتبعة من قبل الجامعة والبيئة الحضرية المتواجدة فيها.

6-1-5 الفضاءات الخارجية في البيئة الجامعية: يمثل الفضاء الخارجي جزءاً هاما في تصميم الحرم الجامعي، ويمكن تمييز نوعين رئيسيين من المكونات الأساسية للفضاءات الخارجية الجامعية، وكالاتي :

أولاً: العناصر المادية: للمكونات المادية دور مهم في وظيفة الفضاءات الخارجية والتي تدعى في كثير من الأحيان بأثاث الفضاء، وتمثل أحد العناصر الأساسية المهمة في خلق التكوينات الجمالية للفضاءات الخارجية، وتشمل أماكن الجلوس والإضاءة والأكشاك والمسقفات وصناديق النفايات.

ثانياً: العناصر الطبيعية: وتشمل النباتات والمياه ، **مازن ،2012.**

6-1-6 التنظيم الفضائي- الكتلي:

ان العلاقة التجميعية والتراكبية مابين الانماط المختلفة للكتل والفضاءات ينتج عنها الشكل الحضري، حيث ان هذه العلاقات تتخذ اشكالا متباينة تعتمد على طبيعة تشكيل الابنية ومواقعها والنظام الحركي فضلا عن الاشجار والجدران وغيرها، وبشكل عام فان شكل العلاقات بين الكتل والفضاءات تشكل من خلال :

- شكل وموقع الابنية.
- تصميم العناصر الخارجية كالاشجار والجدران.
- ممرات الحركة ، **Trancik, 1986.**

ويمكن تصنيف العلاقات بين العناصر كالاتي:

- علاقات تجميعية: كالتقارب والتعاقب، ومنها التجاور، والتداخل.

- علاقات تنظيمية: كالإيقاع، والتدرج، والهيمنة، والتناسب، والتوافق والتكرار (العمودي والأفقي)، **Antoniades,1990.**

-علاقات نسقية: اي الطريقة التي تجتمع بها العناصر وفقا لخواصها المتعلقة بالحجم والموضع والهيئة وقد تعتمد على التدرج والتناظر والتحول والمحورية والايقاع.

-علاقات منظومية : وهي الطريقة المعتمدة على الخواص التموضعية للعناصر عند تجميعها وتتمثل بالتنظيمات الفضائية الاتية (المركزي والخطي والشعاعي والعنقودي والشبكي)، **Ching, 1996**. ان اي مجمع حضري يبنى من خلال طبيعة العلاقات والتوليفات المتنوعة مابين الكتل والفضاءات، ويجب مراعاة تحقيق التوازن بين ارتفاعات الكتل في خط السماء، وتحقيق بيئة حضرية واضحة المعالم ومتماسكة اعتمادا على العلاقات التبادلية بين الكتل والفضاءات، **Antoniades,1990.**

6-1-7 التنظيم البصري-الحركي : تمثل المحاور البصرية احدى العناصر التصميمية الموازية لاهمية الادائية الحركية ومحاورها ولها دور في تحقيق الفعل الترابطي لمكونات البيئة الحضرية، وقد تشترك المحاور البصرية مع الحركية في تعزيز الادراك البصري من خلال توحيدها للتاكيد على اهمية معينة او استقطاب الجذب باتجاه ما، او قد ينفصل المحورين لتحقيق مشهد حضري يعزز الاحساس بالاستمتاع والتنوع. وكلما كان هناك توافق بين المحورين (البصري والحركي) كلما تعمق الشعور بالانتماء المكاني للبيئة الحضرية التي ستكون اكثر فاعلية وثراءاً،**Chapman, 1993.** الكثير من الجامعات تعاني من هيمنة طرق المركبات وتترك المشاة في صراع بين مواقف السيارات وساحات الخدمة، الا ان التصميم الجيد للحرم الجامعي يعطي اولوية لحركة المشاة

وبمساحات واسعة للتنقل مشيا في الطرق الرئيسة اما الثانوية فهي تتفرع منها وتقترب الى المناطق الخلفية لمباني الحرم الجامعي. ويجب ان تتميز طرق المشاة كونها مباشرة وواضحة وامنة وممتعة ومرتبطة بالطبيعة ،حيث تساعد مسارات المشاة في التفاعل العلمي وتبادل الافكار بين الطلبة ذوي الاختصاصات المختلفة، **Edwards, 2000.** ان البيئة الحضرية في الحرم الجامعي تتميز بكونها بيئة تحترم المشاة من خلال اعتماد مسافات تحرك سلسة مريحة بين ارجاء ومكونات الحرم وضمن حدود الراحة البشرية بحيث لاتتجاوز الـ(10 دقائق)، **Dober,2000.**

ومن هنا يتضح ارتباط جميع اجزاء الحرم الجامعي ارتباطاً وظيفياً بحكم تواجدها داخل حرم جامعي واحد، ويجب ان يتاكد هذا الارتباط ماديا بشبكة جيدة ومنظومة متكاملة من الطرق وممرات المشاة وفضاءات التجمع تصل بين جميع اجزاء الحرم الجامعي ويتحقق بها الانتقال السهل والكفوء مع مراعاة تحقيق وتشجيع التفاعل الاجتماعي على مستوى اللقاءات الفكرية بين الطلبة من جهة وبين الطلبة واساتذتهم مما يعمق الروابط ويشجع العلاقات بينهم، ويجب ان تتميز هذه الشبكة باحترام المقياس الانساني فلا تزيد مسافة سير اي شخص عن 15 دقيقة ويكون السير ضمن ممرات مخصصة للمشاة، واضفاء العناصر الجمالية المحببة الى النفس للترويح عن الطلاب اثناء انتقالهم .

6-1-8 الاعتبارات البيئية : هناك العديد من العوامل البيئية التي تؤثر على تخطيط وتصميم مباني الحرم الجامعي، منها العوامل الطبيعية المرتبطة بظروف الموقع الطبيعية ومن اهمها عاملا المناخ والطوبغرافية التي يعتبر التفاعل معها وتطويعها من اهم اسس التصميم المعماري الجيد، ويتم التحكم فيها بداية من تخطيط الموقع العام حتى تصميم المبنى الواحد داخليا وخارجيا،ان طبيعة المناخ الحار(المميز للبيئة المحلية) يؤثر تاثيرا كبيرا على اختيار طريقة اواسلوب البناء المتبع للوقاية من الحرارة وتحسين الظروف المناخية، وهناك عدة طرق تستخدم في حالة المناخ الحار يمكن ان تؤدي الى تحسن ملحوظ في الظروف المناخية منها: تجميع المباني بطريقة اندماجية (تجميعية) وتجميع المباني على فناءات داخلية بالاضافة الى المعالجات البيئية كالتشجير واستخدام المسطحات المائية مما يؤدي الى خفض درجات الحرارة وحماية مستخدميه من الظروف المناخية القاسية، **سحر،1995 .**

6-1-9 استخلاص مؤشرات المستوى التخطيطي الشامل: ويمكن تلخيص اهم المفردات الاساسية من الاطار النظري الخاصة بالمحور الاول (المستوى التخطيطي الشامل) في جدول(1).

6-1-10 المستوى التوسعي (التغيرات المستقبلية) Expansion Scale Design:

ان التحديات التي تواجهها الجامعات سواء كانت داخلية متمثلة بالزيادات المطردة في اعداد الطلاب او التحديات الخارجية متمثلة بالتطورات العلمية والتكنولوجية وظاهرة العولمة وغيرها، تحدث فيها تغييرات مستمرة في الادارة الجامعية والاحتياجات التدريسية، وبالتالي لابد للجامعات ان تكون مؤهلة لمواجهتها، وقد تبين من التجارب العالمية في مجال التخطيط الجامعي بان المستقبل سوف يجعل من الحُرُم الجامعية ديناميكية ومستمرة في النمو والتوسع بدرجة تفوق الحدود القصوى وبمرافق مادية او افتراضية، فالاتجاه الاساس للاستعداد لذلك يكون باعطاء الجانب التخطيطي اهمية كبيرة وهو يعبر عن الفلسفة التصميمية التي تحقق عادة التوازن بين المتطلبات الاساسية القصيرة المدى والاهداف بعيدة المدى،**Duncan, et al,2012 .**

أن توسع الحرم الجامعي يمثل حقيقة ثابتة يظهر بعدة انماط هي:

- النمو والتوسع الشامل Overall Growth and Expansion وهو التوسع بشكل طردي مع الزيادة في الطاقة الاستيعابية .

- النمو المتباين Differential Growth التوسع في اقسام معينة مع تزايد معدلات القبول .
- المرونة الداخلية Internal Flexibility وهو التغير نتيجة لاستحداث اقسام والغاء اخرى، **السليفاني ،1989.**

وبالرجوع الى عامل الزمن، تتضح نقطتان اساسيتان وهما:

اولا: يجب ان لاننظر الى فكرة المخطط العام على انه تصميم مثالي ومتكامل وثابت، فمثل هذه النظرة غيرصالحة تماما اذا ماوضعنا في الاعتبار التغير السريع والمتلاحق في المستجدات المادية والاجتماعية، لذلك لابد ان يكون اساس المخطط العام هو حلقة او سلسلة متصلة من خطط العمل المتتابعة والمتكاملة يربط بينها اسلوب او نمط عام يحدده مايسمى بالمخطط الشامل الذي يجب ان يبقى مرناً قابلاً للتطورات بما قد يستجد من عوامل ومدخلات، دون ان يفقد خصائصه الاساسية.

ثانيا: يجب على المصمم اوالمخطط ان يضع عامل المرونة Flexibility نصب عينيه ويعطيه اهمية بالغة، اذ لابد للمستقبل ان يكون له شروط ومتطلبات جديدة سواء كانت تكنولوجية او اجتماعية او ادراية تعليمية، او سواها من المتغيرات التي يشهدها عالم اليوم، **عبد الله ، 1983.**

ان من السمات الدائمية لتخطيط الجامعات هي التوسع والتغيير ما يتطلب مرونة عالية لمجابهة التحديات المتعلقة لتحقيق التماسك التصميمي والاحساس بالانتماء والهوية في جميع مراحل التنمية والتطور، **العلوان،1988.**

6-1-11 الاعتبارات التصميمية للمباني الجديدة المضافة لتوسيع الحرم الجامعي: في مجال نمو الحرم الجامعي، تسعى الجامعات لايجاد الحلول الذكية لنمو الحرم الجامعي، فان كل من المباني الجديدة والمجددة يجب ان تكون مصممة بطريقة تكمل بها صورة الحرم الجامعي، ومن بين العديد من الاعتبارات التصميمية المستخدمة لدمج الوحدات الطلابية مع الوجود القائم بنجاح داخل نسيج الحرم الجامعي هي تعزيز ثلاث مفاهيم مهمة، **Kyle,2006**. وكالاتي:

1. الاتصالات البصرية
2. العلاقات المادية
3. التمثيل الرمزي، شكل(8)

ان اهم الاعتبارات الواجب مراعاتها من قبل المعماريين ومهندسي الفضاءات الخارجية (Landscape) والمتعلقة بالمباني الجديدة المضافة للحرم هي :

1-المقياس والتناسب Scale And Proportion :لما له من دورعلى الاحساس بالمكان واحترام المقياس الانساني والاخذ بالاعتبار اثر مواد البناء المستخدمة في تأثيراتها على قراءة مقياس المبنى.

2-تحديد موقع المبنى Building Siting : يجب توخي الحذر عند توقيع المبنى بحيث ينتج عنه اتصال ايجابي بين المباني ومسارات المشاة، فلابد للمبنى ان يعترف بالارتداد او محاذاة المباني المجاورة وعلاقته معها من حيث مواقع الدخول وتطوير وتعزيز المساحات الخارجية بين المباني.

3-الشـــكل Form : ان شكل المبنى يمكن ان يؤثر بشكل كبير على نسيج الحرم الجامعي، فالشكل المتسق المستخدم في جميع انحاء المنطقة المحددة يوفر تماسكاً ومظهراً معرفاً ومحدداً لتلك المنطقة. كما ان استخدام اشكال بناء مترابطة يمكن ان يحقق الوحدة لدرجة عالية بين مباني الحرم الجامعي، حتى وان كانت المباني مختلفة بالطراز المعماري.

4-مـــــواد البناء Materials : ان المواد المستخدمة في تشييد المباني او عناصر المشهد الخارجي يمكن ان يكون لها تاثير كبير على صورة الحرم الجامعي، حيث ان مواد البناء المناسبة اضافة الى تجانسها يمكن ان تسمح بحرية التعبير للمصمم لخلق الوحدة بين مباني الحرم.

5-مزروعات الموقع Site Plantings: ينبغي توفر مساحات مزروعة حول المباني الاكاديمية والوحدات السكنية والفضاءات المفتوحة بين المباني، وينبغي اعطاء مساحة كافية من الاهتمام بمداخل المبنى وتكاملها مع النباتات المختارة ويمكن استخدام الاشجار لعزل مواقف السيارات ومناطق الخدمة والمخازن والشوارع التي تكون مصدراً للتلوث الصوتي والبصري، **John**,and **David,2002**.

6-1-12 استخلاص مؤشرات المستوى التوسعي

من خلال الطرح الخاص بالمستوى التوسعي، يمكن استخلاص اهم المفردات والقيم الخاصة بالمستوى التوسعي في الجدول(2).

6-2 المستوى الثاني- الجانب التنفيذي

ان تنفيذ ومتابعة السياسات والمخططات التنموية يعتبرجزءاً لايتجزأ من مسار التخطيط العمراني، والمقصود بالتنفيذ هو تطبيق أي قرار ينطوي على سياسة معينة، حيث ان للتنفيذ والمتابعة متطلبات مرتبطة بتوفر المعلومة الصحيحة والكفاءات البشرية المؤهلة في المجال والتنسيق الشامل من الجهات التي ساهمت في عملية التصميم والتخطيط ، ويعتبر اشتراك الجهات التي اعدت التصاميم في عملية تنفيذها حتمي لنجاحها فهي الاكثر دراية بمكوناتها وتفاصيلها وان ضعف نجاح كثير من الخطط التنموية يرتبط باختلاف الجهات المعدة للخطة عن الجهات المنفذة لها، **الشهري،2006**. إن من مهام وأهداف عملية المتابعة في مرحلة التنفيذ كشف مواطن الخلل والانحرافات التي قد تحدث ونوعها وأسبابها وتقييم نتائجها والاستفادة من ذلك عند إعداد الخطط اللاحقة، التأكد من أن عملية التنفيذ تجري كما هو مرسوم لها وتعمل على تحقيق الأهداف الواردة في الخطة، والتعرف على مدى واقعية الخطة أو الخطط من خلال مقارنة الإنجازات بالأهداف المرسومة فكلما كان الانحراف كبيراً عن الأهداف المنشودة كلما كانت الخطة غير واقعية، كذلك تحديد الجهات المسؤولة عن مواطن الخلل والانحرافات وهل هي داخلية أم خارجية وهل هذه الانحرافات ناجمة عن تقصير الجهات المنفذة أم تلك التي أعدت الخطة، تحديد الصعوبات والمشاكل التي تواجه عملية التنفيذ وكيفية التغلب عليها وتجنبها مستقبلاً عند وضع خطط جديدة، **الشهري،2006**.

أن مقومات الجانب التنفيذي يمكن اعتمادها بمرحلتين اساسيتين يتوقف عليهما مدى نجاح المشروع المعد وفقا للفكر التصميمي والفلسفي، فهو يمثل المرحلة التي يُترجم فيها الجانب الفكري الى واقع ملموس، ونجاحها يعزز نجاح الجانب الفكري للمشروع، وتتمثل هذه المقومات بالمرحلتين الاتيتين: مرحلة اعداد المخططات والرسومات التنفيذية التفصيلية المتعلقة بالمخططات المعمارية(خرائط+ مواصفات فنية) والمتطابقة معها والتي تعد من قبل الاستشاري المصمم او قد تحال الى استشاريين اخرين، والمرحلة الثانية تمثل مرحلة التنفيذ الفعلي على ارض الواقع من قبل الجهة المنفذة(الاستشاري المصمم او المقاول) والخاضعة لاشراف الاستشاري المصمم. ويمكن ان نلخص مفردات الجانب التنفيذي بالجدول (3).

7-الدراسة العملية : جـامعة الكـــــوفة وضع المخطط الاساس للحرم الجامعي في الموقع الحالي للجامعة الذي يقع بين مدينة النجف والكوفة، من قبل المعمار المحلي_الدكتور ساهر القيسي وفق رؤيا فلسفية شمولية نابعة من خصوصية المدينة وتراثها الحضاري، وسيتم تحليل الحرم الجامعي وفقا لمؤشرات الاطار النظري، وكالاتي:

7-1التحليل على وفق المستوى الاول من التطبيق... (المستوى التخطيطي الشامل Macro Scale Concept):تتضمن ادوات وعناصر تحقيق الفكر التخطيطي العام للحرم الجامعي الذي يشمل الأتي:

أ-التنظيم التخطيطي: أن طبيعة الشكل الطولي للموقع المخصص للمشروع، قد فرض نمط التخطيط الخطي (الشريطي)، والذي استثمره المصمم بطريقة حققت خصوصية متميزة في تنطيق وتوزيع استعمالات الارض، حيث تم تقسيم مكونات الموقع الى قطاعين اساسيين هما القطاع العام والقطاع الخاص(تحقيق مفهوم الخصوصية-العام والخاص).ويضم القطاع العام المنشآت والمرافق الخاصة بالفعاليات المشتركة والمتبادلة بين ادارة وجمهور الجامعة وبين مجتمع المدينة، اما النطاق الاخر يشمل المنشآت الرياضية والصحية، وهما يمثلان قطبي الجامعة مكانيا. اما القطاع الخاص فيشمل المنشآت الاكاديمية التدريسية والمختبرية وخدماتها وهو يتضمن الانطقة العلمية حيث يحتوي كل نطاق على عدد من الكليات التي لها علاقة علمية وتخصصية مشتركة ومتبادلة مع بعضها، حيث يمكن ان تشترك وظيفيا من خلال الاستخدام المشترك لبعض المختبرات المتخصصة اوالاستفادة علميا في بعض الجوانب المعرفية المشتركة. اما قطاع العلوم الانسانية، فيشمل نطاق الاداب والادارة ونطاق القانون ونطاق الشريعة، وقد روعي عند التخطيط التركيز في تجميع الفعاليات لتكون ضمن مسافة انتقالية(10 دقائق)على مستوى القطاع الواحد.كما في الشكل (9).

ب-التنظيم الفضائي -الكتلي : استخدم المصمم مبدأ التدرج الفضائي على مستوى النطاق الاكاديمي الواحد العلمي والانساني، حيث اتبع مبدأ الاحتواء والتدرج من الفضاء الخاص(الفناءات الداخلية لكل كلية) الى الفضاء شبه الخاص المتمثل بالفضاء الذي يجمع الفعاليات الترفيهية والخدمية لكل كلية الى الفضاء العام للمجمع والمتمثل بالمحور الحركي الوسطي للجامعة والذي يمثل المفصل الانتقالي بين الفضاءات العامة والخاصة، وبالتالي تحقيق التجانس والتسلسل الفضائي بين الفضاءات المتنوعة، وهو بذلك يتبع التنظيم التدريجي المميز لبنية النسيج الحضري الخاص بالمدن التقليدية والتي اعتمدها المصمم بشكل اساسي في تنظيم البيئة الحضرية الجامعية. كما في الشكل(10). وقد عمد المصمم الى تحقيق التوازن الكتلي على مستوى خط السماء من خلال اتباع مستوى متناغم لارتفاعات المباني، وعلى مستوى المخطط تم تحقيق التوازن من خلال العلاقة المتكاملة بين الفضاءات الخارجية وارتفاعات المباني والكتل وحسب المقياس الانساني. شكل(11).

ج-تنظيم البيئة الخارجية والمناخية: إن فكرة الكيان الجامعي المراد تحقيقها يتطلب ان يستمد مقومات خاصة به نابعة من طبيعة الموقع وخصوصية المدينة البيئية، وأن من هذه المقومات التي روعيت في التخطيط والتصميم الأساسي لجامعة الكوفة هو أهمية دراسة تأثير الطبيعة الجغرافية والمناخية في التصميم العام، وتصاميم المفردات التي يتكون منها هذا التخطيط، وقد كان بالنتيجة هذه إن التصميم قد اهتم في اسلوب توزيع فضاءاته وتجمعها بعوامل المناخ والبيئة المحلية الخاصة،فطبيعة المناخ في مدينة الكوفة والذي يتميز بكونه حار جاف صيفا، جعل من المصمم يتخذ خطوات تصميمية خاصة للمعالجة البيئية، وابراز الحلول الملائمة لهذا الغرض، فعلى مستوى المخطط للابنية، اعتمد على النسيج الحضري العضوي المتضام، وأكدت الفضاءات الخارجية باستعمالاتها وبتحديد مواقعها وتنظيم الفسح وإحاطتها بالأروقة المكشوفة، وتمثلت باستخدام سلسلة من الفناءات الوسطية المترابطة والمتداخلة مع بعضها البعض والتي تخلق تيارات هوائية مريحة بين الابنية، فضلا عن توفير عناصر الفضاءات المفتوحة في الفناءات الداخلية من تشجير ونباتات وظلال ونافورات وغيرها من العناصر التي تخلق مناخا بيئيا ملائما، بالاضافة الى جعل بعض الابنية متقاربة مع بعضها لاغراض وظيفية، وخلق ممرات ضيقة بينها للحصول على حماية اكبر من اشعة الشمس،

واستخدام ممرات الحركة المسقفة والاروقة للتقليل من قساوة المناخ. فضلا عن استخدام التشجير بكثرة وخاصة النخيل لتوفير الظلال للابنية والمماشي ومواقف السيارات، وكان لاعتماد الحزام الاخضر بصورة واسعة في الحرم الدور الفعال في خلق مناخ مريح والتقليل من التلوث البيئي.

د–التنظيم الحركي –البصري: تم اعتماد مبدأ الفصل بين حركة المشاة وحركة الاليات(السيارات)، حيث تصنف الحركة داخل المجمع التعليمي بشكل اساسي الى نوعين من الانماط الحركية تمثلت بالاتي :

- حركة المشاة: والتي تنقسم الى مسارات رئيسة ومسارات ثانوية، فالمسارات الرئيسة والمتمثلة بوجود شريان الحركة الرئيس(المحور الوسطي)، والذي قسّم الحرم الجامعي الى قطاعين، اضافة الى التفرعات الثانوية منه التي تغذي مرافق الجامعة المختلفة والمكونات المتوزعة على جانبيه، الامر الذي اعطى دورا اساسيا لهذا الشريان في تحديد بنية الموقع وصورته الشكلية، هذا المبدأ التنظيمي الحركي عزز من نفاذية الامتدادات البصرية وانسيابية مسارات الحركة ومرونتها للتنظيم الفضائي للحرم الجامعي وبما يحقق الوضوحية ومتعة الحركة اثناء التنقل بين ارجاء الحرم وادراك الصورة الكلية وكأنها لوحة لايمكن ادراكها كاملة الا عند التنقل بين اجزاءها يساعدها في تحقيق ذلك المحاور البصرية وعناصر الدلالة التي وظفها المصمم في هذا الجانب. اما المسارات الثانوية والخاصة بحركة المشاة داخل كل نطاق في الحرم الجامعي فقد اعتمدت على مبدأ التدرج والالتواءات بحيث تتسع في نقاط معينة لتشكيل الباحات والفناءات الوسطية والتي صممت لتكّون الفضاءات الرابطة بين الاقسام والكليات، بحيث تحافظ على الوحدة البصرية والتماسك الشكلي مع تحقيق وخلق المتعة البصرية من خلال مبدأ المفاجاة والاستكشاف المتحقق من التداخل الفضائي والمسارات ذات الاتجاه المتغير والاتصال البصري اللامباشر وبشكل انسيابي مرن.
- حركة السيارات: اعتماد نمط الطريق الحلقي المحيطي كاساس لحركة السيارات وابعادها عن اختراق المجمع التعليمي قدر الامكان الا في حالات وصول سيارات الخدمة وفي اماكن محددة ومخصصة وبمسارات محورية مستقيمة لتؤدي الغرض المرجو منها، لجعل البيئة الجامعية خالية من السيارات ومعتمدة بشكل اساسي على حركة المشاة وعدم تقاطعه مع حركة السيارات لتامين السلامة اولا ولتجنب الملوثات الصادرة عن المركبات سواء كانت الضوضاء او الغازات المنبعثة. شكل(12)

2-7 التحليل على وفق المستوى الثاني من التطبيق –المستوى التوسعي(التغيرات المستقبلية): تم وضع المخطط الاساس للجامعة وفق رؤية شمولية انية ومستقبلية لجميع مكونات ومتطلبات الحرم الجامعية، فاعتمد التخطيط الاساس للجامعة على قطاعين اساسين للجانب الاكاديمي والتدريسي تم الفصل بينهما من خلال المحور الحركي الوسطي بفعالياته الترفيهية والاجتماعية، وقد تمثل كلا القطاعين على تشكيل مجاميع فيزياوية هندسية الشكل، على ان يؤخذ التوسع المستقبلي بها في مساحات خصصت لاغراض النمو وبطريقة لاتؤثر على الفكر الفلسفي الذي قام عليه المخطط الاساس. والجامعة في الوقت الحالي لاتزال في طور اكمال مكونات المخطط الاساس الحالي لاستيعاب الاعداد المتنامية للطلب.

3–7 التحليل على وفق المستوى الثالث من التطبيق – المستوى التنفيذي : بعد انتهاء مرحلة اعداد التصاميم المعمارية المعبرة عن الفكر والفلسفة التصميمية واعداد المخطط الشاملMaster Plan المتكامل، توقف دور الاستشاري المصمم عن المشروع، واخذ المكتب الاستشاري الخاص بجامعة الكوفة مهمة اعداد المخططات التنفيذية والمواصفات الفنية والاشراف على التنفيذ. عبّرت هذه المرحلة المتمثلة بانقطاع وغياب دور المصمم في مرحلة التنفيذ، عن بداية تعرض المشروع الى الانفصال مابين الفكر والفلسفة التصميمية وبين التطبيق الفعلي على ارض الواقع، حيث ان قلة الخبرات في اعداد المخططات التفصيلية من جهة وفي

الاشراف على مشاريع بهذا الحجم والمواصفات، فضلا عن قلة خبرة الجهة التنفيذية في اعداد البدائل والمخططات التنفيذية اضافة الى القرارات الذاتية للسياسة الادارية التي ارتأت تغيير بعض الجوانب التخطيطية والتوقيعية للمكونات الفيزياوية وبمنظور انفرادي دون تحسس أثر ذلك على المنظومة الكلية للحرم الجامعي، ادى الى ظهور بعض المشاكل على ارض الواقع، اعتمد الاسلوب التنفيذي في انشاء جامعة الكوفة، على تنفيذ مباني منفردة وفقا للحاجة الاكاديمية وليس كمجموعات متكاملة تعكس الفكر والفلسفة التصميمية وفقا لمخططات معمارية متكاملة. اي تكامل المخططات المعمارية يقابله ضعف في المخططات التنفيذية وفي الادائية التنفيذية على ارض الواقع.

7-4 اختبار الحرم الجامعي (جامعة الكـوفــة) وفقا لمؤشرات الاطار النظري للتخطيط الاستراتيجي

بعد تحليل مكونات الحرم الجامعي وفقا لمعطيات الجانب النظري، سوف يؤشر البحث استقراءه لمجموعة مؤشرات الاطار النظري والخاصة بسياسات التخطيط العمراني لتحقيق عملية التنظيم والترابط الوظيفي والفضائي لمكونات البيئة الحضرية الجامعية جدول (1)،(2)،(3)، وكما يوضح الجدول (4).

7-5 مناقشة النتائج : اظهرت نتائج تحليل جامعة الكوفة ان تصميم الجامعة -من قبل معمار محلي وفقا لفكر وفلسفة تصميمية تجمع بين التراث والمعاصرة، ومؤكدا من خلاله على أهمية البيئة المحلية وخصائصها المتميزة والتي ظهرت بصورة جلية في نتاجه العمراني المتميز على المستوى التخطيطي والمعماري- اعتمد على فكر تصميمي وسياسة تخطيطية ممنهجة قادت الى تحقق نسبة جيدة من مؤشرات البيئة الجامعية المنتظمة، حيث برز دور التخطيط العمراني في رسم السياسة التخطيطية الموحدة للصورة الكلية للنسيج الحضري في مرحلة التصميم كفكر وفلسفة، اما في مرحلة التنفيذ ونتيجة لاعداد المخططات التنفيذية بشكل يفتقر الى القدرة على تفعيل تلك السياسات الفكرية والنهج الفلسفي على ارض الواقع، وبسبب غياب الدور الفعال لاشراف الاستشاري المصمم على التنفيذ، قد حال تحقيق بعض المؤشرات في المرحلة الحالية ومن المتوقع غيابها بنسبة اكثر في المنظور المستقبلي، في حالة استمرار النهج والسياسة التنفيذية وفق السياق الحالي، كما ان بعض الفقرات الغير متحققة يمكن ارجاعها الى عدم اكتمال تنفيذ مكونات الحرم الجامعي فهو لايزال في طور النمو والانشاء.

8- الاستنتاجات : أن ما توصل اليه البحث في مجال اطاره النظري هو تقصي واستكشاف وتوضيح مفاهيم التخطيط العمراني وابراز دوره الفاعل في تنظيم البيئة الحضرية للحرم الجامعي، وقد توصل للاتي:

- تبرز فاعلية التخطيط العمراني في معالجة مشكلات الاوضاع الراهنة من خلال وضع الاليات والسبل اللازمة والكفيلة بمعالجتها لاي جزء من اجزاء المجمع الحضري، فهو يمثل مرحلة موازية لمسار التنمية العمرانية على المستوى الشمولي.
- إن وضع سياسات عملية فعالة لتحقيق الاهداف العمرانية هي غاية التخطيط العمراني الاستراتيجي في المجمعات الحضرية
- تمثل الجامعات البيئة الحضرية الاكثر عرضة للتغيير في بنيتها الحضرية بفعل المتغيرات العلمية والفكرية والاكاديمية المستمرة والتي تلقي بظلالها على نمط الحياة الاكاديمية والاجتماعية، وهذا يقابله تغيرات على المستوى العمراني لاستيعاب تلك المستجدات والتي تستوجب اتخاذ الخطط والتدابير المستقبلية لتجاوز الاخفاقات المحتملة الحدوث في المجال العمراني في الحرم الجامعي .
- القيمة المثلى للبيئة الحضرية الجامعية تكمن في كيفية التعامل بين الجانبين الفكري والتنفيذي بشكل متكامل ومتوازن وبما يحقق سياسات استراتيجية ومبادئ اساسية تسهم في رسم وتنظيم الملامح العامة للبيئة الحضرية والحفاظ عليها في المراحل الزمنية المختلفة .

- ان مقومات نجاح تنظيم البيئة الحضرية الجامعية على المستوى الفكري والفلسفي هو النظر بشمولية لمكونات الحرم الجامعي واعتباره منظومة واحدة(كلٌ مكون من اجزاء) كل جزء فيها يؤثر في اخراج الصورة الكلية ضمن نظام من العلاقات التي تحكم ترابط الاجزاء مع بعضها انطلاقا من التوجهات الفكرية والفلسفية والمبادئ التصميمية للبيئة الحضرية الجامعية تعززها الفعالية التنفيذية.
- مبادئ التنظيم للبيئة الحضرية الجامعية على المستوى الفكري والفلسفي تتمحور بالمستويات الاتية:

– المستوى التخطيطي الشامل

– مستوى التوسعات المستقبلية

- تشكيل لجان متخصصة تتألف من مختصين معماريين ومخططين ومصممين حضريين تتولى على عاتقها مهمة اعداد الدراسات المستفيضة لتحليل الاوضاع والمستجدات التي تواجه البيئة الجامعية وتتابع الامور الطارئة كي تقوم بتحديث المخطط الاساس بطريقة تستوعب تلك المتغيرات ولا تؤثر على الفكر التصميمي.

9– التوصيات

- يوصي البحث باهمية اعداد تصاميم معمارية لمجمعات الحُرُم الجامعية وفق رؤية شمولية مستقبلية وفكر وفلسفة تصميمية محددة، واعداد تصاميم المخطط الاساس ومصادقتها مع الجهات المستفيدة على ان تؤخذ توقعات التوسع المستقبلي والتطورات في اساليب التعليم ووسائل نقل المعلومة ضمن حدود المخطط الاساس Master Plan .
- يوصي البحث باهمية وضرورة العمل على تحديد الاليات الملائمة للتنفيذ وفقا لاطار زمني محدد والمتضمنة مايأتي:

✓ اعداد الرسومات التنفيذية التفصيلية المطابقة للمخططات المعمارية والتي يقوم باعدادها الاستشاري المصمم، وبالتعاون والاستئناس بآراء الاستشاريين على ان ترتبط وتتطابق مع المخططات المعمارية المعبرة عن الفكر والفلسفة التصميمية.

✓ اعداد التصاميم التنفيذية والتفصيلية المرتبطة بتصميم الخدمات الخاصة بالمخطط الاساس Master Plan او المخطط المعد لها شاملة لكل الخدمات والبنى التحتية وتفاصيلها اضافة الى اعداد جداول الكميات والمواصفات الفنية والتي تكون ملزمة في عملية التنفيذ.

- تشكيل لجان متخصصة تتألف من مختصين معماريين ومخططين ومصممين حضريين تتولى على عاتقها مهمة اعداد الدراسات المستفيضة لتحليل الاوضاع والمستجدات التي تواجه البيئة الجامعية وتتابع الامور الطارئة كي تقوم بتحديث المخطط الاساس بطريقة تستوعب تلك المتغيرات ولا تؤثر على الفكر التصميمي.

- **المصادر**

1. الجميلي، سعد خضير محمود، 2012 ،*اثر تنظيم البيئة الجامعية على زيادة كفاءتها وتوجيه الموارد الاقتصادية*، مجلة المخطط والتنمية العدد25،ص5.
2. سحر مرسي محمد علي ،الاسس المعمارية لتصميم المباني الجامعية في مصر،رسالة ماجستير مقدمة الى كلية الهندسة– جامعة اسيوط–1995،ص52–54

3. السليفاني ، هدى صالح عمو ، 1989،*الاسس التخطيطيه والتصميميه للابنيه الجامعيه والتجربه العراقيه : اقسام العلوم في جامعتي بغداد والمستنصريه*، رسالة ماجستير مقدمة الى قسم الهندسة المعمارية ، جامعة بغداد،ص30.
4. الشهري، فائز سعد، 2006 ، *ممارسات التخطيط العمراني بالمملكة العربيةالسعودية: دراسة استكشافية وإطار عام مقترح من السياسات لتحقيق التنمية المستدامة*، مجلة البناء ،العدد السادس، ص22،21،13.
5. عبد الله يحيى بخاري، 1983،*الجامعات الاسلامية – البناء والدور*، مجلة عالم البناء العدد32، ص11.
6. عزالدين، محمد ، 1993، *تخطيط الجامعات*، مجلة عالم البناء، مركز الدراسات التخطيطية والمعمارية،القاهرة، العدد146 ،جامعة الكويت،ص11.
7. مازن إسماعيل رحيم، 2012 ،*تكاملية مواقع الأبنية الجامعية وفضاءاتها الخارجية*، رسالة ماجستير مقدمة إلى قسم الهندسة المعمارية في كلية الهندسة – جامعة بغداد،ص 49-50.
8. Antoniades,A.C., 1990 ,*Poetics of Architecture*, Van Nostrand Rein-hold,New York, ,p. 260-261, 264
9. Campos, P., 2014, *From Typological Analysis to Planning: Modern Strategies for University Spatial Quality*, CIAN-Revist e Historia de las Universidades,p.47,44.
10. Chapman, DW. and Larkhan, PJ. ,1993,*Discovering the Art of Relationship: Urban de-sign*, Aesthetic Control and design Guid-ance – University of Central England – Birmingham –.p.52
11. Ching, F. D. K., 1996*, Architecture: Form, Space and Order* , New York, Van Nastrand Reinhold Company, ,p.320.
12. Dober, R., *Campus Landscape: Functions, Forms, Features*, 2000, John Wiley & Sons, Inc., U.S.A.
13. Dober,R.,*Campus Architecture* , 1996,Mc Graw-Hill,Washington D.C., ,p.216-218.
14. Duncan, W.,et al.2012, *Campus of the future, Arup 2012*, ,http://www.driversofchange.com/download/1190/pdf
15. Edwards, B., 2000, *University Architecture*, Spoon Press, Taylor & Francis Group, London and New York, ,p.150,41.
16. Flavia ,C. M., 2013,*The universi-ty campus and its urban development in the context of the knowledge economy*, , p.4,available ,from www.eura.org /media/Full_papers_ Track_5/127_ Curvelo-Magdaniel_The_university_campus_ and_its_urban_development_ in_the_context.pdf
17. Hashimshony, R. and Haina, J., 2006, *Designing the University of the Future*, Society for College and University Planning (SCUP). http://pdc.ucr.edu/campus/2007design.pdf
18. John, A.B., and David K.P. , 2002,*University of Nebraska-Lincoln,* Published research,. p.15-18

19. Kyle, T., 2006, Student Unions-Campus as Facilities Manager. from, http://www.appa.org/FacilitiesManager/article.cfm?ItemNumber=2563&parentid=2542
20. Neuman,David J., 2013,*Building Type Basic For College And University Facilities*, ,Willy,Second Edi-tion.p.12,23,25,37.
21. Peter, A.G, 2004,*The Evolving Campus - American School and Universi-ty*,.,http://asumag.com/mag/university_evolving_campus , Nov 1.
22. Trancik, R., 1986,*Finding Lost Space: Theories of Urban Design* – VNR – VAn nostrand Reinhold Company – New York –,p. 101
23. Turnel, P., *Campus an American planning Tradition*, The Architecture History Foundation, 1984,.NY,.p.186-188,88-89,248,268,267,281,269,282.
24. Yang, H., *Campus Landscape Space Planning and Design Using QFD*, 2007, Thesis submitted to the Faculty of the Virginia Polytechnic, p.4.

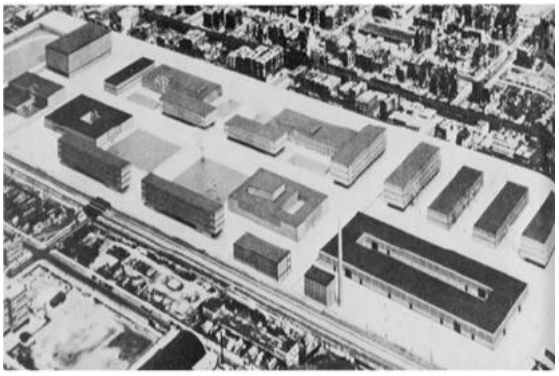

شكل(1) معهد التكنولوجيا بالينويميس فان دوروه(Turnel,1984)

شكل(2)مركز الدراسات العليا في جامعة هارفارد لـ والتر كروبيوس(Turnel,1984).

شكل(3) المركز الفني في جامعة هارفارد Turnel,1984

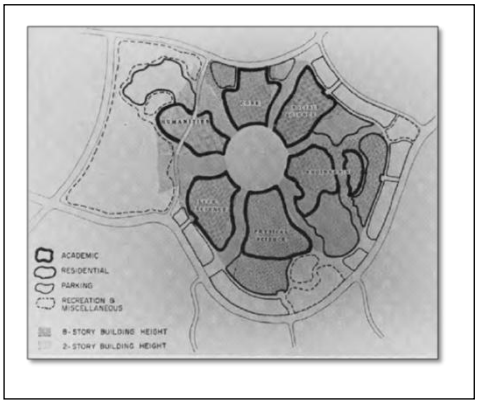

شكل(4) جامعة Irvine بكاليفورنيا، ((Turnel, 1984

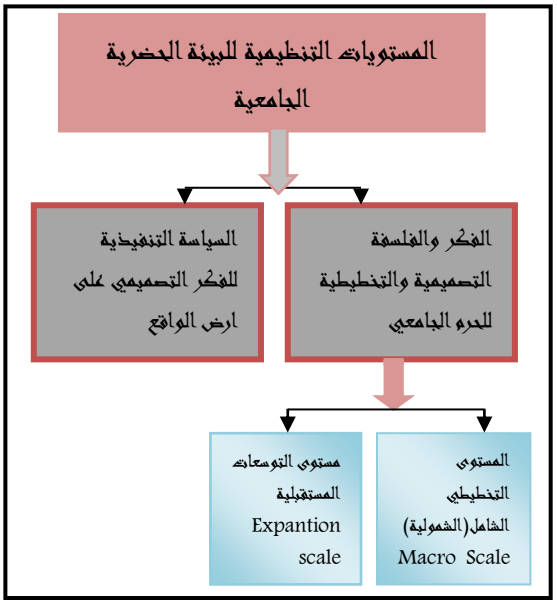

شكل(5) المستويات التنظيمية للبيئة الجامعية م-الباحثة

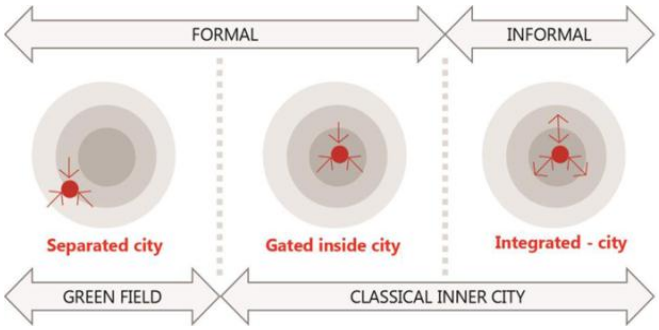

شكل(6)علاقة الجامعة بالمدينة [Flavia,2013]

شكل (7)الانماط التخطيطية للجامعات وفقا لـ Campos (Campos,2014)

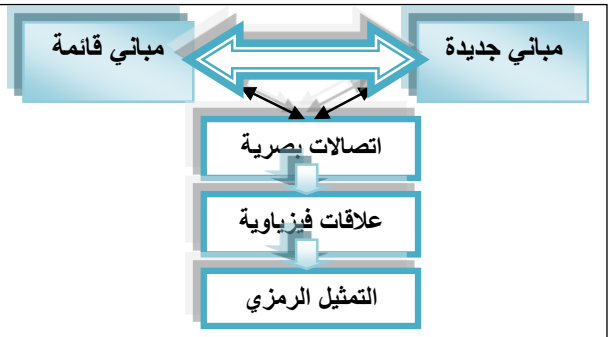

شكل(8) الاعتبارات التصميمية للمرافق الجديدة في الحرم الجامعي-الباحثة

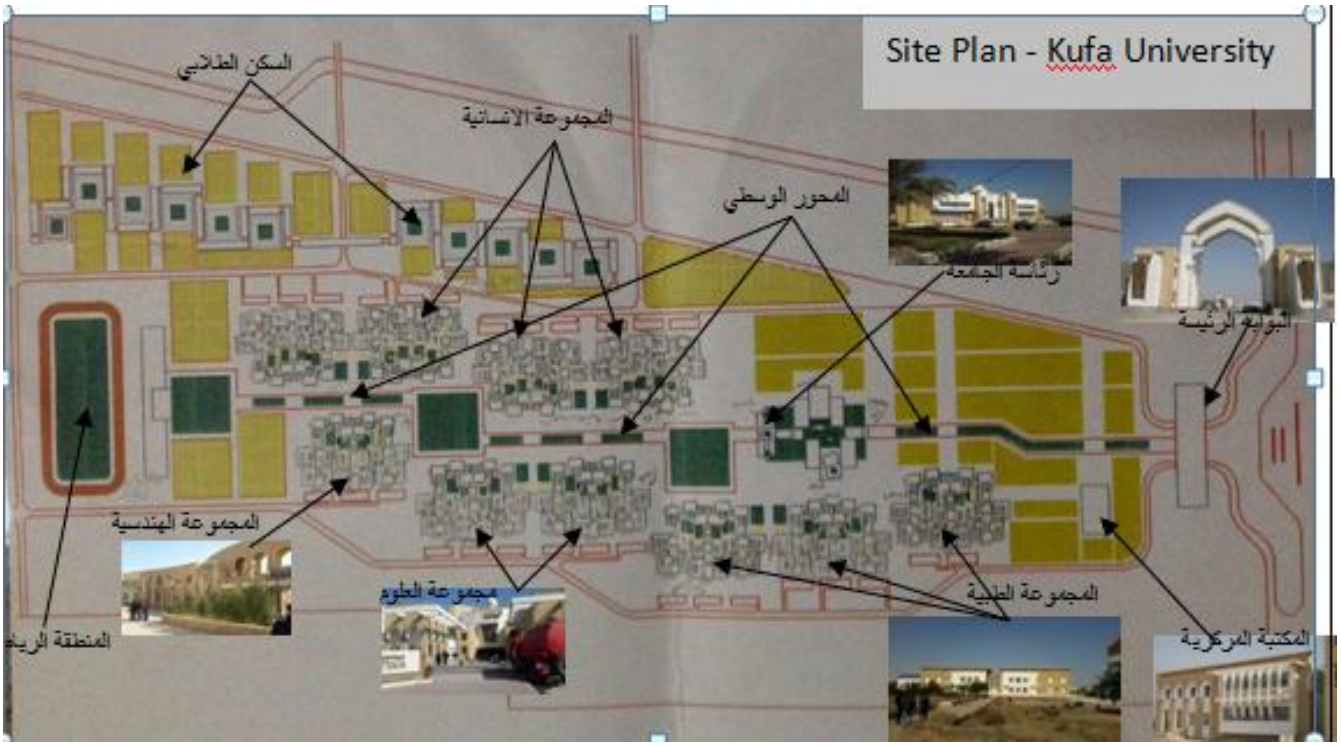

شكل(9)المخطط الاساس لجامعة الكوفة ،(مكتب الاستشاري المصمم) بتصرف من الباحثة

شكل(10) الفناءات الداخلية للمجموعة الطبية

شكل(11)السياسات العمرانية لجامعة الكوفة– التوازن الكتلي على مستوى خط السماء لجامعة الكوفة من خلال اتباع مستوى واحد لارتفاعات المباني، العناصرالتصميمية للمعالجة البيئية (الاروقة والتشجيروالفناءات الوسطية) التي استخدمت باساليب متنوعة ولجميع مكونات الحرم الجامعي، مسارات المشاة والسيارات وتحديدها باعمدة الانارة واشجار النخيل مع توفير مواقف السيارات

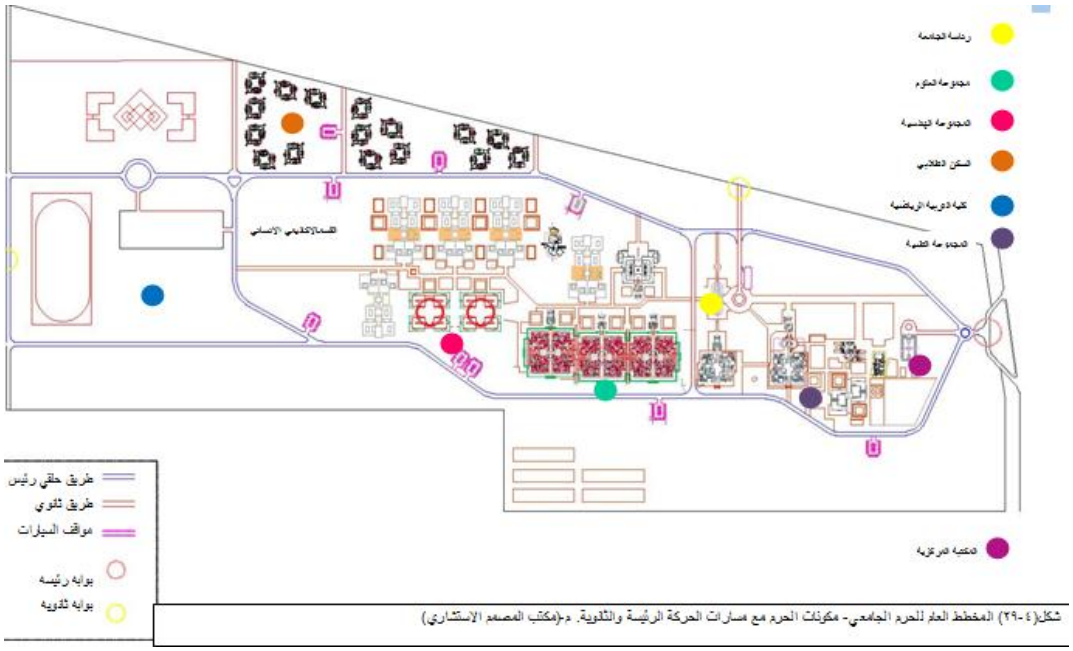

شكل(٤-٢٩) المخطط العام للحرم الجامعي- مكونات الحرم مع مسارات الحركة الرئيسة والثانوية. م(مكتب المصمم الاستشاري)

شكل(12)المخطط العام للحرم الجامعي-مكونات الحرم مع مسارات الحركة الرئيسة والثانوية

جدول(1) مفردات المستوى التخطيطي الشامل،م- الباحثة

المستوى التخطيطي الشامل	المفردات الرئيسة	المفردات الثانوية	القيم الممكنة			
	الجانب الوظيفي	**التنظيم التخطيطي**	التكوين المكاني		نمط تخطيطي واضح (مركزي،شعاعي،خطي،شبكي)	
			الفكر التنظيمي والشكل الحضري		تخطيط القطاعات و تنسيق الموقع وتنطيق وظيفي للفعاليات وتقسيم الموقع الى انطقة موزعة حسب العلاقة بين العام والخاص (اكاديمي،اداري،سكني،خدمي)	
			الحدود وسهولة الوصول	انفتاح المؤسسة على المجتمع	حدود مادية	
					حدود مفاهيمية	
		التنظيم الفضائي والتنظيم الكتلي	التنظيم الفضائي	العلاقات بين العناصر	علاقات تجميعية	الهرمية في علاقة الفضاءات مع بعضها (التدرج الفضائي من الفضاءات العامة الى الفضاءات الخاصة)
					علاقات نسقية	التجانس الفضائي بين الفضاءات العامة والخاصة والذي يحقق الانسيابية الفضائية
					علاقات تنظيمية	الوضوحية والارتباط والتكامل لشبكة فضاءات موصولة تربط بين العام والخاص والداخل والخارج والكل والجزء
				السمات الفضائية	خصائص وظيفية	تحقيق هوية مميزة للحرم الجامعي
						توفر مواقع ملائمة لكافة الانشطة المختلفة داخل الحرم الجامعي
						توفر حماية للبيئة الطبيعية
						تحقيق الجودة البصرية من خلال المتعة والجمال
			التنظيم الكتلي		تحقيق التوازن بين ارتفاعات الكتل في خط السماء	
					التوازن في علاقة الكتل بالفراغات المحيطة	
					ترابط متماسك بين الكتل والفضاءات الحضرية -المقياس الانساني	
					تحقيق شكل حضري واضح المعالم ويمكن ادراكه من خلال التوازن الكتلي	
		تنظيم البيئة الخارجية والمناخية	العوامل الطبيعية		الانسجام مع طوبغرافية الموقع	
			العوامل المتغيرة		التوجيه المناسب	
					المعطيات المناخية (التظليل ،التشجير،النافورات .الفناءات الداخلية ،المسطحات المائية ،عناصر تنسيق وتأثيث الموقع)	
					تعزيز البيئة الخضراء	
		التنظيم الحركي والبصري	مسارات حركية	التتابع الحركي	مدة التنقل لاتزيد عن10 دقائق	
					تحسين كفاءة مسارات المشاة(تسييج الحافات ووضع النباتات أو الأشجاروالمسقفات للتظليل والحماية من أشعة الشمس)	
					تحسين كفاءة مسارات حركة السيارات(زراعة النباتات أو الأشجار للتظليل والحماية من أشعة الشمس)	
					التقليل من دخول السيارات ومواقفها داخل الحرم الجامعي	
			الاتجاهية البصرية	نفاذية بصرية	تحقيق مشهد حضري متسلسل ومتكامل الصورة	
					اتصال بصري بين الفضاءات المتنوعة	

جدول(2)مفردات المستوى التوسعي،م-الباحثة

	المفردة الرئيسة	القيم الممكنة
مستوى التوسعات المستقبلية	اتصالات ونفاذية بصرية	تحقيق الاستمرارية
	علاقات مادية	الانسجام والوحدة الشكلية مع النسيج
	الرمزية	الحفاظ على الطابع والجانب الرمزي المميز للحرم الجامعي
	التوازن في المقياس والتناسب للجزء مع المجاورات	
	التوقيع الملائم للمبنى (السلامة في أختيار مواقع الأبنية الجديدة)	
	الوحدة والتنوع في مواد البناء	
	كفاءة التنظيم البيئي (تكامل الموقع مع البيئة المجاورة)	
	الأعتماد على وحدة تخطيطية تتقبل الأضافة والتداخل والترابط	
	الأخذ بنظر الأعتبار الفضاء المفتوح المحيط والذي يتميز بالوحدة والتنوع	
	نمو وتوسع متوافق مع الفكر والفلسفة التصميمية	

جدول(3) المفردات الخاصة بالجانب التنفيذي- الباحثة

	المفردة الرئيسة	القيم الممكنة
المستوى التنفيذي	الخصائص التنفيذية للمخططات	اعداد المخططات والرسومات التنفيذية التفصيلية الانشائية والخدمية(البنى التحتية) (Working Drawing) مقرونة بنصوص كتابية توضيحية، والمطابقة للمخططات المعمارية
	الواقع الفعلي كانعكاس للفكر التصميمي	ضمان التنفيذ وفقا للمخططات المعدة مسبقا(المعمارية والتنفيذية) مع اعداد مخططات (Shop Drawing) من قبل المقاول لتقديم البدائل الممكنة .

جدول(4) اختبار حرم جامعة الكوفة-الباحثة

الاستراتيجيات	المفردة الرئيسة	المفردة الثانوية		القيم الممكنة		جامعة الكوفة: تحقق القيمة بالاتجاه الايجابي	جامعة الكوفة: تحقق القيمة بالاتجاه السلبي
السياسة التخطيطية	التنظيم التخطيطي	النمط التخطيطي	التكوين المكاني	اتباع نمط تخطيطي واضح للحرم(خطي)		✓	
		الفكر التنظيمي والشكل الحضري		تنطيق وظيفي للفعاليات وتقسيم الموقع الى قطاعات وفقا للعلاقة بين العام والخاص		✓	
				تعريف حدود النطاقات في الحرم الجامعي تسهل ادراكها والتعرف اليها (حدود معرفة وواضحة)		✓	
		الحدود وسهولة الوصول	انفتاح المؤسسة على المجتمع	حدود مادية		✓	
				حدود مفاهيمية			✓
	الفضائي والتنظيم الكتلي	التنظيم الفضائي	العلاقات بين العناصر	علاقات تجميعية	الهرمية في علاقة الفضاءات مع بعضها: تتدرج الفضاءات من الفضاء الخاص الى الفضاء شبه الخاص الى الفضاء العام	✓	
				علاقات نسقية	التجانس والتسلسل الفضائي بين الفضاءات العامة والخاصة تحقق درجة من الانسيابية الفضائية	✓	

				علاقات تنظيمية	الوضوحية والارتباط والتكامل لشبكة فضاءات موصولة تربط بين العام والخاص والداخل والخارج والكل والجزء	✓	
				سمات تعريفية	الخصائص الوظيفة للفضاءات الخارجي: تحقق هوية مميزة للحرم الجامعي	✓	
					توفر مواقع ملائمة للانشطة المختلفة داخل الحرم الجامعي		✓
					توفر حماية للبيئة الطبيعية	✓	
					تحقق الجودة البصرية من خلال المتعة والجمال	✓	
				االتنظيم الكتلي	تحقيق التوازن بين ارتفاعات الكتل مع خط السماء	✓	
					التوازن في علاقة الكتل بالفراغات المحيطة: ان عدم اكتمال تنفيذ مشاريع الجامعة بصورة مجاميع لم يظهر التوازن بشكل ملحوظ		✓
					ترابط متماسك بين الكتل والفضاءات الحضرية -المقياس الانساني : عدم اكتمال اعمال الفضاءات المحيطة بالكتل قللت من هذا الجانب		✓
					تحقيق شكل حضري واضح المعالم وسهل الادراك من خلال التوازن الكتلي	✓	
	تنظيم البيئة الخارجية والمناخية			العوامل الطبيعية	الانسجام مع طوبغرافية الموقع	✓	
				العوامل المتغيرة	الملائمة والتوافق مع العوامل المناخية المتغيرة: التوجيه المناسب نسبة الى الاشعاع الشمسي والرياح	✓	
					المعطيات المناخية (التظليل ،التشجير،النافورات ،التجميع المتضام العضوي للمباني)	✓	
					تعزيز البيئة الخضراء: قلة الاهتمام بالمساحات الخضراء من قبل الجامعة الا في مواقع معينة ادى الى قصور دورها البيئي والجمالي		✓
	التنظيم الحركي والبصري			مسارات حركية	التتابع الحركي: مسافة التنقل ضمن النطاق الواحد لاتزيد عن 10 دقائق		✓
					تحسين كفاءة مسارات المشاة :قصور الاهتمام بالجانب التنفيذي قلل من كفاءة المسارات		✓
					تحسين كفاءة مسارات حركة السيارات(زراعة النباتات أو الأشجار للتظليل والحماية من أشعة الشمس	✓	
					التقليل من دخول السيارات ومواقفها داخل الحرم الجامعي (توقيع مواقف السيارات في محيط الحرم الجامعي	✓	
				الاتجاهية البصرية	النفاذية البصرية: تحقيق مشهد حضري متسلسل ومتكامل الصورة عبر النفاذية البصرية	✓	
					اتصال بصري بين الفضاءات المتنوعة	✓	
سياسة التوسعات	بيئة عمرانية متكيفة مع التغيرات			المبادئ التنظيمية للمكونات الجديدة في الحرم الجامعي (العلاقة بين الوجود القائم والاضافات	اتصالات ونفاذية بصرية: تحقيق الاستمرارية	✓	
					علاقات مادية: الانسجام والوحدة الشكلية مع النسيج	✓	
					الرمزية: الحفاظ على الطابع الرمزي المميز للحرم الجامعي	✓	

		الجديدة للحرم).	التوازن في المقياس والتناسب للجزء مع الكل	✓	
			التوقيع الملائم للمبنى: (تم تغير بعض المواقع المخصصة للمكونات الجامعية عن المخطط الاساس الى مواقع اخرى غير مدروسة)		✓
			الوحدة في مواد البناء	✓	
			كفاءة التنظيم البيئي (تكامل الموقع مع البيئة المجاورة)	✓	
			الأعتماد على وحدة تخطيطية تتقبل الأضافة والتداخل والترابط	✓	
			الأخذ بنظر الأعتبار الفضاء المفتوح المحيط والذي يتميز بالوحدة والتنوع	✓	
		نمو وتوسع متوافق مع الفكر والفلسفة التصميمية			✓
السياسة التنفيذية	تنفيذ متوافق مع الفكر التصميمي	الخصائص التنفيذية للمخططات	اعداد المخططات والرسومات التنفيذية التفصيلية الانشائية والخدمية(البنى التحتية)(Working Drawing) مقرونة بنصوص كتابية توضيحية، والمطابقة للمخططات المعمارية: ظهرت بعض الاشكالات بسبب غياب دور المصمم الاستشاري في مرحلة الاعداد .		✓
		علاقة الواقع بالفكر التصميمي	ضمان التنفيذ وفقا للمخططات المعدة مسبقا(المعمارية والتنفيذية) مع اعداد مخططات(Shop Drawing) من قبل المقاول لتقديم البدائل الممكنة		✓
					✓
مجموع الفقرات المتحققة				38/28	
نسبة التحقيق				%73.7	

ENGINEERING

College of Engineering University of Baghdad No.6 Vol. 23 June 2017

List of Contents

English Section: Page

Stress Analysis of Spiral Bevel Gear Drives 1 - 13
Mohammad Qasim Abdullah
Humam Abdulrahiem Abdulwahid

Evaluating the Performance of High Modulus Asphalt Concrete Mixture for Base Course in Iraq 14 - 33
Amjad H. K. Albayati
Roaa H. Lateif

Stabilization of Clay Soil Using Tyre Ash 34 - 51
Mahmood Dheyab Ahmed
Ahmed Mohamed. Adkel

Synthesis of Nanozeolite NaA from Pure Source Material Using Sol Gel Method 52 - 62
Najwa Saber Majeed
Jwan Taher Majeed

A Study of Parameters Affecting the Solvent Extraction-Flocculation Process of Used Lubricating Oil 63 - 73
Hussein Qasim Hussein
Ali Laith Abdulkarim

Design and Implementation of Classical Sliding Mode Controller for Ball and Plate System 74 - 92
Marwa Mohammed Alwan
Dr. Laith Jasim Saud

The Effect of Cyclic Bending Loads on Crack Growth in Pipes for Inclined and Transverse Cracks with or Without Internal Pulsing Pressure 93 - 107
Dr.Fathi Alshamma
Shwan Abdulmuhsin Zainalaabdeen

E-ISSN 2520-3339

P-ISSN 1726-4073

Journal of Engineering

A Scientific Refereed Journal
Published by
College of Engineering
University of Baghdad

June
2017

Number 6

Volume 23

E-ISSN 2520-3339

P-ISSN 1726-4073

مجلة الهندسة

مجلة علمية محكمة تصدرها
كلية الهندسة ـ جامعة بغداد

حزيران
2017

العدد 6
المجلد 23

رقم الايداع في دار الكتب والوثائق ببغداد
2231 لسنة 2017

قائمة المحتويات

القسم العربي:

العنوان	الصفحة
السياسات العمرانية في الحرم الجامعي دراسة تحليلية لسياسة التخطيط العمراني في حرم جامعة *طالب حميد الطالب* *زمن عودة عمران*	**1 - 24**